NASA CR-132615

EVALUATION OF DISPERSION STRENGTHENED NICKEL-BASE ALLOY HEAT SHIELDS FOR SPACE SHUTTLE APPLICATION

Phase II Summary Report
May 1975
MDC G5241

Prepared under Contract No. NAS1-11654
McDonnell Douglas Astronautics Company
Huntington Beach, California
for
NATIONAL AERONAUTICS AND SPACE ADMINISTRATION
Langley Research Center
Hampton, Virginia 23365

NASA CR-132615

EVALUATION OF DISPERSION STRENGTHENED NICKEL-BASE ALLOY HEAT SHIELDS FOR SPACE SHUTTLE APPLICATION

Phase II Summary Report
May 1975
MDC G5241

R. Johnson, Jr.
D. H. Killpatrick

Prepared under Contract No. NAS1-11654
McDonnell Douglas Astronautics Company
Huntington Beach, California
for
NATIONAL AERONAUTICS AND SPACE ADMINISTRATION
Langley Research Center
Hampton, Virginia 23365

ABSTRACT

The work conducted from 15 May 1973 through 31 May 1975 in a program to evaluate dispersion-strengthened nickel base alloy heat shields for Space Shuttle application is described. The work reported constitutes the second phase of a two-phase program. The design, fabrication, and testing of a full-size, full-scale TD Ni-20Cr heat shield test array in simulated mission environments is described. The design and fabrication of two additional full-size, full-scale test arrays to be tested in flowing gas test facilities at the NASA Langley Research Center is also described. Cost and reusability evaluations of TD Ni-20Cr heat shield systems are presented, and weight estimates of a TD Ni-20Cr heat shield system for use on a Shuttle Orbiter vehicle are made. Safe-life expectancy of a TD Ni-20Cr heat shield system is assessed. Non-destructive test techniques are evaluated to determine their effectiveness in quality assurance checks of typical TD Ni-20Cr components such as heat shields, heat shield supports, close-out panels, formed cover strips, and edge seals. Results of tests on a braze reinforced full-scale, subsize panel are included in test evaluations of the contractor test array. Phase II test results show only minor structural degradation in the main TD Ni-20Cr heat shields of the contractor test array during 25 simulated mission test cycles. More extensive degradation occurs in the test array close-out panels as a result of interference from the test fixture edge seals and from larger thermal gradients near the edge of the test fixture. Results of cost studies show the initial unit cost of a TD Ni-20Cr metallic radiative thermal protection system, including heat shields, supports, fasteners, closure strips, and insulation, to be $721 per square foot. A refurbishment rate of four percent per mission is indicated, and such a rate yields a total cost for 100 missions of $1,943 per square foot.

Page intentionally left blank

FOREWORD

This report presents results of Phase II work that was performed between 15 May 1973 and 31 May 1975 under Contract NAS1-11654. The program described herein is being performed by the McDonnell Douglas Astronautics Company (MDAC) of the McDonnell Douglas Corporation for the National Aeronautics and Space Administration, Langley Research Center, Hampton, Virginia. Technical direction of the contract is being performed by Mr. W. B. Lisagor of the Materials Division, Materials Research Branch.

The program is being managed by Read Johnson, Jr., under the direction of Dr. J. F. Garibotti, Chief Structures Engineer, Research and Development, Structures, Development Engineering. Major contributions were made to the program by Dr. D. H. Killpatrick, Material and Process, Development Engineering. Others who contributed to the program and to the preparation of this report are: Ralph Lilienkamp, in charge of Space Simulation Chamber tests; John McDaniels, Space Simulation Test Engineer; W. B. Shelton, Acoustic Test Engineer.

Page intentionally left blank

CONTENTS

Page intentionally left blank

FIGURES

TABLES

Section 1
INTRODUCTION AND SUMMARY

The objective of this program was to evaluate TD Ni-20Cr material for application in reusable radiative metallic heat shields as part of a Space Shuttle thermal protection system (TPS). The evaluations encompassed analytical and experimental efforts designed to assess the potential of TD Ni-20Cr heat shields in terms of reuse capability, refurbishment requirements, TPS weight, and TPS costs.

TD Ni-20Cr, a dispersion-strengthened metal for which production techniques were recently improved (Reference 1), was selected for this evaluation program because it extends the service temperature limits for uncoated metallic structures by 111°K to 333°K (200°F to 600°F) above those of current superalloys. Thus, a maximum reuse temperature of 1477°K (2,200°F) has been projected for TD Ni-20Cr heat shields.

To achieve program goals efficiently, the work was organized into two sequential phases covering a total time span of 35-1/2 months. Phase II efforts, covering the period from 15 May 1973 to 31 May 1975, are reported herein.

The work conducted under this program is part of an overall effort by the NASA to evaluate advanced thermal protection systems for application in reusable space vehicles capable of entry from earth-orbital missions, maneuvering flight after entry, and horizontal landing. Such advanced thermal protection systems are also projected as being applicable to vehicles capable of sustained hypersonic flight within the earth's atmosphere at speeds ranging from Mach 6 to 12. A reusable space vehicle having the capabilities mentioned above is currently under development as a key part of the NASA Space Shuttle Program (SSP). This vehicle, designated the Orbiter, will be capable of at least 100 missions to earth orbit followed by entry flight and return to a designated landing site.

The Orbiter TPS has been recognized as a key system in determining the vehicle weight. Durability of the TPS will also be a significant factor in refurbishment requirements; hence, costs associated with refurbishment will be directly affected by the TPS performance in terms of reuse capability. A third design goal, TPS reliability, is a primary requirement for successful operational service of the Space Shuttle. The goal of improving these key TPS performance requirements - weight, cost, and reliability - resulted in establishment of the current program to evaluate TD Ni-20Cr heat shields. The evaluations undertaken in this two-phase program are based upon a coordinated analytical and experimental approach that have led to demonstration tests to determine the performance and behavior of a full-size, full-scale TD Ni-20Cr heat shield array when tested under simulated Space Shuttle TPS environmental conditions.

Phase I efforts (Reference 2) were devoted to (1) a definition of Shuttle Orbiter environments critical for its TPS, (2) material evaluations of TD Ni-20Cr sheet material to be used in this program, (3) parametric studies of TPS designs, and (4) tests of two subsize, full-scale TPS panel designs. As a result of Phase I evaluations, a corrugation-stiffened single-face panel design was selected for the full-size, full-scale TPS test arrays tested in Phase II. Phase I tests of two panel edge closure designs in the simulated entry flow conditions of a plasma-arc facility led to the selection of a cover strip design to close the space between panels.

During Phase II three full-size TD Ni-20Cr heat shield arrays were designed and fabricated, one for cyclic simulated mission tests in the McDonnell Douglas Space Simulation Laboratory and two for testing in flowing gas facilities at the NASA Langley Research Center. All three test arrays used the same basic heat shield panel design, a corrugation-stiffened single-face panel with nominal planform dimensions of 48.2 cm by 46.0 cm (19 in. by 18.1 in.). When the interpanel cover strip dimensions are accounted for, the nominal heat shield module size is 50.4 cm by 50.4 cm (20 in. by 20 in.). The full size heat shield arrays for Phase II tests included surface panels, panel closeouts, a simulated substructure, panel supports and attachments, and insulation packages between the panels and the substructure. Differences

in test fixture planform sizes, depths, and attachment requirements caused differences in each test array, particularly in the closeout panels, the edge details, and in the insulation depth between the heat shields and the simulated substructure.

Specific objectives of the Phase II efforts included evaluations of TD Ni-20Cr heat shield systems for use in the Shuttle Orbiter in terms of life expectancy, weight, and in installation requirements and ease of replacement. Also, refurbishment frequency and overall TPS unit costs for 100 missions were evaluated from Phase II test results.

Page intentionally left blank

Section 2
HEAT SHIELD TEST ARRAY DESIGNS

The three Phase-II heat shield arrays were all designed to meet requirements of the Shuttle Orbiter TPS environment defined in Phase I of the program. The defined environment included typical acoustic levels and duration during each mission, temperature profiles for a full mission, and differential pressure loads on a specific TPS area on the Orbiter lower surface where TD Ni-20Cr heat shields are applicable. The projected meteoroid environment was also defined during Phase I. Meteoroid impingement effects were evaluated in Phase I (Reference 2) and thus were not a part of Phase II evaluations.

While designed to the same basic Orbiter requirements, the three test arrays were to be tested in three different facilities, and each was therefore to sustain a different test environment. The McDonnell Douglas Space Simulation Laboratory was used to evaluate heat shield performance under programmed differential pressure and thermal loads. Acoustic load effects were also evaluated in a separate test chamber at the McDonnell Douglas test laboratories in St. Louis. Two TD Ni-20Cr heat shield arrays were also designed and fabricated for aerodynamic testing in Langley test facilities, one for the 8-foot High Temperature Structures Tunnel (HTST) and the second for the Langley Thermal Protection System Test Facility (TPSTF). Tests in the Langley HTST and TPSTF were not completed during Phase II and performance evaluations of TD Ni-20Cr heat shields were thus based on the tests conducted in contractor test facilities.

Each heat shield array designed for Phase II tests employed the same basic design for the main surface panels and the smaller close-out panels. The basic design, selected from Phase I evaluations, consisted of a corrugation-stiffened, single-face configuration with stiffening members at each edge. The heat shield panels were designed as wide beams supported at each end by transverse beams formed from TD Ni-20Cr sheet. A sheet thickness of 0.0254 cm (0.010 in.) was used for both face sheet and corrugation in each panel

design. Reinforcing members on the panel sides were made from 0.0254 cm (0.010 in.) thick sheet for the MDAC test array; however, initial thermal and differential pressure tests indicated a requirement to increase the edge stiffness. Consequently, the lateral edge members for the HTST and TPSTF main test panels were made from 0.0508 cm (0.020 in.) thick TD Ni-20Cr sheet. Other changes from the Phase I panel designs are discussed in greater detail subsequently in this section.

The remainder of this section presents details of the baseline Orbiter configuration, the TPS environment defined from the Orbiter mission trajectories, the three TPS test arrays designed and fabricated in Phase II, and the design temperatures and stresses for the test arrays.

2.1 ORBITER CONFIGURATION AND TPS ENVIRONMENT

The Shuttle Orbiter configuration selected as the baseline vehicle for heat shield evaluations is shown in Figure 2-1 in the launch configuration in which the orbiter is mated with the external tank and solid rocket motors (SRM). The delta-winged Orbiter configuration is typical of those designed to orbit a 27,250 kg (60,000 lb) payload and to have a cross-range on entry of approximately 2,040 km (1,100 nm). Dimensions of the baseline Orbiter are shown in greater detail in Figure 2-2.

The basic design pressures and temperatures experienced by the TPS surface panels were determined by the vehicle trajectories during boost, entry, and terminal approach phases of the mission. To define the TPS panel pressure and temperature histories, the trajectories for the baseline Orbiter were reviewed in Phase I and a critical set of boost, entry and cruise trajectories were selected. From the selected trajectories critical flight parameters were defined as shown in Figure 2-3. After selecting critical trajectory parameters, a typical TD Ni-20Cr heat shield area on the lower surface of the Orbiter was chosen for the purpose of deriving specific time-histories of TPS temperatures, differential pressures, and ambient pressures to be used in Phase I studies and in subsequent Phase II designs of full-size, full-scale TD Ni-20Cr heat shield arrays. As a criterion for initial selection of a typical surface area for

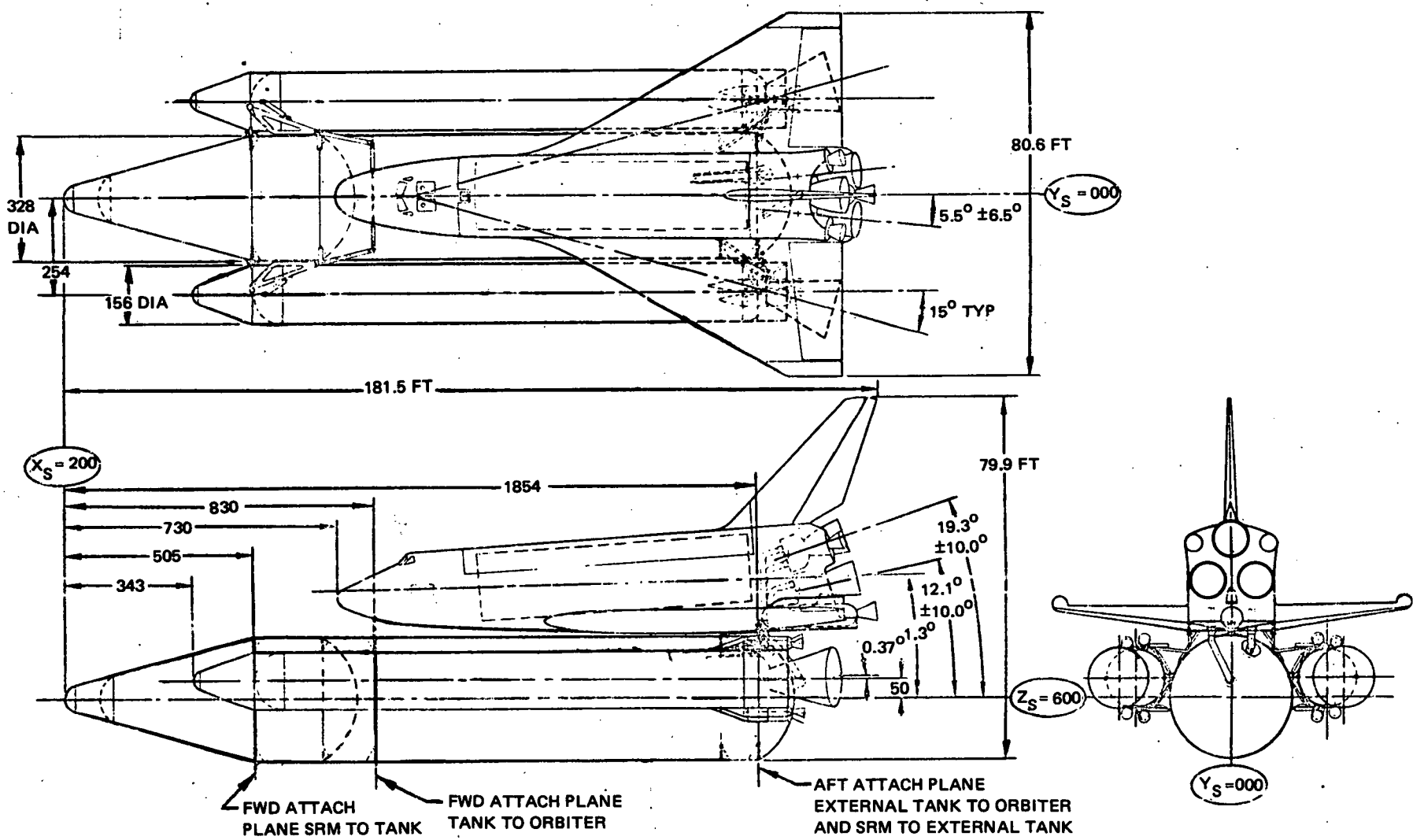

Figure 2-1. Shuttle Mated Configuration

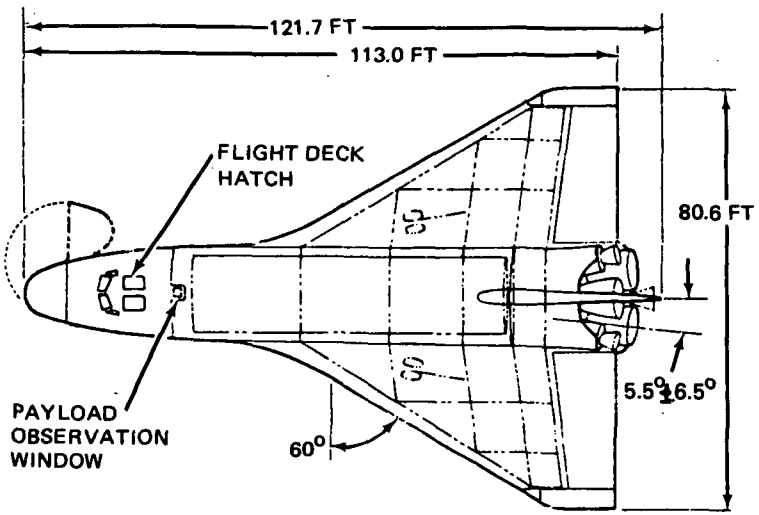

WING	
THEO AREA	3,800 FT^2
EXPOSED AREA	2,416 FT^2
AR	1.71
ELEVON AREA	548 FT^2
WETTED AREA W PODS	5,074 FT^2
WING BODY INTERSECTION	462 FT^2
ML VOLUME W PODS	5,988 FT^2
AIRFOIL	NACA 0008–64
TAIL	
THEO AREA	450 FT^2
EXPOSED AREA	432 FT^2
ASPECT RATIO	1.74
RUDDER AREA	161 FT^2
WETTED AREA	888 FT^2
TAIL BODY INTERSECTION	30 FT^2
ML VOLUME	410 FT^3

TOTAL VEHICLE	
WETTED AREA	13,258 FT^2
PROJECTED PLANFORM	4,406 FT^2
ML VOLUME	40,745 FT^3
FUSELAGE	
WETTED AREA FT^2	
FWD	1,382 FT^2
MID	4,450 FT^2
AFT W OMS AND BODY FLAP	1,585 FT^2
BASE	371 FT^2
TOTAL	7,788 FT^2
ML VOLUME FT^3	34,347 FT^3
PROJECTED PLANFORM	1,990 FT^2

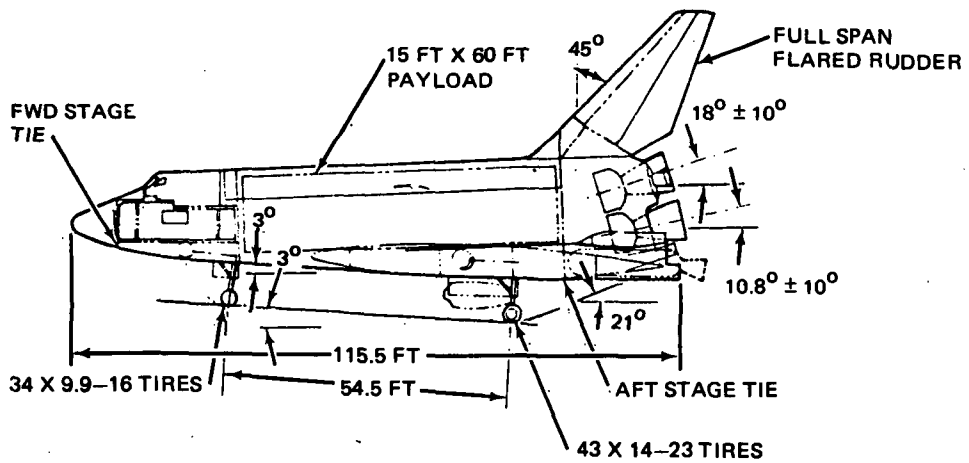

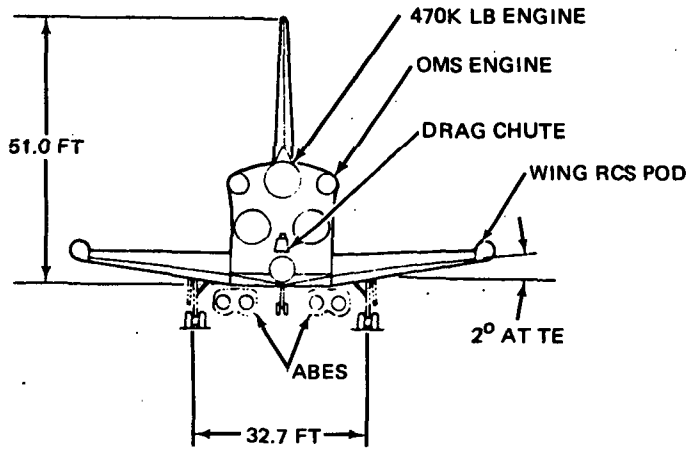

Figure 2-2. Baseline Orbiter Configuration

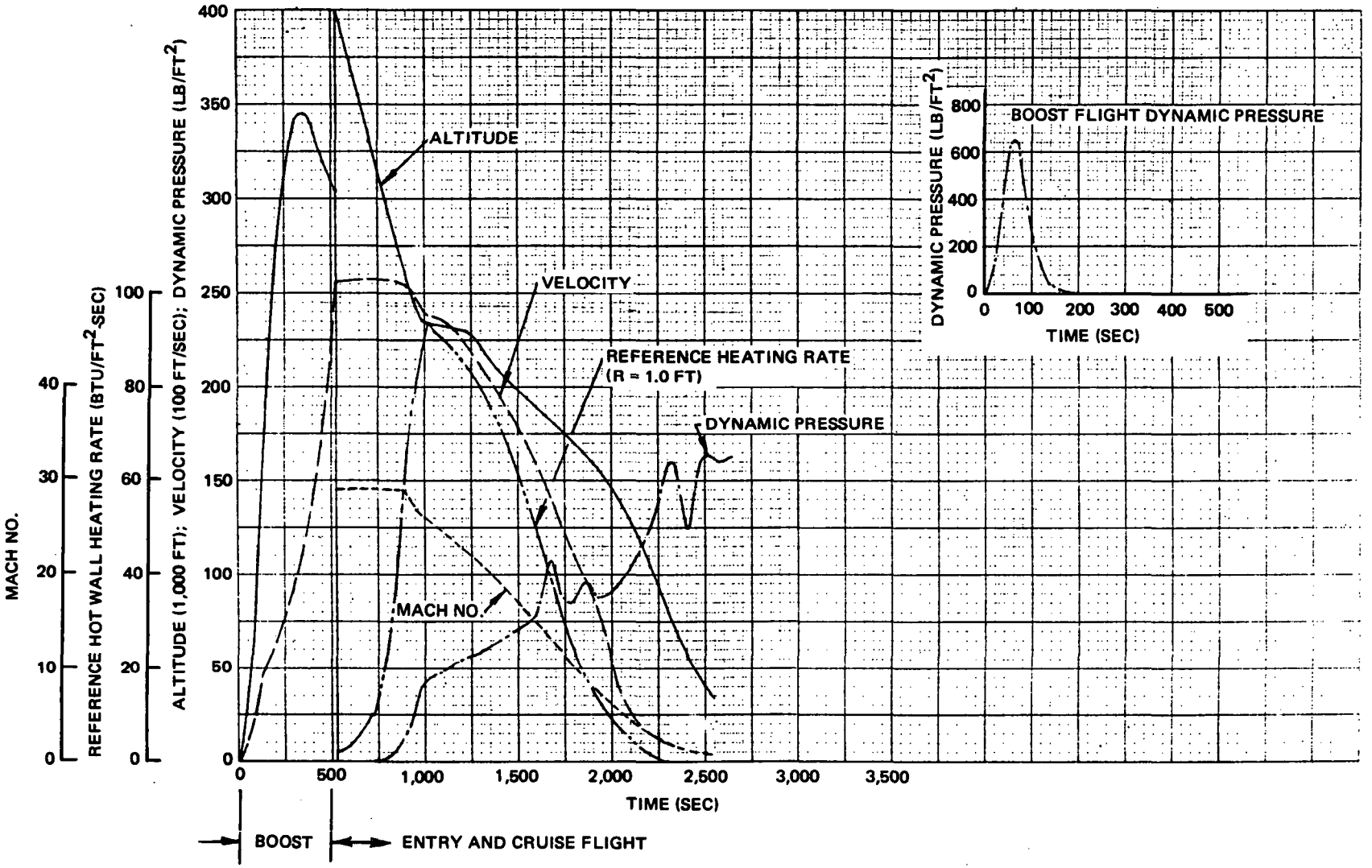

Figure 2-3. Baseline Orbiter Flight Parameters

a TD Ni-20Cr TPS, a maximum reuse temperature of 1,478°K (2,200°F) was chosen, along with 100 entry flights as the nominal number of missions. Thermal analyses of the baseline Orbiter showed maximum lower surface temperatures to range from 1,368°K to 1,699°K (2,000°F to 2,600°F) during entry flight. The maximum temperature isotherms for the Orbiter configuration are shown in Figure 2-4. From the isotherms shown in Figure 2-4, a position on the lower surface centerline at X/L = 0.35 was chosen to define panel design parameters. The selected position sustains a maximum temperature of 1,478°K (2,200°F) and it is also subjected to maximum temperatures for a significant portion of the entry period due to the early initiation of turbulent flow. Figure 2-5 shows the selected position on the vehicle.

The overall sound pressure levels predicted for the baseline Orbiter configuration are shown in Figure 2-6 for launch and ascent conditions. The full-scale subsize panel designs developed for Phase I tests were analyzed for resistance to fatigue failures at a maximum overall sound pressure level (OASPL) of 160 db in accordance with the predicted values for the Orbiter forward lower surface shown in Figure 2-6. The acoustic fatigue analysis conducted for the Phase I test panels (Reference 2, Appendix D) was reviewed during Phase II and the analytical results were found to be valid for Phase II panels due to similarity of design and test conditions. A duration of 30 seconds at 160 db during liftoff was selected as being the critical acoustic environment. Fatigue analyses were based on the 160 db level for 100 missions with a life factor of 10.

2.2 HEAT SHIELD ARRAY FOR CONTRACTOR TESTS

The contractor TPS tests were conducted in the Space Simulation Laboratory and the Acoustic and Vibration Laboratory at the McDonnell Douglas Test Laboratory complex at St. Louis. The Space Simulation Laboratory was used to apply programmed differential pressure load and temperature profiles in a reduced atmosphere test chamber. Such test profiles were applied in cycles to simulate repeated missions that would be experienced by the TPS on the selected lower surface area of the Orbiter. Acoustic loadings were applied separately in the Acoustic Laboratory. To eliminate disassembly and reassembly of the heat shield array when it was moved from one laboratory to the other, the test fixture was designed to be mounted in either laboratory.

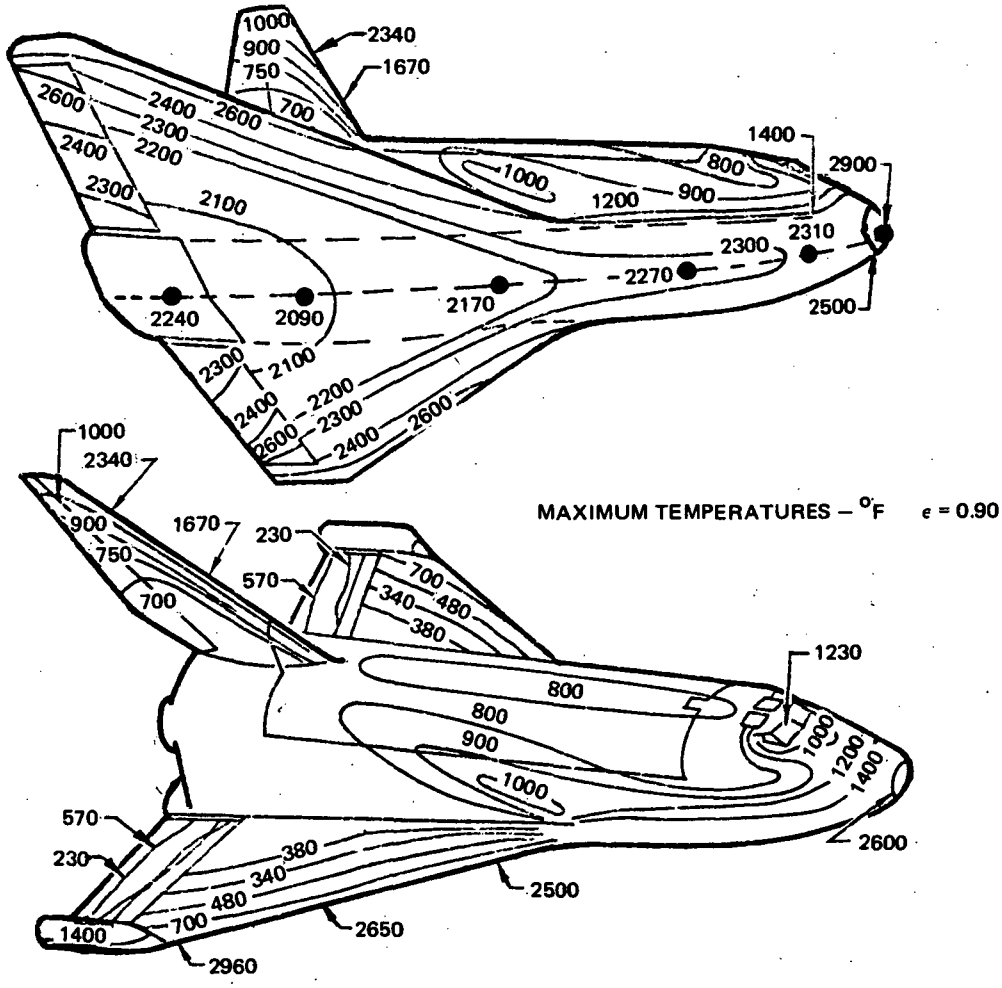

Figure 2-4. Maximum Temperatures During Critical Entry Trajectory

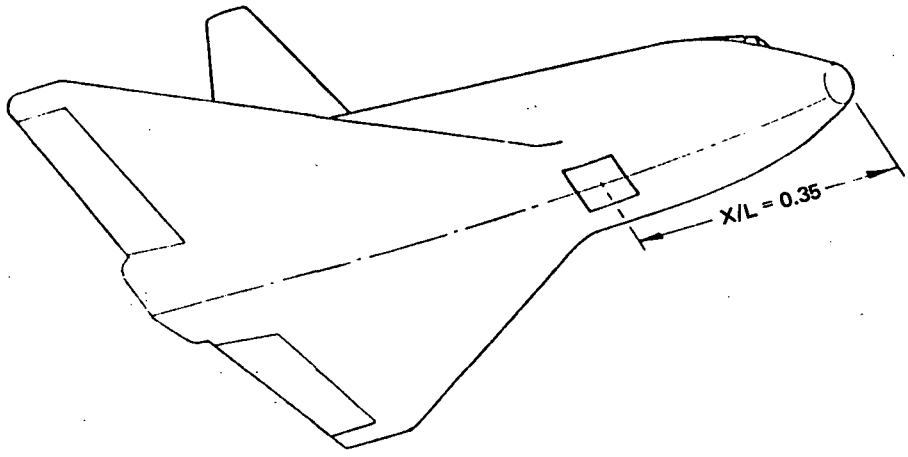

Figure 2-5. Orbiter Surface Area for TPS Study

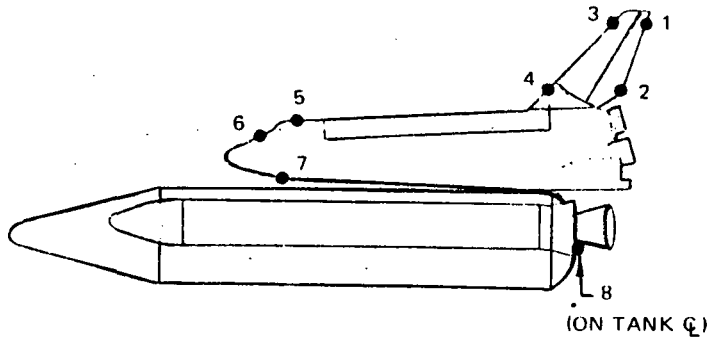

	OVERALL SOUND PRESSURE LEVEL (dB)		
	LAUNCH*	ASCENT**	
1	164.6	161	
2	165.9	161	*BASED ON TEST
3	163.6	155	FIRINGS OF SATURN
4	163.3	146	J-2 ENGINES AT
5	158.2	161	NASA-MSFC
6	157.6	148	
7	158.0	160	**BASED ON AMES WIND
8	165.0	153	TUNNEL TEST DATA

Figure 2-6. Orbiter Overall Sound Pressure Levels

The heat shield array tested at the McDonnell Douglas laboratories was designed to fit a test fixture with a 78.5 cm by 128.2 cm (30.9 in by 50.5 in) opening. The complete test fixture consisted of two halves, the upper half forming a holding frame in which the TPS components were mounted and the lower half forming a mating closed cavity that contained the quartz lamp heating units. The test fixture upper half is seen in Figure 2-7, which shows the low-density fibrous insulation packages that were mounted in the upper portion of the fixture between the heat shield panels and the simulated substructure. Although not shown in Figure 2-7, an aluminum simulated substructure was also mounted on the upper half of the test fixture. The lower half of the fixture formed a closed cavity containing three groups of quartz lamps. The three groups of quartz lamps, each covering approximately one-third of the heat shield array surface area, were controlled separately to provide relatively uniform temperatures over the test array. The lower half of the test fixture is shown in Figure 2-8. The heat shield, cover strips, and edge seals formed a continuous surface at the intersection of the two

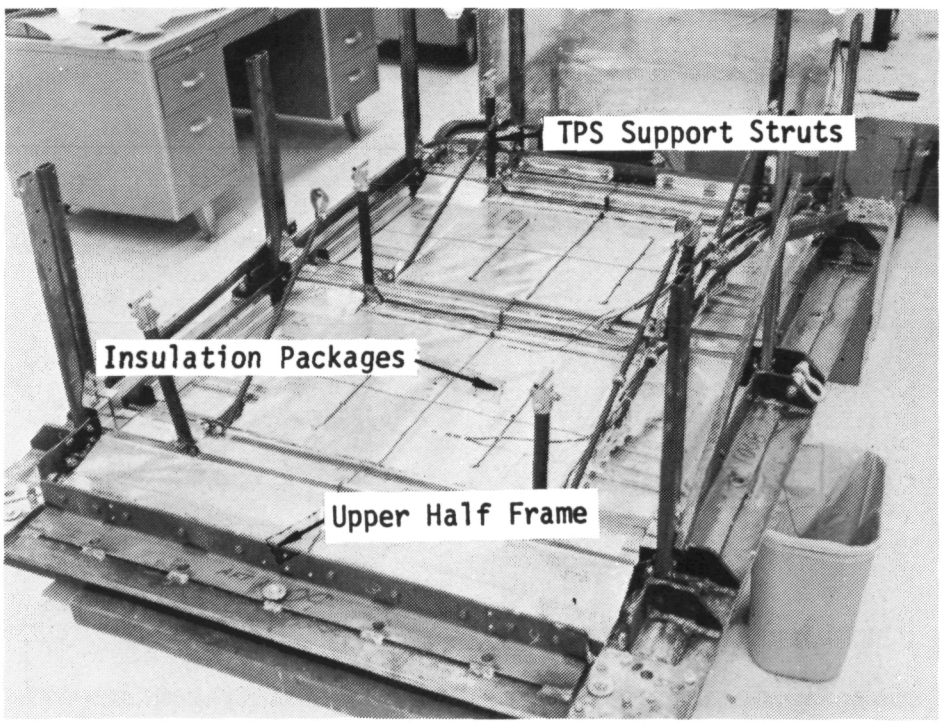

Figure 2-7. Upper Half of Contractor TPS Test Fixture

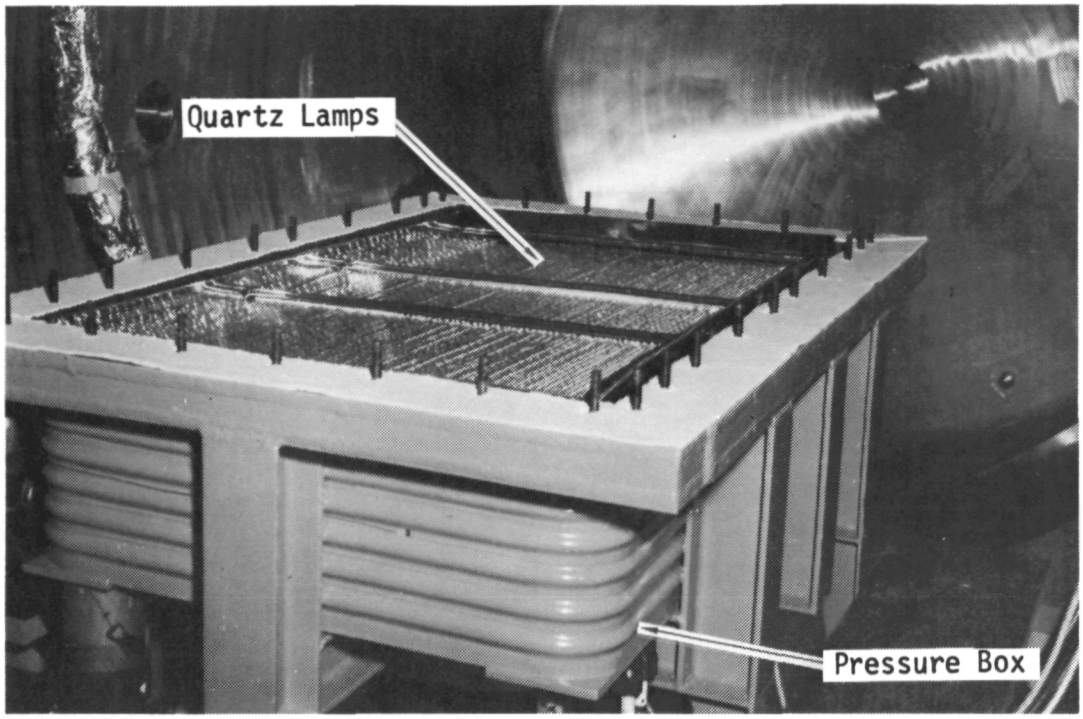

Figure 2-8. Lower Half of Contractor TPS Test Fixture

halves of the test fixture, and in this manner allowed programmed differential pressure loads to be applied to the heat shields by adjusting the pressures in the main test chamber and in the closed half of the test fixture. The test fixture halves, TD Ni-20Cr heat shield array, insulation packages, and simulated aluminum substructure are shown schematically in Figure 2-9.

2.2.1 TPS Design Configuration

The basic TPS concept, derived in Phase I and developed to a full-scale, full-size array in Phase II, consisted of discrete panels attached to a TD Ni-20Cr support structure in a manner to permit expansion between panels at elevated temperatures and thus to minimize the effects of thermal stresses. Floating nutplates were used to provide the required expansion for each panel. For contractor tests, the TD Ni-20Cr heat shield panel array consisted of two main test panels, four side close-out panels, two end close-out panels, and cover strips to span the gaps between panel edges. Support beams and fasteners were also made from TD Ni-20Cr material, as were the seal strips used at the edges of the holding fixture.

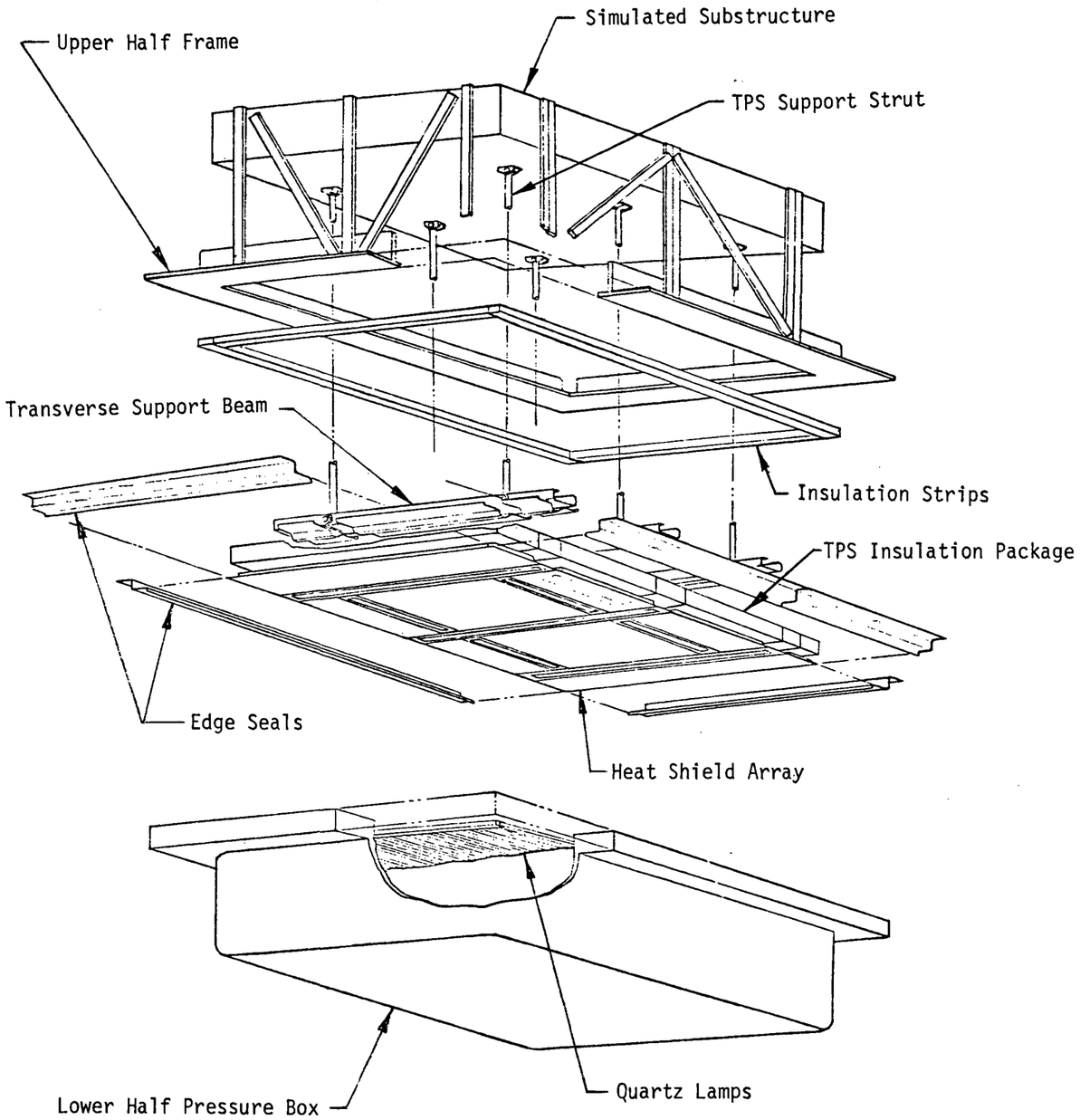

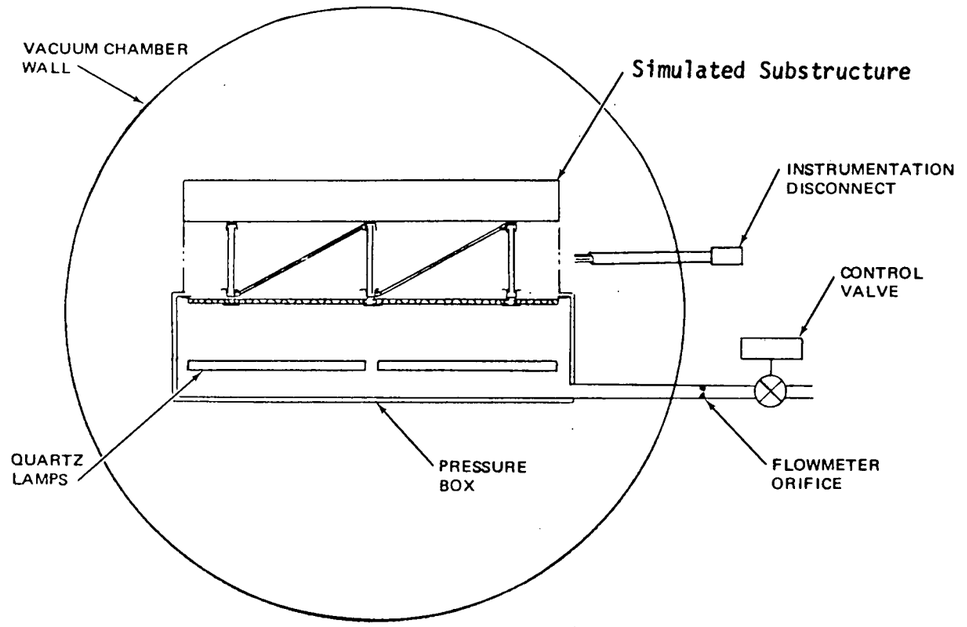

Test Array and Fixture in Space Simulation Chamber

Figure 2-9. Schematic of Contractor TPS and Test Fixture

The complete TPS array, shown in Figure 2-10, was composed of the external heat shields and cover strips, the support beams, standoff struts, foil-enclosed insulation packages, and a simulated aluminum substructure. As shown in Figure 2-9, the substructure was mounted to the test fixture frame by a series of struts at the frame periphery. The TD Ni-20Cr support beams were in turn mounted to the substructure by a series of struts that penetrated the insulation packages at discrete points. Attachment of the panels, cover strips, and insulation packages completed the upper half of the test assembly except for installation of the TD Ni-20Cr edge seals. The latter members were used to provide an overlapping set of seals to close the gap between the close-out panels and the internal edges of the test fixture frame. Cross-sectional details and overall dimensions of the TPS components are also shown in Figure 2-10.

The nominal thickness of all panels was 2.54 cm (1.0 in). Formed beads were incorporated in the face sheets of all main test panels and in a majority of the closeout panels with the design objective of permitting controlled deformation in the panel surfaces at elevated temperature conditions. The outward projecting beads added approximately 0.25 cm (0.10 in) to the panel thickness at their maximum height. A continuous corrugation was spot-welded to the inner surface of the face sheet to provide bending and torsional strength in the panels. The ends of the panels were closed off with zee-shaped stiffening members made from 0.0508 cm (0.020 in) thick TD Ni-20Cr sheet. The panel lateral edges were reinforced by the corrugation terminations which mated with the face sheet edges. The face sheet and corrugation edges were spot-welded together, and a formed lip at the panel edge provided additional stiffness.

Transverse beams made of 0.102 cm (0.040 in) thick TD Ni-20Cr formed sheet were located at the panel ends and provided the basic support members to which the panels were attached. Pan head TD Ni-20Cr bolts of 0.635 cm (0.25 in) diameter were used to attach the panels to floating nuts that were also made from TD Ni-20Cr and were mounted on the transverse beams. Support struts made from L605 cobalt alloy were used to attach the support beams to the

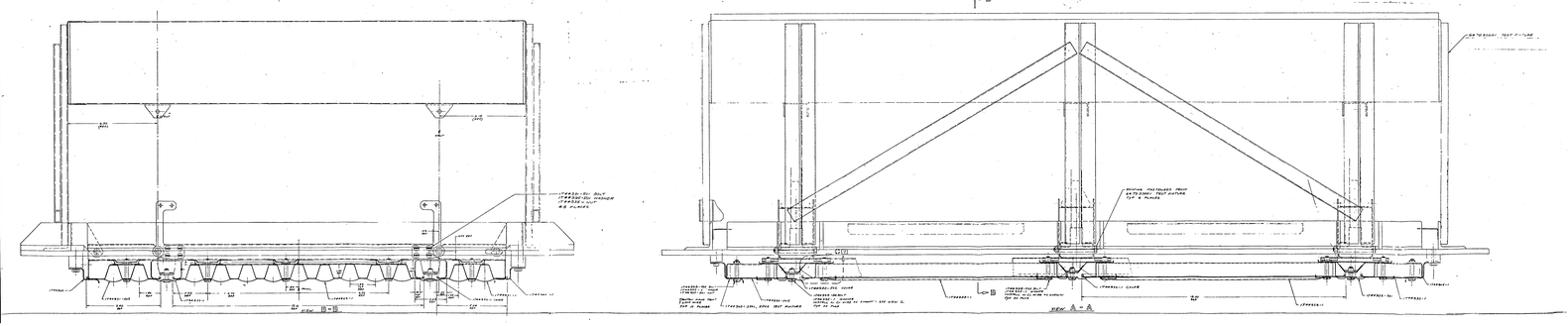

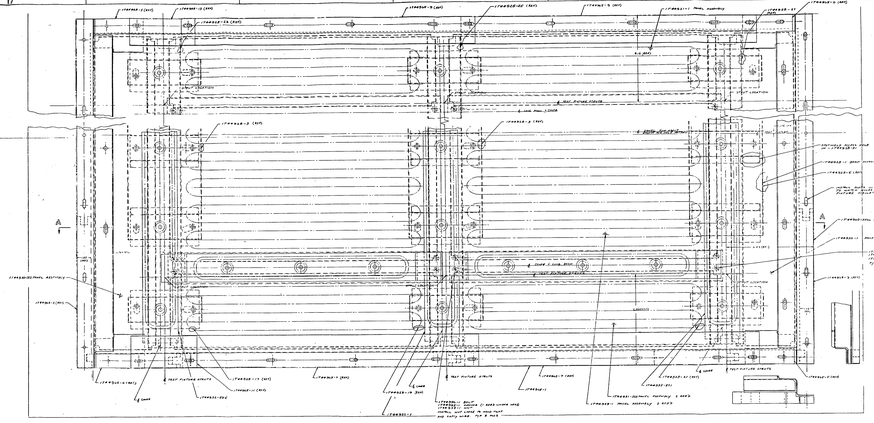

Figure 2-10. Contractor TPS Test Array Design.

Page intentionally left blank

simulated aluminum substructure. Diagonal struts braced the support structure in a longitudinal direction, while the segmented transverse beams were allowed to expand in a lateral direction through use of slotted holes at one end of each beam where it was attached to the test fixture.

Packages of low-density insulation with a nominal thickness of 6.35 cm (2.50 in) were located between the heat shield panels and the substructure. The insulation was enclosed in a metallic foil package made of 0.0102 cm (0.004 in) thick Hastelloy X. Five 1.27 cm (0.50 in) thick layers of insulation made up the total insulation thickness, the outer (hottest) layer being 192.2 kg/m^3 (12 lb/ft^3) Dynaflex and the inner four layers being 56.0 kg/m^3 (3.5 lb/ft^3) Microquartz. As shown in Figure 2-7, a number of insulation packages were used to fill the space beneath the heat shield array. The largest packages were located beneath the main test panels and smaller packages were mounted beneath the support beams and under the closeout panels.

Each of the main test panels was attached with a total of six bolts, one bolt providing a fixed location point for the panel and the others allowing expansion of the panel in radial directions from the fixed point.

Closure strips were mounted independently from the heat shield panels at all four edges so that the strips overlapped the edges of adjacent panels and closed off the expansion space provided between panels. The closure strips were formed from 0.0508 cm (0.020 in) thick TD Ni-20Cr sheet, and, like the heat shield panels, were attached to floating nuts mounted on the support beam so that expansion of the closure strips could occur without restraint along the length of the strips when they were at elevated temperatures.

The external surface of the heat shield panels are shown in Figure 2-11 while the interior sides of the panels are seen in Figure 2-12. The panels are shown in Figures 2-11 and 2-12 prior to preoxidation, a process used to produce a dark, high-emittance surface on the panels and cover strips. Figure 2-13 shows the support beams mounted in a mockup of the test fixture before

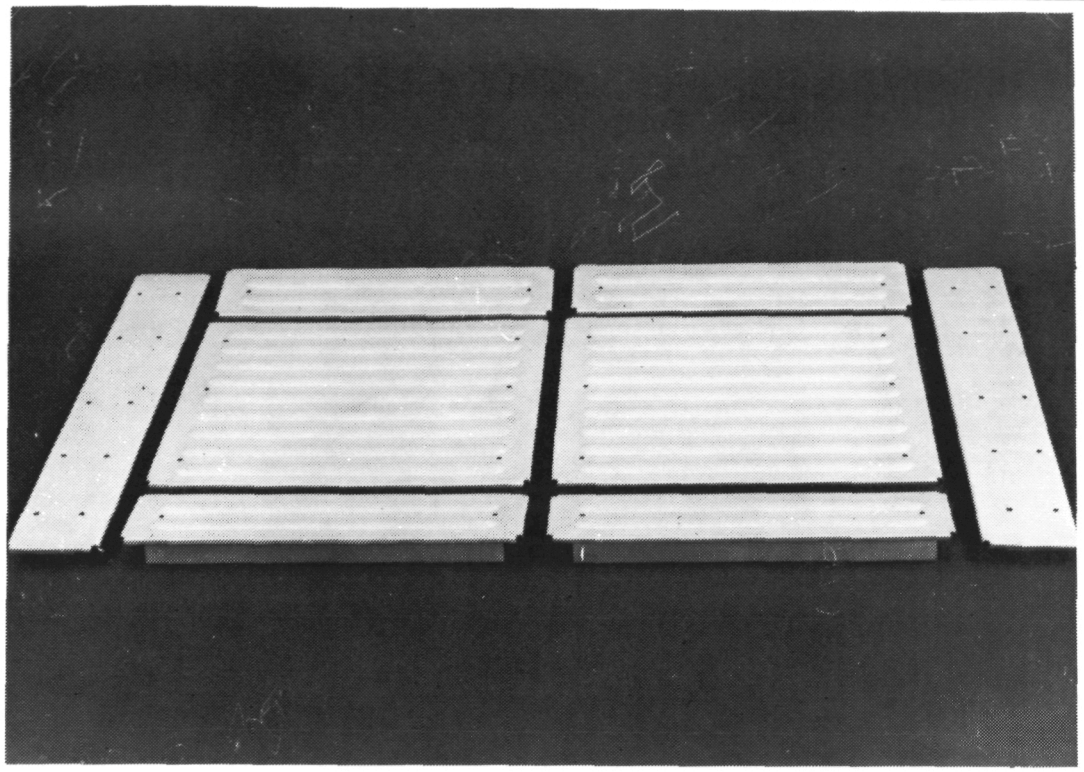

Figure 2-11. Completed TD Ni-20Cr Heat Shield Panels – Outer Surface

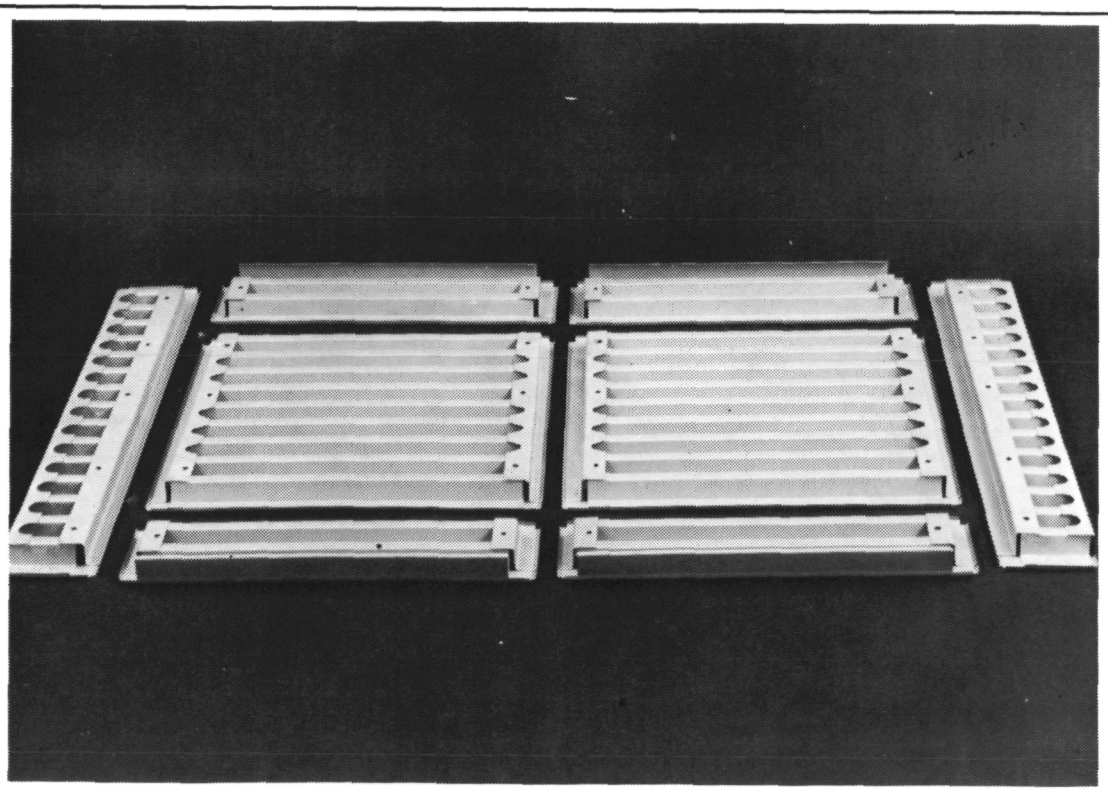

Figure 2-12. Completed TD Ni-20Cr Heat Shield Panels – Inner Surface

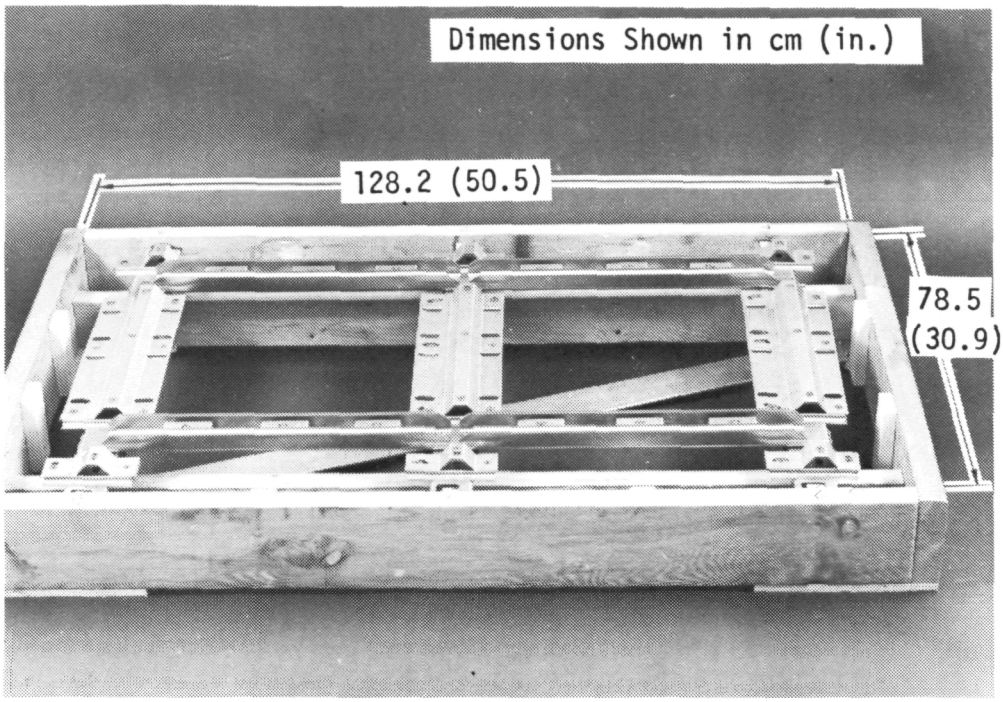

Figure 2-13. Completed Support Beam Assembly

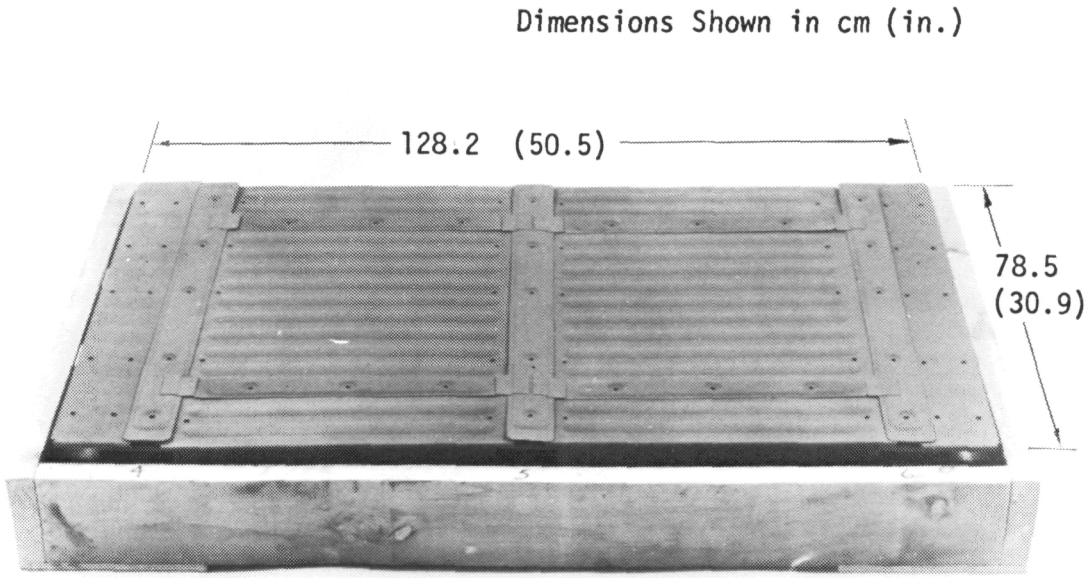

Figure 2-14. Pre-Oxidized Panels in Place on Support Beams

installation of the surface panels, and Figure 2-14 shows the panels and cover strips in position on the beams before the fasteners were installed. As seen in Figure 2-14, the surface components had been preoxidized before installation on the mockup.

Unit weights for the contractor test array were derived from actual weights of the TD Ni-20Cr components combined with computed weights of the insulation packages. Actual component weights and weight per unit area are presented in Table 2-1.

Since the support system and insulation depths required for the HTST and TPSTF arrays differed from those of the contractor test array, the unit weights were slightly different for each of the remaining TPS arrays. Such differences are discussed subsequently in Section 2.3 and 2.4.

As a result of Phase I evaluations a braze-reinforced panel was included in the Phase II contractor test array. Evaluations of braze-reinforced spotwelded samples conducted in Phase I showed improved fatigue life (Reference 2) for braze-reinforced joints when compared to simple spotwelded joints. Such evaluations led to the decision to test one of the side close-out panels as a braze-reinforced panel in the contractor TPS tests. A spare side close-out panel was therefore fabricated to the same configuration as the basic design with the exception that its spotwelded areas were braze-reinforced and the panel fasteners were recessed in a full-depth pocket. The latter feature, shown in Figure 2-15, was incorporated in the braze-reinforced panel to assess the thermal effects of an attachment system with a smaller mass and with a fastener that did not act as a conductive path from the outer surface to the interior of the heat shield panel.

The braze-reinforced panel was fabricated at MDAC facilities up to the point of actual brazing. Initial fabrication at MDAC included manufacture of detail parts, cleaning, emplacement of braze alloy, and assembly by spotwelding. The panel was then shipped to the Langley Research Center where brazing and pre-oxidation processes were accomplished. The panel was shipped subsequently

Table 2-1

TPS WEIGHTS OF CONTRACTOR TEST ARRAY

NOTE: See Figure 2-10 for TPS Description

COMPONENT	WEIGHT kg (lb)	UNIT WEIGHT kg/m^2 (lb/ft^2)
MAIN PANEL	1.420 (3.13)	5.78 (1.185)
LATERAL COVER STRIP	0.236 (0.52)	0.96 (0.197)
LONGITUDINAL COVER STRIP	0.095 (0.21)	0.39 (0.080)
SUPPORT BEAM	1.175 (2.59)	4.79 (0.981)
EDGE CHANNEL	0.377 (0.83)	1.53 (0.314)
PANEL ATTACH BOLTS	0.095 (0.21)	0.39 (0.079)
COVER STRIP BOLTS	0.196 (0.43)	0.79 (0.163)
INSULATION PACKAGE(1)	2.330 (5.14)	9.49 (1.945)
INSULATION ATTACH	0.091 (0.20)	0.37 (0.076)
	TOTAL	24.49 (5.020)

(1) Insulation Thickness: 6.35 cm (2.50 in).

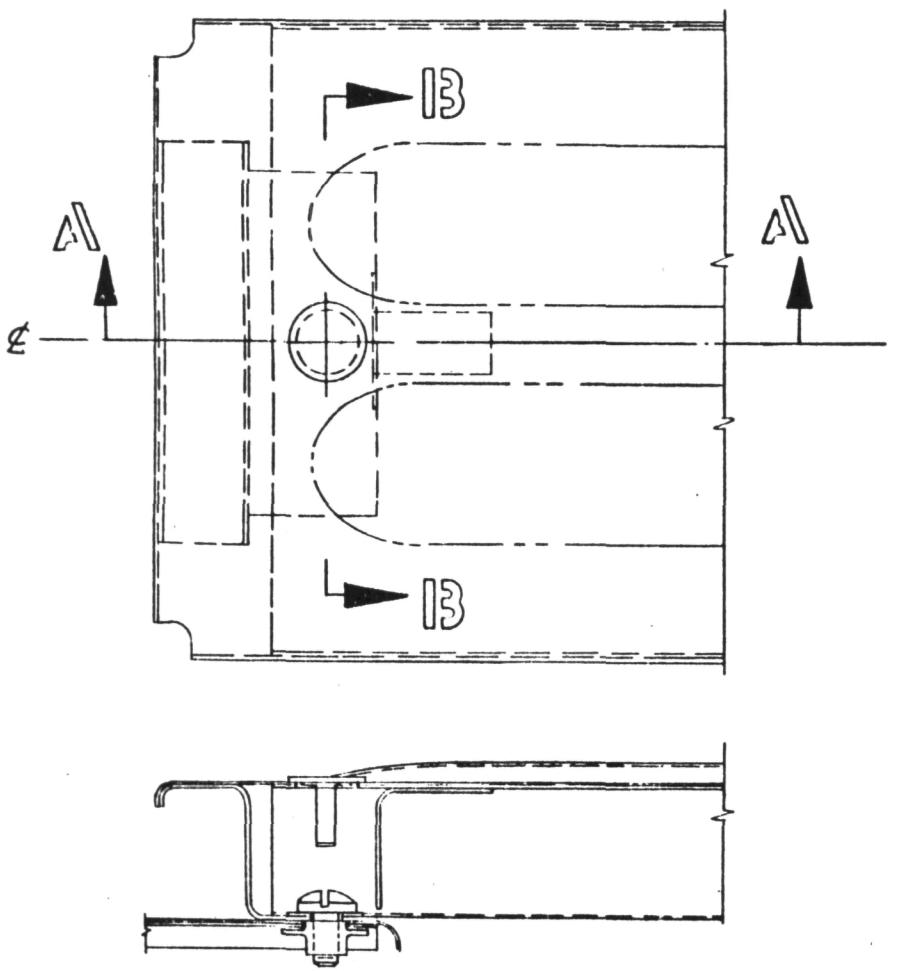

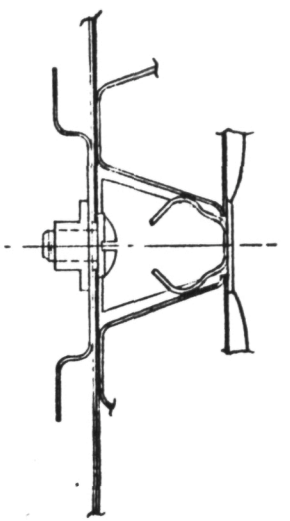

Figure 2-15. Panel Fastening Design for Braze-Reinforced Panel

from Langley Research Center to MDAC facilities at St. Louis. It was then installed in the test array as a replacement component for a spotwelded panel.

The braze-reinforced panel is shown in Figure 2-16 before being subjected to the brazing cycle, and Figure 2-17 shows the panel after brazing but before it was grit-blasted and pre-oxidized. Figure 2-18 shows the panel appearance after completion of pre-oxidation processes. The light areas seen in Figure 2-18 indicate the extent of the brazed areas in the faying surfaces of the panel. The lighter areas seen in Figure 2-18 were not as clearly discernible by visual inspection alone and the different shadings seen in the photographs of the panel are believed to be the result of slightly different oxide formations that occurred in the brazed regions during pre-oxidation of the panel. Such differences in the oxide were judged to be caused by lower temperatures locally in the brazed areas due to the larger thermal mass of the braze alloy. No thermocouples were attached to the panel during pre-oxidation and thus temperature variations that are judged to have existed were not verified during pre-oxidation processing. However, oxide formations

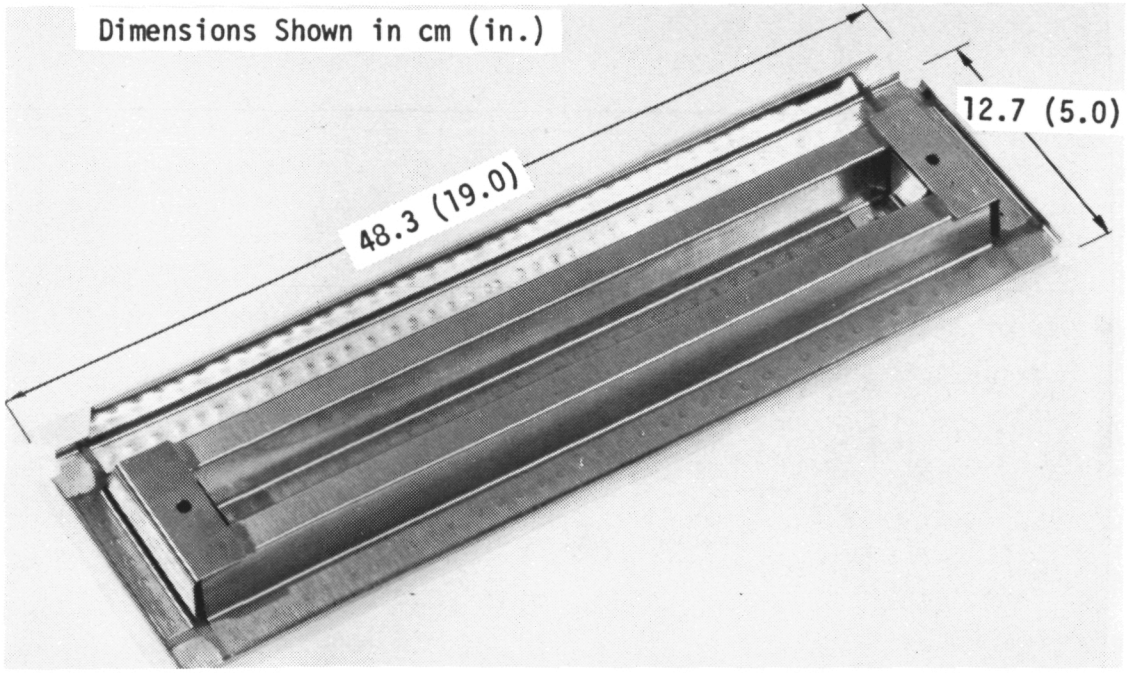

Figure 2-16. Braze-Reinforced Panel Prior to Brazing Cycle

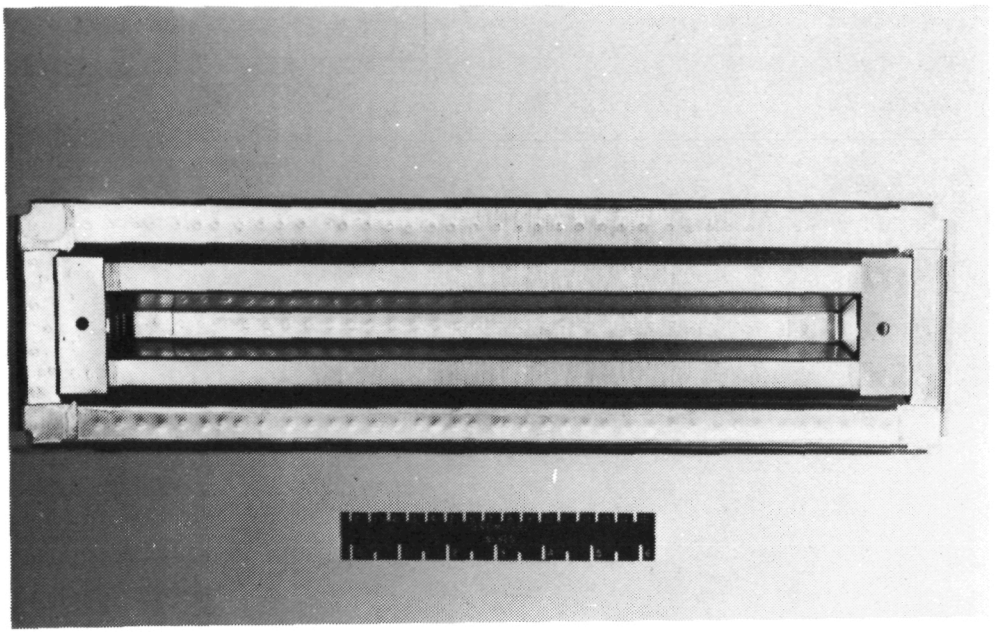

Figure 2-17. Braze-Reinforced Panel After Brazing Cycle

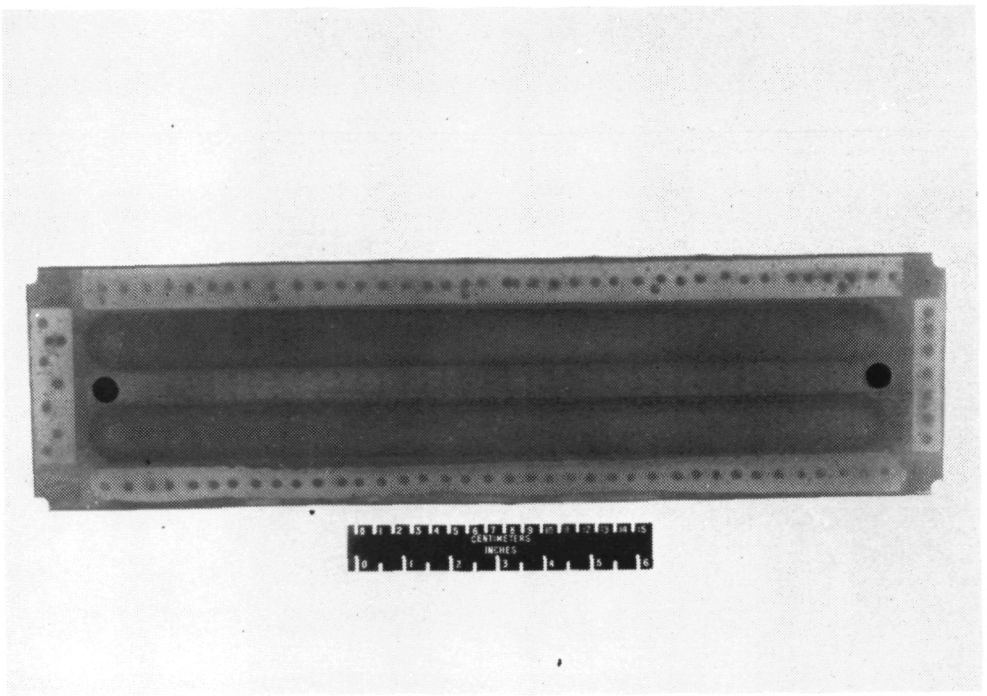

Figure 2-18. Braze-Reinforced Panel After Pre-Oxidation Cycle

have been shown to be a function of temperature in nickel-chromium alloys (Reference 5), and differences in shading or coloration have been shown to occur when different oxides are formed on nickel-chromium alloys.

2.2.2 Design Criteria and Analyses

The criteria developed in Phase I were applied to the full-size, full-scale heat shield arrays designed for Phase II tests. Specific criteria, presented in Reference 2, are summarized here for clarity and convenience. TPS design criteria included effects of differential pressure loads, acoustic loads, panel flutter, meteoroid impact, creep, and thermal stresses. The basic criteria used for Phase II heat shield designs are summarized in Table 2-2. While test facility environments differed for the three test arrays, each facility environment was checked for compatibility with the basic design criteria derived from the Orbiter mission environments. Such checks showed that normal facility operations did not exceed the TPS design conditions.

Allowable stresses, also derived in Phase I, were based on cyclic stress and temperature evaluations conducted as a part of Phase I efforts. Data from References 3 and 4 were also used extensively in developing TD Ni-20Cr material allowables during Phase I. Phase I test results confirmed the basic panel design for the corrugation-stiffened single-face configuration in terms of creep resistance and overall panel strength under acoustic, thermal, and pressure loads simulating 100 missions. However, considerable panel face sheet cracking occurred at the fastener positions in Phase I tests. Such cracking was judged to occur as a result of both acoustic load and thermal stress effects. The panel design for Phase II therefore employed the same basic cross-section, but the panel fasteners and attachment details were revised to increase the strength at and near the panel attach points.

The contractor TPS panels were analyzed for thermal and mechanical stresses at several points on the main panel using the criteria developed in Phase I. Temperature time-histories of several areas were used to define thermal stresses in the panels at critical time points in the test cycle and the thermal and mechanical stresses were then combined according to criteria

Table 2-2

SUMMARY OF HEAT SHIELD DESIGN CRITERIA

Mission Phase	Limit Differential Pressure (psi)	Overall Sound Pressure Level	Panel Flutter	Meteoroid Impact	Cumulative Creep In 100 Missions cm (in.)	Factor of Safety(1)
Boost Flight	+3.30 (Collapse) -1.00 (Burst)	160 db	No flutter at 1.5 times local dynamic pressure.	--	--	1.50
Orbital Mission	--	--	--	Designed for a 0.95 probability of one or less puncture in a 7-day mission.	--	--
Entry Flight	+0.50 (Collapse) -0.50 (Burst)	--	Same as Boost Flight	--	$\delta = 0.254 + 0.0254\ L$ ($\delta = 0.10 + 0.01L$) (See Section 2)	1.50

taken from Appendix A of Reference 2. In accordance with the referenced criteria, external mechanical and thermally induced loads or stresses were combined in the following manner:

$$K_1 L_{ext} + K_2 L_{ther} \geq 1.40\ \Sigma L \qquad (1)$$

where

K_1, K_2 = Ultimate to limit ratios for external and thermal loads respectively.

L_{ext} = Mechanical externally applied loads; e.g., inertial loads.

L_{ther} = Thermally induced loads.

K_1 = 1.4 for boost conditions when the term is additive to the algebraic sum, ΣL

K_1 = 1.5 for entry, atmospheric cruise, and landing when the term is additive to the algebraic sum, ΣL

K_2 = 1.5 when the term is additive to the algebraic sum, ΣL

K_1, K_2 = 1.0 when the term is subtractive to the algebraic sum, ΣL

Using the above criteria, critical heat shield stresses were determined for the contractor TPS array in several different locations.

The programmed differential pressure loads and external surface temperatures for contractor tests, presented in Figure 2-19, were used to develop panel temperature time-histories and to evaluate the combined effects of thermal and mechanical stress levels at three places on a typical full-size panel. The programmed test temperature profile was also used to develop internal temperature time-histories for the test array insulation package and substructure. Temperature time-histories at points through the TPS and substructure are shown in Figure 2-20. In the temperatures of Figure 2-20, an initial run in a series was assumed so that external surface temperatures were at room temperature at the start of the test run.

Panel temperature distributions were evaluated in three areas, one area being at the center of a main panel, a second being at the panel edge at midspan, and a third at the panel edge near the support struts. Such areas corresponded closely to thermocouple locations of the instrumented TPS array

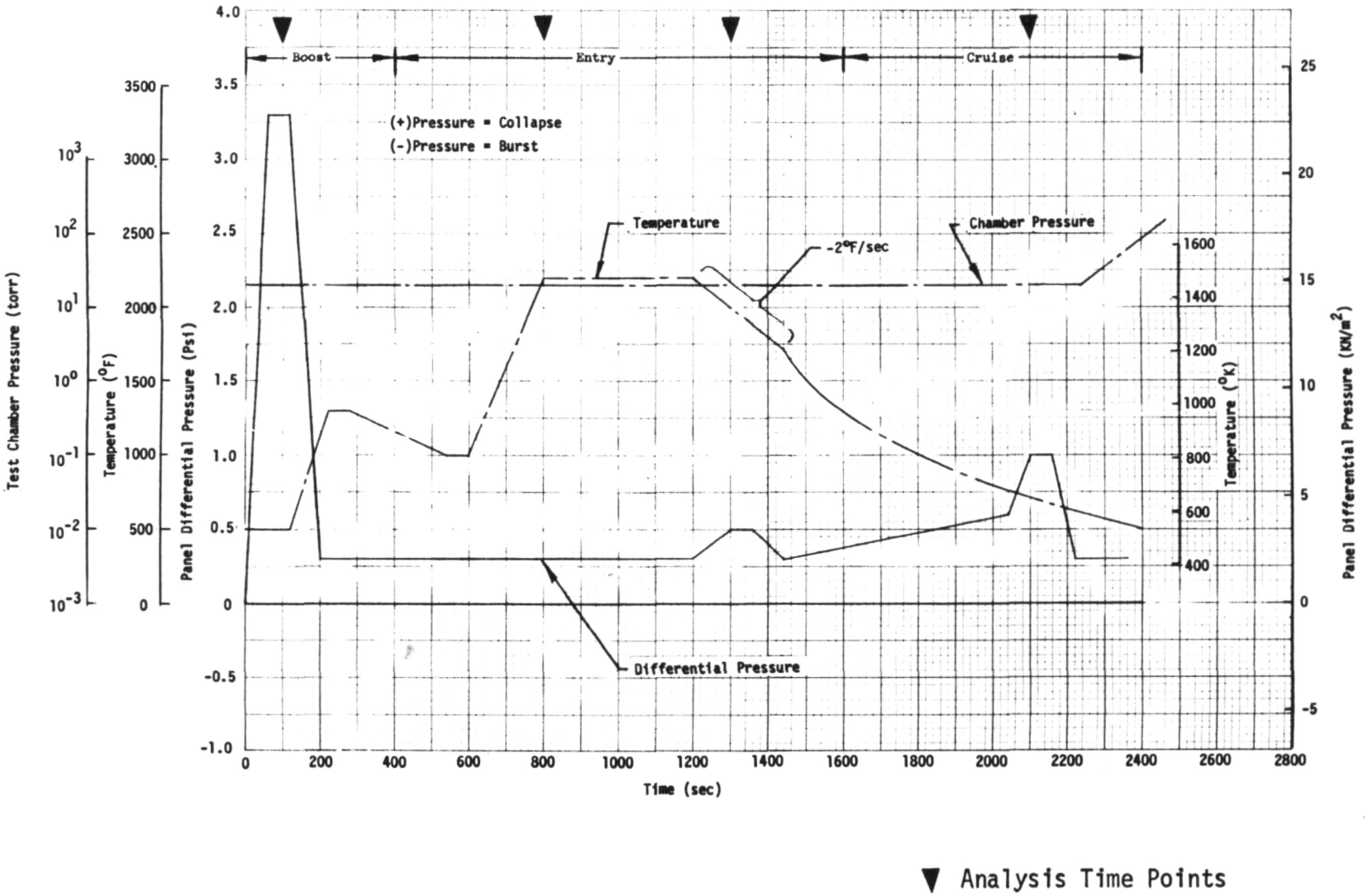

Figure 2-19. Programmed Temperatures and Differential Pressures for Contractor Test Array

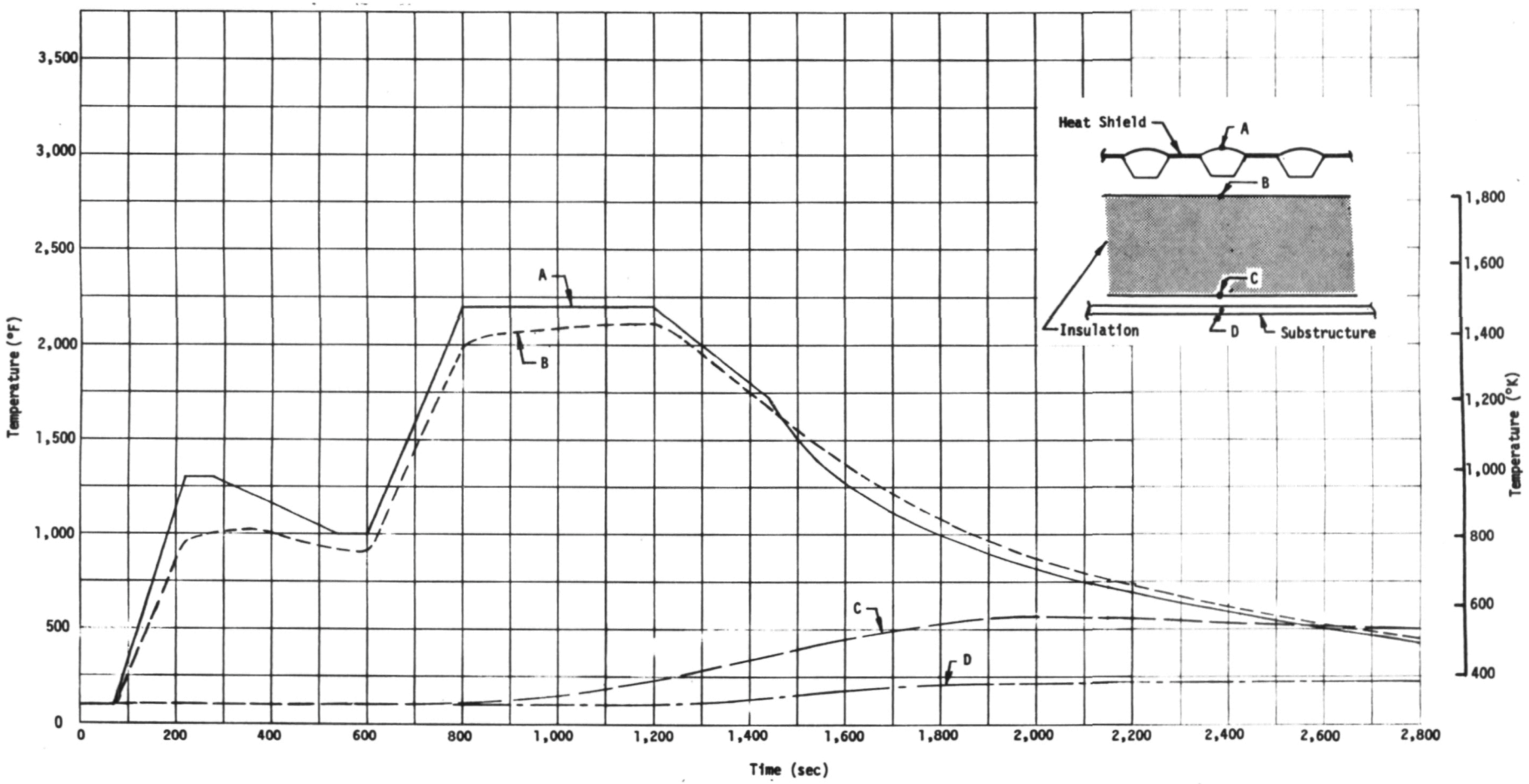

Figure 2-20. Projected Temperature Time-Histories; Contractor Test Array

(see Section 3.0) tested in the Space Simulation Laboratory. Typical temperatures at two locations are shown in Figures 2-21 and 2-22. Four time points were selected in the simulated mission test profile as being critical for thermal and aerodynamic load conditions. The selected times included a point in the boost flight where maximum aerodynamic loads are experienced, a point in the entry flight where surface temperatures have reached a maximum, a point shortly after the start of external surface cooldown from maximum temperature conditions, and a point in the cruise portion of the entry flight where external surface temperatures have decreased at the same time that internal temperatures are still near a maximum. The latter time point also coincided with the period in the cruise flight when aerodynamic loads were at a maximum in the simulated mission profile. The time points selected for panel analysis are noted in Figure 2-19.

Panel stresses were analyzed in the selected panel areas at the four time points and combined according to the previously described criteria. The resultant stresses and margins of safety are summarized in Table 2-3. Critical stresses occurred at two of the four selected time points, the two critical conditions occurring during the simulated boost portion of the test profile and at the point during the simulated entry portion of the test where the heat shield temperature first reaches 1,478°K (2,200°F).

Test results are discussed subsequently in Section 3.0, and comparisons with panel analyses are made at that point.

2.3 TEST ARRAY FOR THE HIGH TEMPERATURE STRUCTURES TUNNEL

The 8-ft. HTST test array was the largest of the three TPS arrays constructed during Phase II. Overall planform dimensions of the array were 108 cm by 152.4 cm (42.5 in. by 60.0 in.) with the larger dimension being parallel to the tunnel flow. While a more detailed description of the 8-ft. HTST may be found in Reference 6, a brief description is given here to indicate general test conditions for the HTST array.

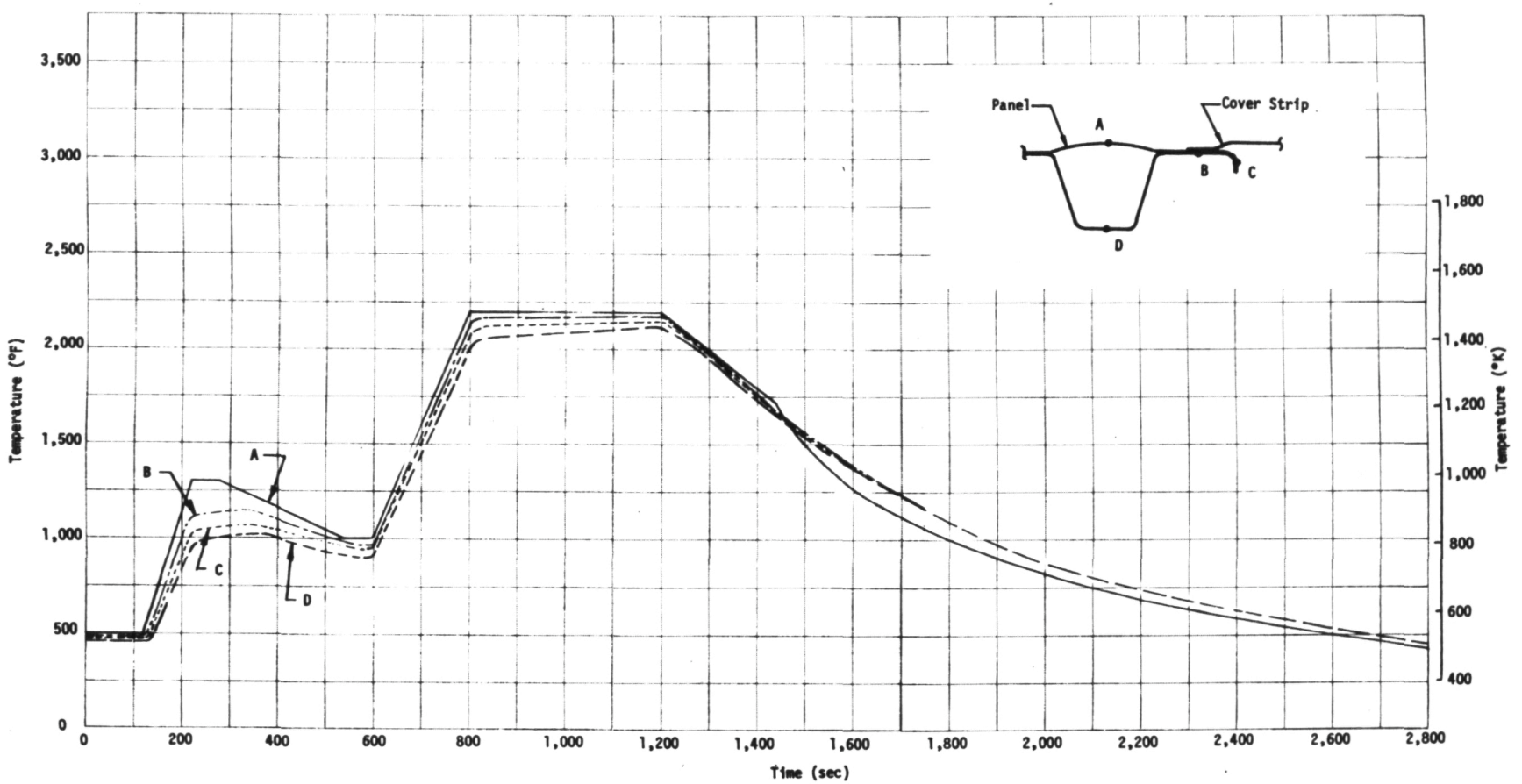

Figure 2-21. Projected Temperature Time-Histories at Panel Edge; Midspan Location

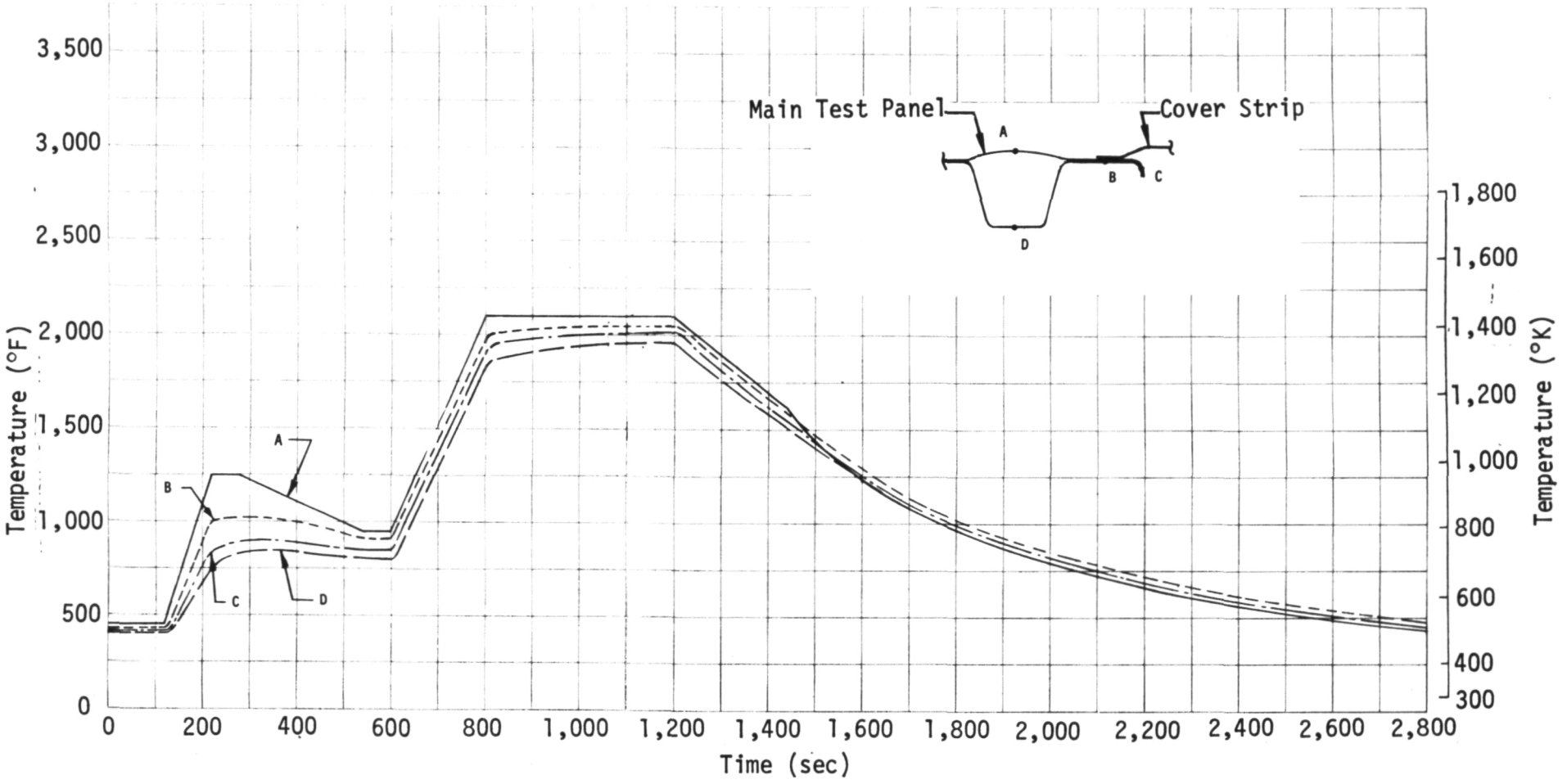

Figure 2-22. Projected Temperature Time-Histories at Panel Edge Near Support Strut

Table 2-3

Contractor Test Array Panel Stresses

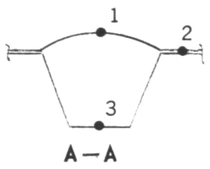

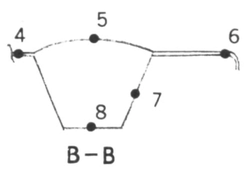

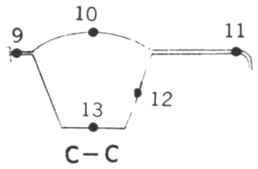

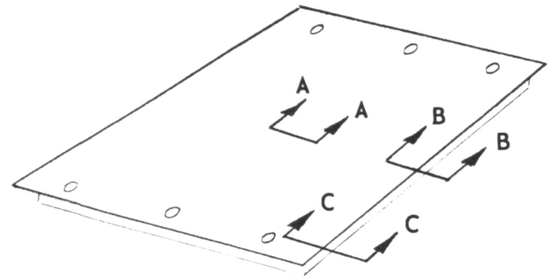

		t = 100 sec			t = 800 sec			t = 1300 sec			t = 2100 sec		
	Panel Ref. Point	Stress MN/m^2 (psi)	Temperature °K (°F)	Margin of Safety	Stress MN/m^2 (psi)	Temperature °K (°F)	Margin of Safety	Stress MN/m^2 (psi)	Temperature °K (°F)	Margin of Safety	Stress MN/m^2 (psi)	Temperature °K (°F)	Margin of Safety
Panel Center	1	-162.0 (-23,500)	533 (500)	.06	36.2 (5,245)	1,477 (2,200)	.98	20.5 (2,945)	1,368 (2,000)	2.90	-12.7 (-1,840)	672 (750)	HIGH
	2	-80.6 (-11,700)	528 (490)	4.21	31.1 (4,510)	1,468 (2,180)	1.30	-10.2 (-1,480)	1,358 (1,980)	HIGH	-16.3 (-2,360)	675 (755)	↓
	3	269.0 (39,000)	486 (415)	1.54	-76.8 (-11,150)	1,368 (2,000)	.03	-9.23 (-1,340)	1,349 (1,965)	8.31	27.2 (3,940)	697 (795)	↓
Panel Edge, Midspan	4	-77.5 (-11,250)	528 (490)	5.42	32.2 (4,660)	1,468 (2,180)	1.04	-8.1 (-1,175)	1,358 (1,980)	HIGH	27.8 (4,030)	661 (730)	HIGH
	5	-111.3 (-16,140)	533 (500)	.55	41.4 (5,995)	1,477 (2,200)	.52	22.4 (3,245)	1,368 (2,000)	2.54	-8.93 (-1,295)	672 (750)	↓
	6	-61.7 (-8,950)	525 (485)	6.48	16.6 (2,410)	1,416 (2,090)	3.06	-20.5 (-2,980)	1,349 (1,965)	7.06	-10.02 (-1,455)	680 (765)	↓
	7	59.0 (8,550)	519 (475)	HIGH	-21.9 (-3,170)	1,410 (2,080)	1.72	-5.45 (-790)	1,351 (1,970)	HIGH	-27.4 (-3,980)	703 (805)	5.28
	8	193.1 (28,000)	511 (460)	2.50	-66.5 (-9,650)	1,373 (2,015)	.06	9.03 (1,310)	1,333 (1,940)	9.00	25.0 (3,630)	709 (815)	HIGH
Panel Edge, Near Attach Point	9	-11.38 (-1,650)	494 (430)	HIGH	29.0 (4,200)	1,382 (2,030)	1.45	31.0 (4,500)	1,304 (1,885)	2.13	-5.17 (-750)	678 (760)	↓
	10	-50.7 (-7,350)	505 (450)	2.61	63.1 (9,150)	1,427 (2,105)	.09	2.07 (300)	1,316 (1,905)	HIGH	-1.03 (-150)	672 (750)	↓
	11	-1.04 (-150)	491 (425)	HIGH	-18.6 (-2,700)	1,351 (1,975)	7.52	10.35 (1,500)	1,245 (1,780)	↓	35.2 (5,100)	675 (755)	↓
	12	33.1 (4,800)	486 (415)	↓	-27.9 (-4,050)	1,318 (1,910)	1.96	-13.45 (-1,950)	1,238 (1,765)	↓	-13.45 (-1,950)	686 (775)	↓
	13	40.4 (5,850)	477 (400)	↓	-55.9 (-8,100)	1,281 (1,845)	1.94	-36.2 (-5,250)	1,139 (1,690)	2.08	-15.51 (-2,250)	689 (780)	↓

The 8-ft. HTST, shown schematically in Figure 2-23, is a hypersonic blowdown wind tunnel that operates at a nominal Mach number of 7, at total pressures between 3.4 and 24.1 MPa (600 and 3,500 psia), and at nominal total temperatures between 1,400°K and 2,000°K (2,040°F and 3,140°F). The corresponding free-stream unit Reynolds numbers are between 1×10^6 and 10×10^6 per meter (0.3×10^6 and 3.0×10^6 per foot). These test stream conditions simulate the aerothermal flight environment at Mach 7 in the altitude range between 25 and 40 km (80,000 and 130,000 ft.). The test simulation envelope is shown in Figure 2-24 in terms of altitude and velocity, and a typical Shuttle Orbiter velocity-altitude entry band is also shown for comparison with the simulation envelope. As shown in Figure 2-24, the Orbiter entry flight conditions are simulated by the 8-ft. HTST at an equivalent altitude of approximately 40 km (130,000 ft.).

The test medium in the HTST consists of the products of combustion of a mixture of methane and air which is burned within a pressurized combustion chamber. The combustion products are then expanded to the test-section Mach number by means of an axisymmetric contoured nozzle having an exit diameter of 2.4 m (8 ft.). In the test section, the stream is a free jet with a usable test core approximately 1.2 m (4 ft.) in diameter over a length of 4.3 m (14 ft.). The stream leaves the test section through a straight tube diffuser where it is pumped to the atmosphere by means of a single-stage annular air ejector. Stagnation temperature is controlled by regulating the fuel-to-air ratio.

A cross-sectional view showing the two basic positions of the test array holder is shown in Figure 2-25. The test array and holder are kept out of the stream until hypersonic flow conditions are established. If required, the test array may be pre-heated by quartz-lamp units prior to insertion in the test stream. The holder and test array are inserted rapidly into the stream on an elevator and programmed through a predetermined sequence of events to simulate the desired test profile. The holder and array are withdrawn from the stream prior to tunnel shutdown at the end of a test. A closed panel separates the test array from the test section during tunnel startup and shutdown to prevent excessive differential pressures on the test array. Overall dimensions of the test array holder are shown in Figure 2-26.

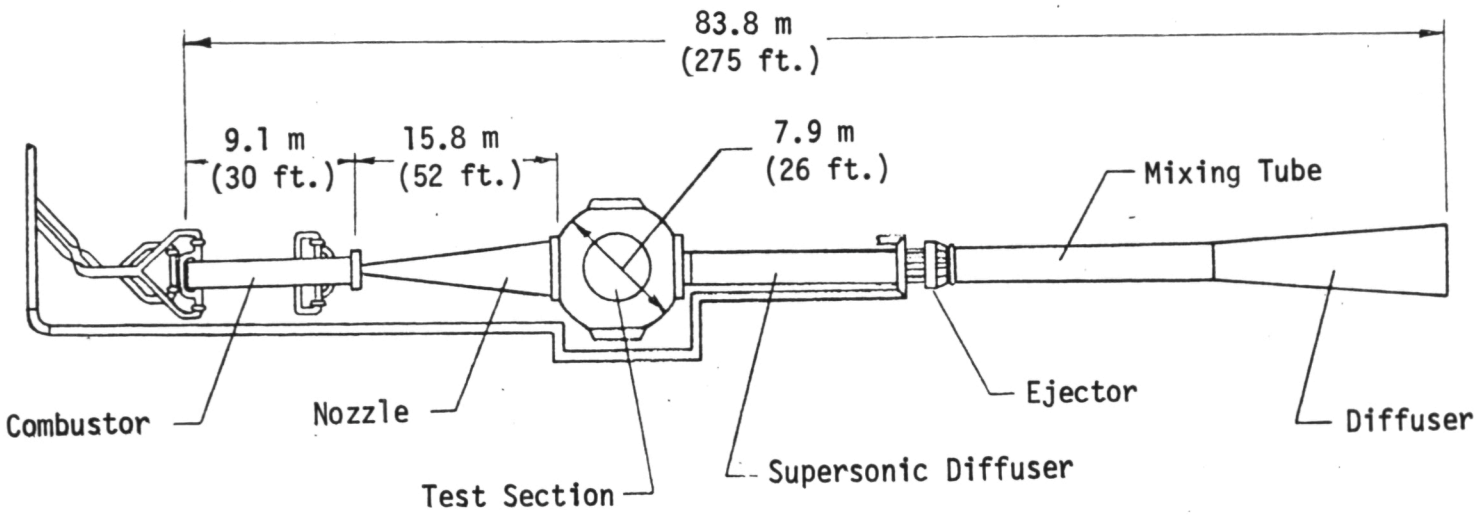

Figure 2-23. Schematic of Langley 8-foot High Temperature Structures Tunnel

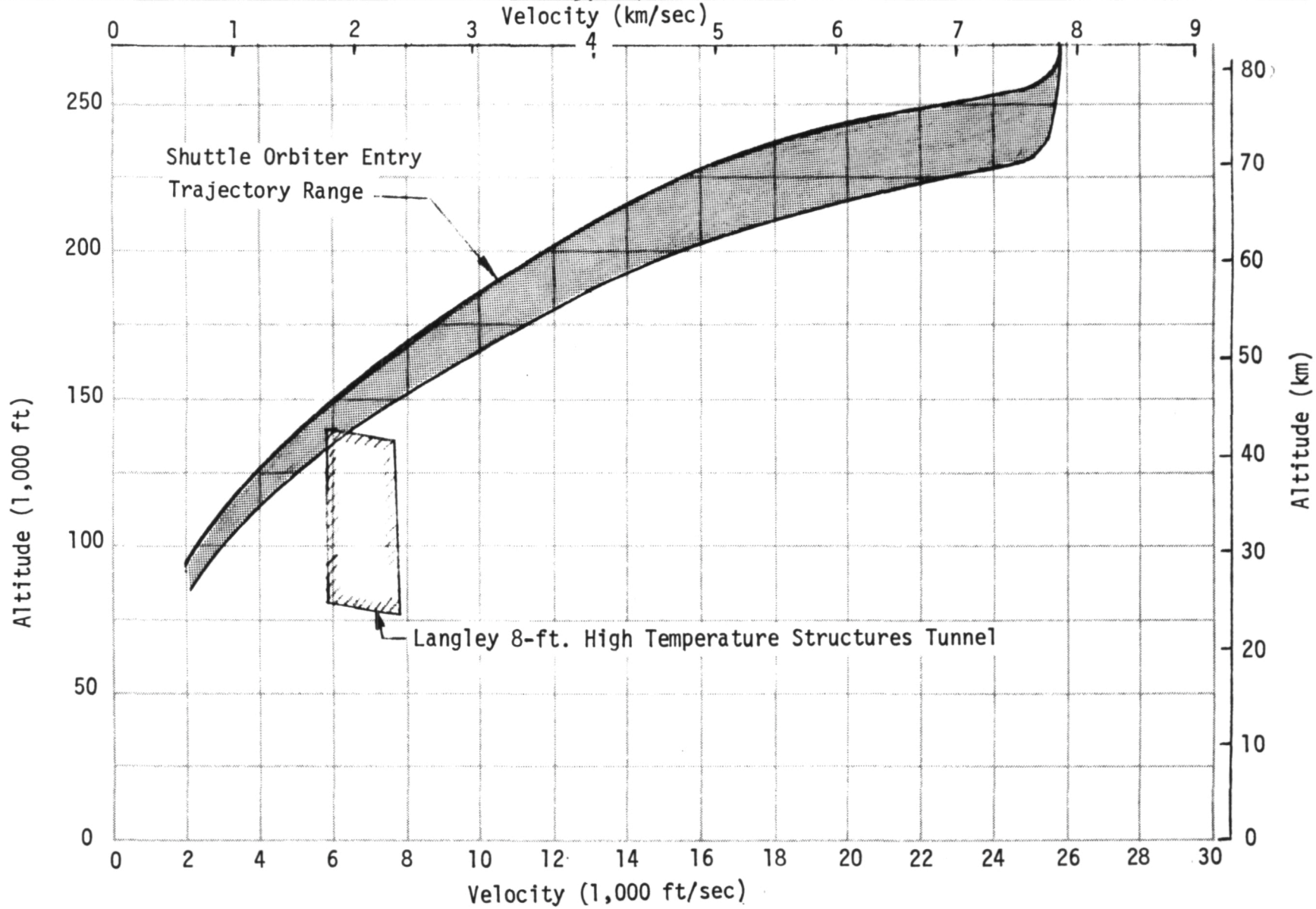

Figure 2-24. Langley 8-Foot High Temperature Structures Tunnel Simulation Envelope

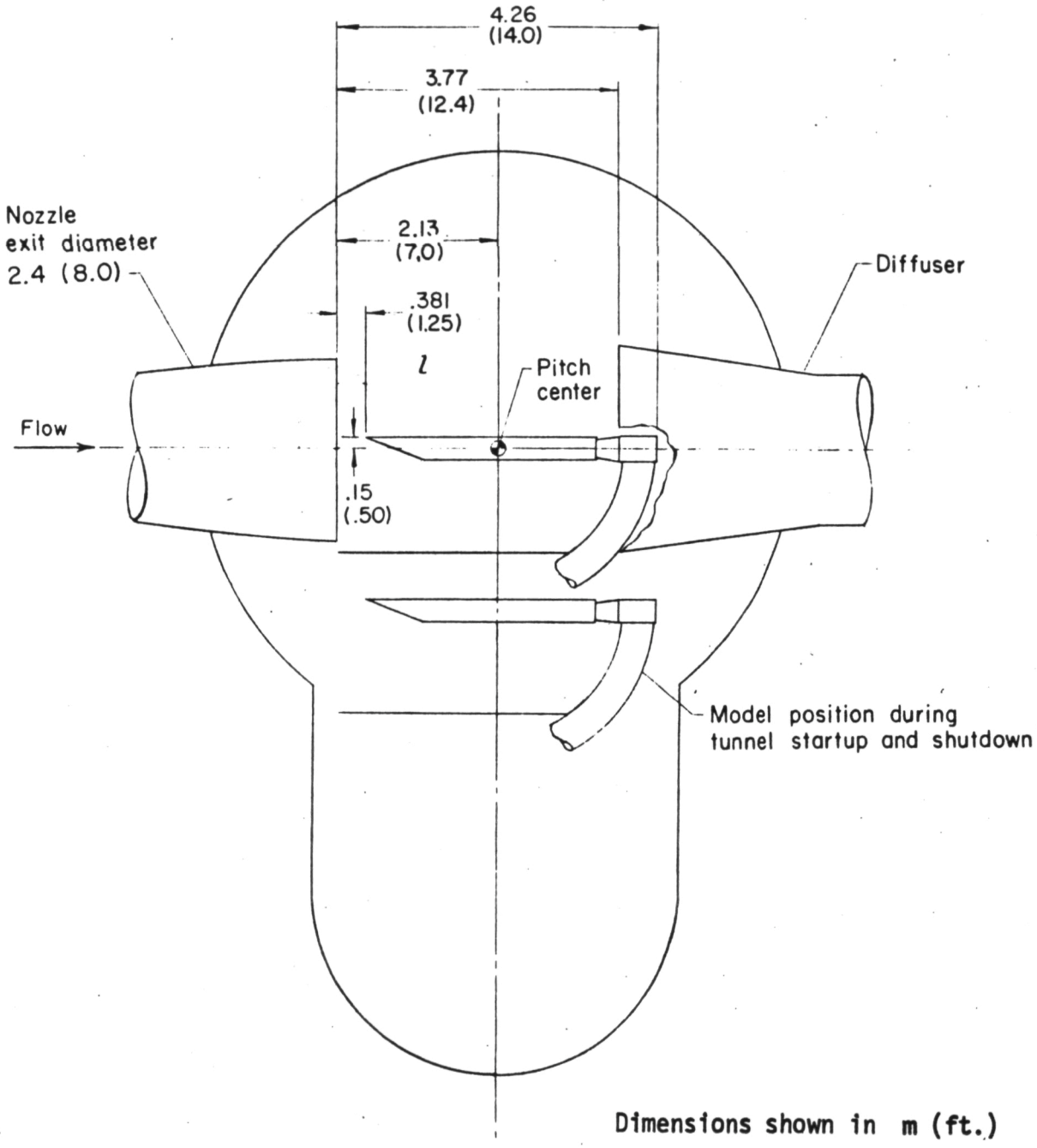

Figure 2-25. Test Section of Langley 8-Foot High Temperature Structures Tunnel

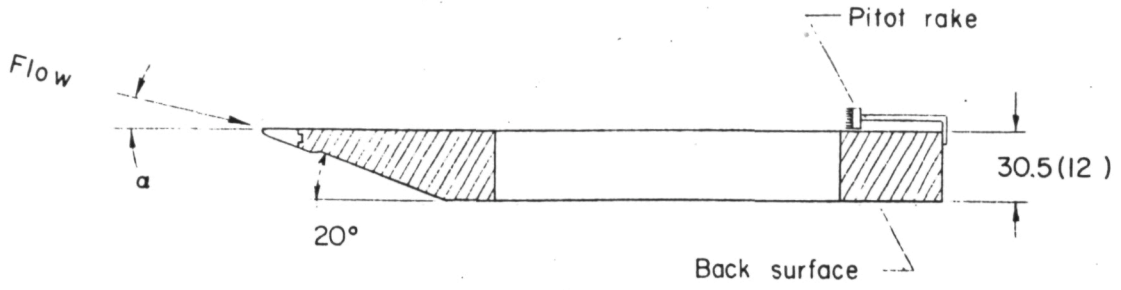

(a) Longitudinal cross section.

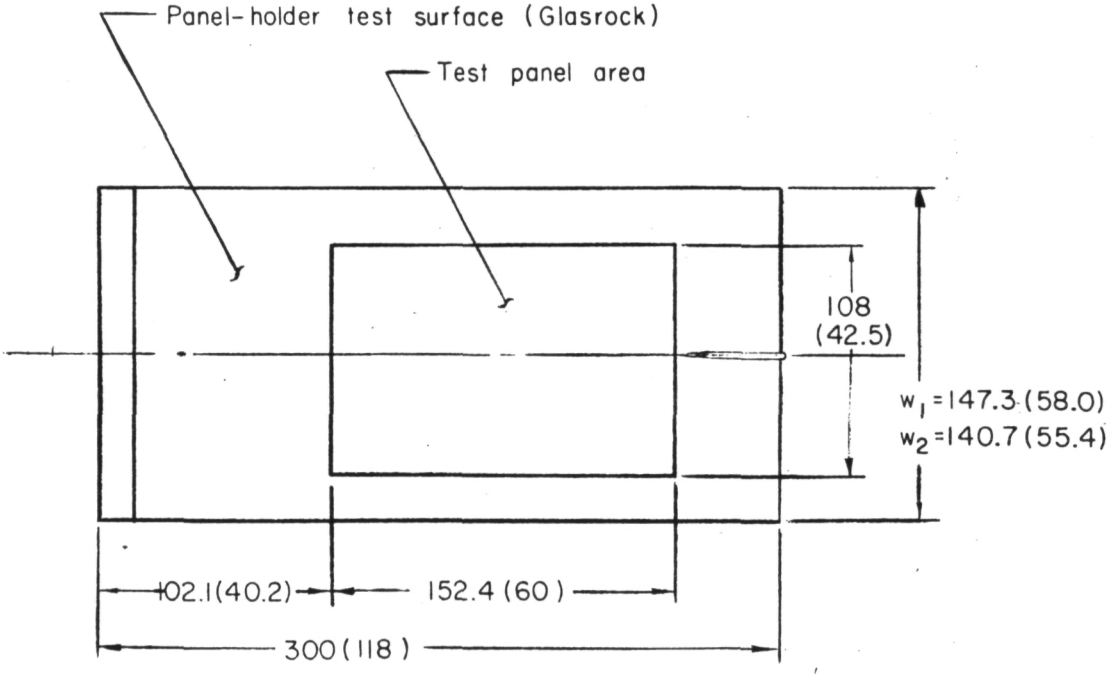

(b) Planview.

Dimensions shown in cm (in.)

Figure 2-26. Langley 8-foot High Temperature Structures Tunnel Test Array Holder

The HTST TD Ni-20Cr test array included two main panels, four side closeout panels, two end closeout panels, cover strips, support structures, insulation packages, and a simulated substructure. The basic dimensions of the array are shown in Figure 2-27, which also shows the panel holder mounting rails and edges of the cavity into which the TPS and substructure are mounted. The simulated substructure was designed for attachment to the set of steel mounting channels located within the cavity of the holder. The location of the mounting channels in the holder limited the total thickness of the TPS and substructure to 12.7 cm (5.0 in.), a thickness that in turn limited the insulation package thickness to approximately 7.6 cm (3.0 in.). Such thickness limitations led to the selection of titanium for the simulated substructure since substructure temperatures in the range of 477°K to 588°K (400°F to 600°F) were projected for the HTST tests.

The panel design of the HTST test array was basically the same as the design used for the MDAC test array with minor modifications at the attach positions to provide recessed fasteners. Additional stiffness was incorporated on the HTST main panel sides by using 0.0508 cm (0.020 in.) thick separate reinforcing edge members instead of employing the 0.0254 cm (0.010 in.) thick corrugation to reinforce the lateral edges. The thickness of all panels in the HTST array was 2.54 cm (1.0 in.) and the basic panel cross-section was the same as that used in the test array panels for contractor tests.

The support structure was changed in the HTST array to reduce the TPS weight and to curtail heat transfer to the substructure. Panel supports in the HTST design consisted of pylon configurations made from 0.0254 cm (0.010 in.) thick TD Ni-20Cr sheet material. Floating attach nuts machined from TD Ni-20Cr bar were mounted in each pylon support.

Figure 2-28 shows the HTST test array substructure and edge frames. The latter members contain the insulation packages and provide mounting supports for the end closeout panels as well as edge seals along the lateral edges of the test array. In Figure 2-29 the heat shield panel array is shown in place on the substructure and supports.

Page intentionally left blank

Figure 2-27. Test Array for the Langley 8-foot High Temperature Structures Tunnel

Page intentionally left blank

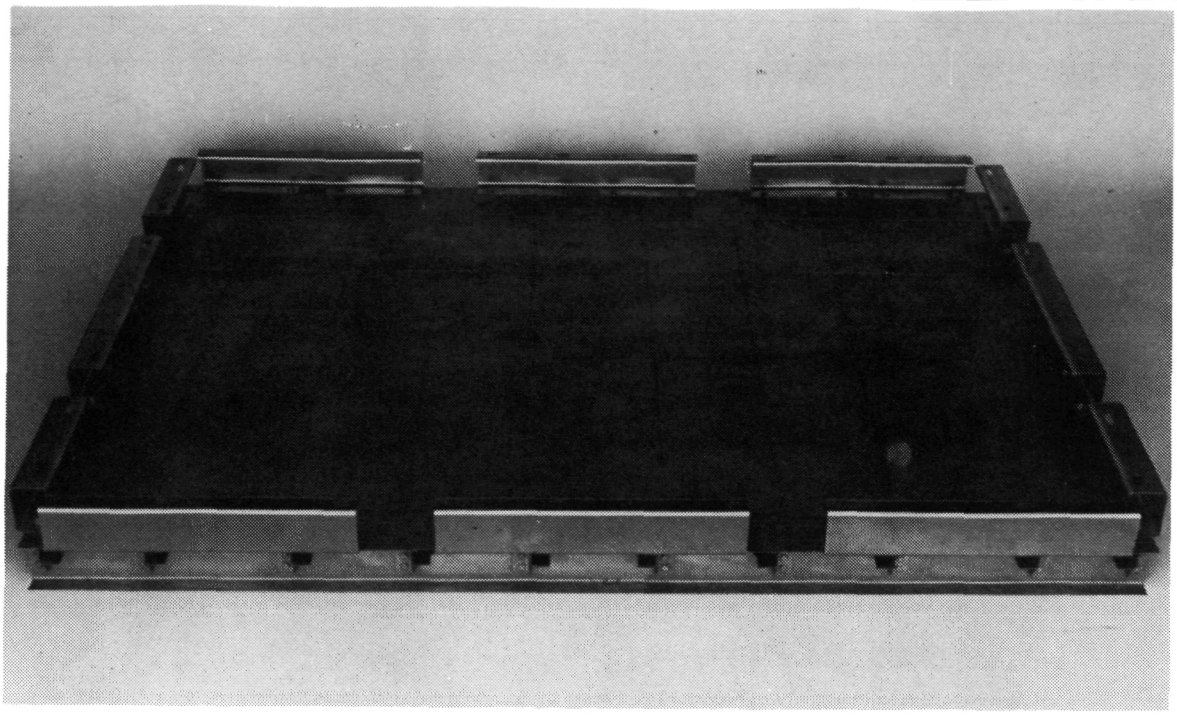

Figure 2-28. Substructure and Side Frames of HTST Test Array

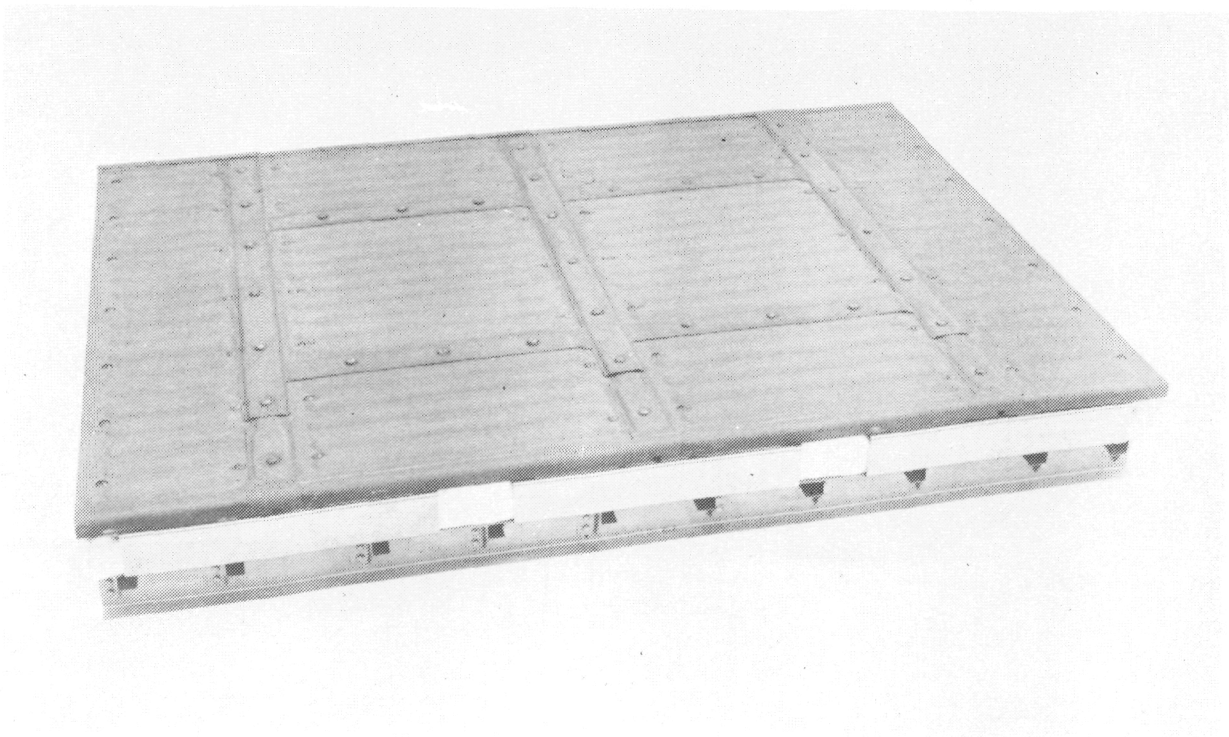

Figure 2-29. Completed HTST Test Array

2.4 TEST ARRAY FOR THE THERMAL PROTECTION SYSTEM TEST FACILITY

The TPSTF test array was the smallest of the three TPS arrays constructed, its planform dimensions being 61 cm by 91.4 cm (24 in. by 36 in.). Design of the TPSTF array was similar to that used for the other two arrays with the exception that only one full-size test panel could be included in the array because of the smaller planform size available in the TPSTF holder. Also, the small transverse dimension of 61 cm (24 in.) left a relatively small gap between the sides of the main panel and the edge of the holder cavity. As a consequence, side closeout panels were eliminated in the TPSTF array and wider edge seals were used as side closeout members.

The TPSTF heat shield array design is shown in Figure 2-30. The TPSTF test array holder, shown in Figure 2-31, has a water-cooled welded steel picture frame as its outer member which is bolted to a larger welded steel inner frame. Slotted holes around the periphery of the inner frame provide attachment positions for mounting the test array in the holder. Ports are also located in the edge members of the inner frame for passage of instrumentation leads.

The Thermal Protection System Test Facility is a supersonic blowdown wind tunnel that is similar to the HTST. However, the TPSTF test medium can reach higher temperatures through the addition of oxygen in the combustion mixture of air and methane. The test medium is made up of the products of combustion resulting from the burning of methane in air and/or oxygen within a pressurized combustion chamber. The combustion gases that form the test medium are then expanded to the test section Mach number by means of a two-dimensional contoured nozzle having an exit size of 30.5 cm by 91.4 cm (12 in. by 36 in.). A Mach number of from 3.5 to 4.3 may be achieved in the test section, the Mach number varying with test stream enthalpy. Total test stream enthalpy at the nozzle exit can range from 1,905 to 8,840 J/g (820 to 3,800 BTU/lb) depending on the test medium mixture ratio of methane, air, and oxygen. The test stream exits from the test section through a straight tube diffuser into a single-stage air ejector which pumps the mixture into the atmosphere.

Figure 2-30. Test Array for the Langley Thermal Protection System Test Facility

Page intentionally left blank

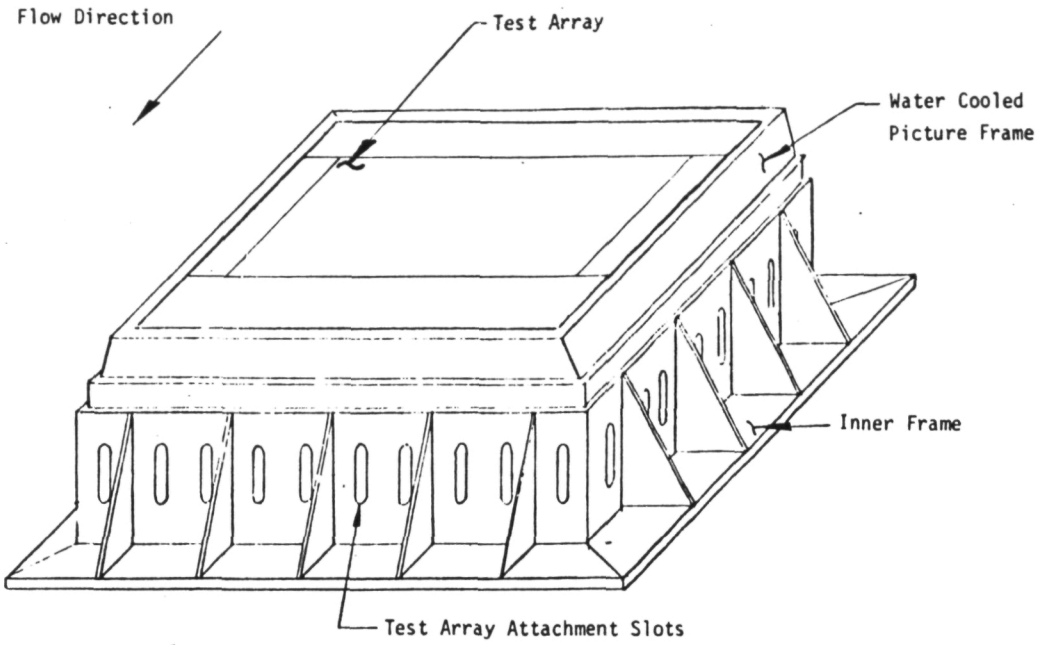

Figure 2-31. Test Array Holder for the TPSTF

The test array's outer surface when mounted in the holding fixture, is flush with the side wall of the test section. A maximum test array size of 61.0 cm by 91.4 cm (24 in. x 36 in.) can be mounted in the holder, and a heat flux range of from 22.7 to 545 kw/m^2 (2 to 48 BTU/ft^2-sec) may be applied to the test array surface parallel to the test stream. The range of surface pressures applied to the test array varies from 557 to 1,013 N/m^2 (.0057 to .01 atm) depending on stream flow conditions.

A maximum test time of 360 seconds can be achieved when the facility is operating at a maximum equivalent power of 134 MW. Tests at lower power can be conducted up to a maximum run time of 1,800 seconds. In contrast, the HTST is limited to maximum run times of approximately 200 seconds. Figure 2-32 presents a comparison of the HTST and TPSTF operating envelopes in terms of panel surface pressures and equilibrium temperatures available in

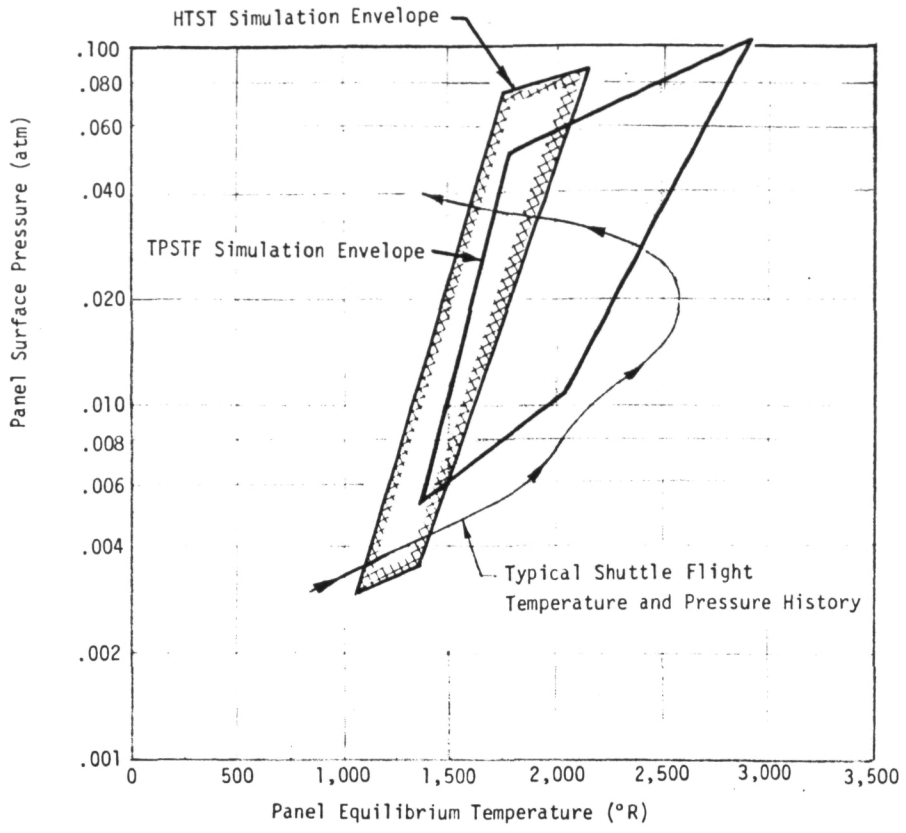

Figure 2-32. Panel Temperature and Pressure Test Envelopes

the two facilities. Combinations of temperatures and pressures are also shown in Figure 2-32 for a point on the lower surface of the Orbiter during nominal boost and entry trajectories.

As in the other two test arrays, the nominal panel thickness in the TPSTF test array was 2.54 cm (1.0 in.). A test fixture cavity depth of 17.6 cm (6.93 in.) permitted a slightly thicker insulation package of 8.88 cm (3.50 in.) to be used in the TPSTF test array. Seven insulation layers were used, each layer being 1.27 cm (0.50 in.) thick. The four outer layers were made of 128-kg/m^3 (8-lb/ft^3) Fiberfrax Hi-Fi fibrous insulation and the three inner layers were made of 96-kg/m^3 (6-lb/ft^3) Microquartz. The insulation was again packaged in high temperature quartz cloth using the same basic approach as that employed in the HTST TPS array.

TD Ni-20Cr pylon panel supports provided attach points for the panels, and alumina insulating pads were located at points where the pylons were attached to the simulated titanium substructure. The substructure formed the floor of an open rectangular box, and the TD Ni-20Cr sides of the box were designed to mate with the interior surfaces of the test fixture cavity. "Z"-shaped clips were located at eight points around the periphery of the test array frame to provide attachment to the inner steel frame of the test fixture. TD Ni-20Cr edge members were mounted on top of the test array side frames to provide closeout members along the lateral edges of the test array.

The TPSTF test array components are shown in Figures 2-33 through 2-36. The substructure and side frames are shown in Figures 2-33, the substructure being a spotwelded titanium structure simulating a skin-stringer-frame segment of the Shuttle primary structure. The TD Ni-20Cr side frames provided containment for the insulation packages and also served as supports for the test array close-out members. The attach clips on the frame members are also visible in Figure 2-33. The heat shield supports and a portion of the insulation packages are shown in Figure 2-34 prior to installation of the surface panels and cover

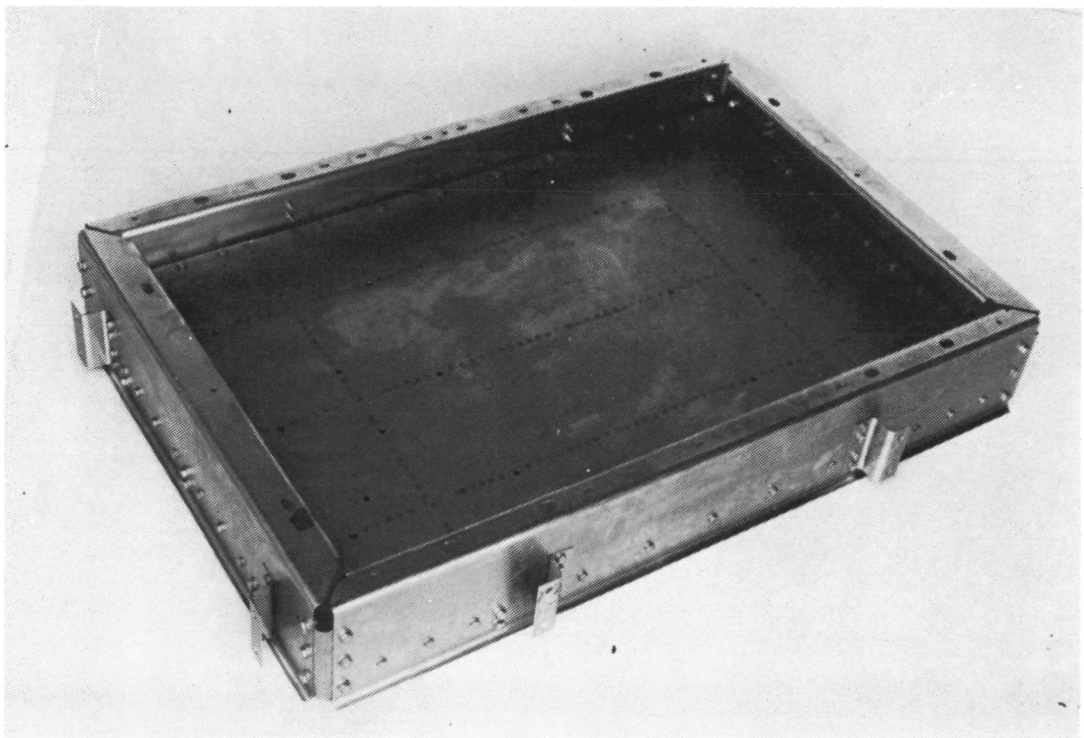

Figure 2-33. Substructure and Side Frames; TPS Test Array

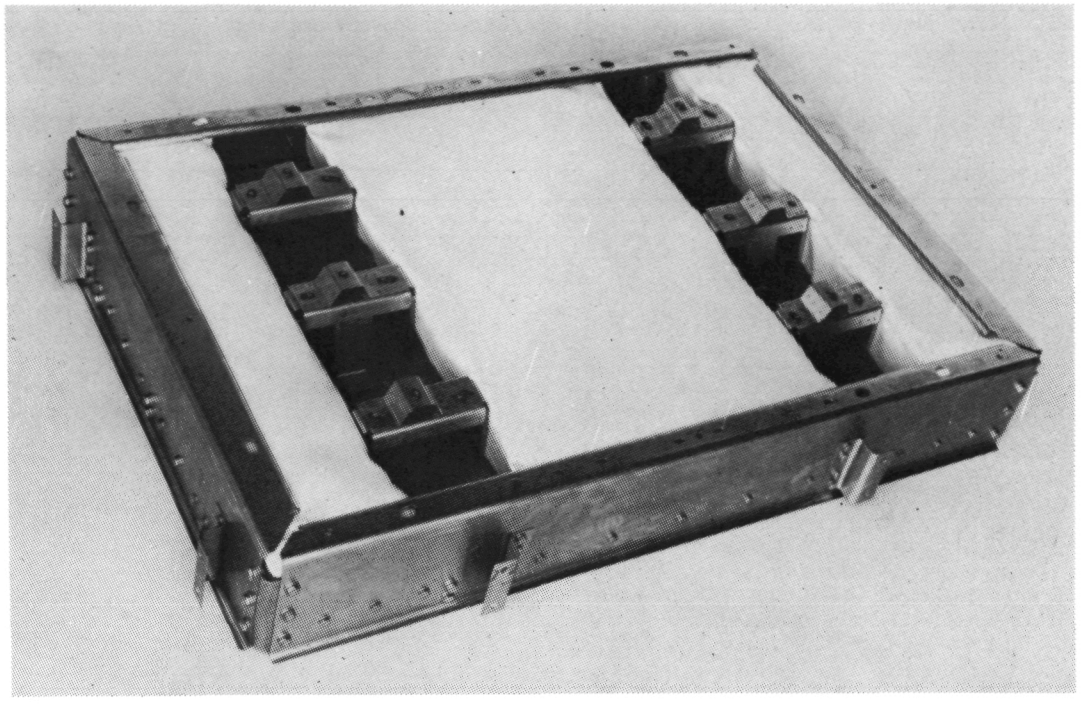

Figure 2-34. Installed Insulation Packages and Heat Shield Supports

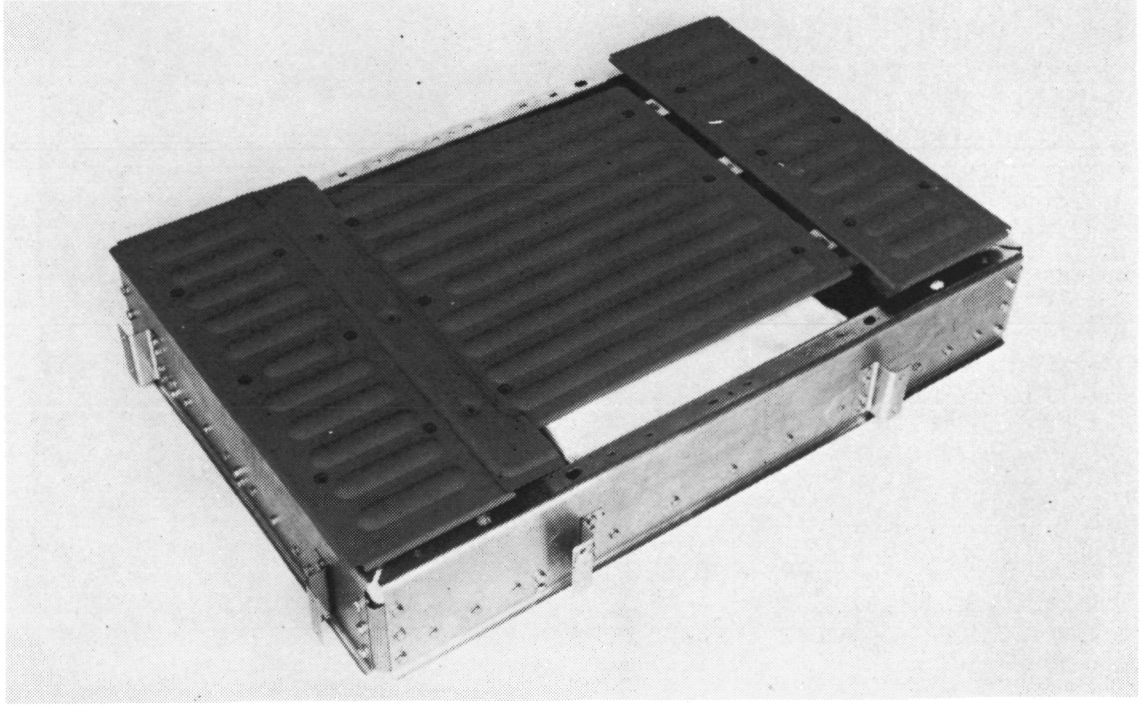

Figure 2-35. Partially Assembled Heat Shield Array

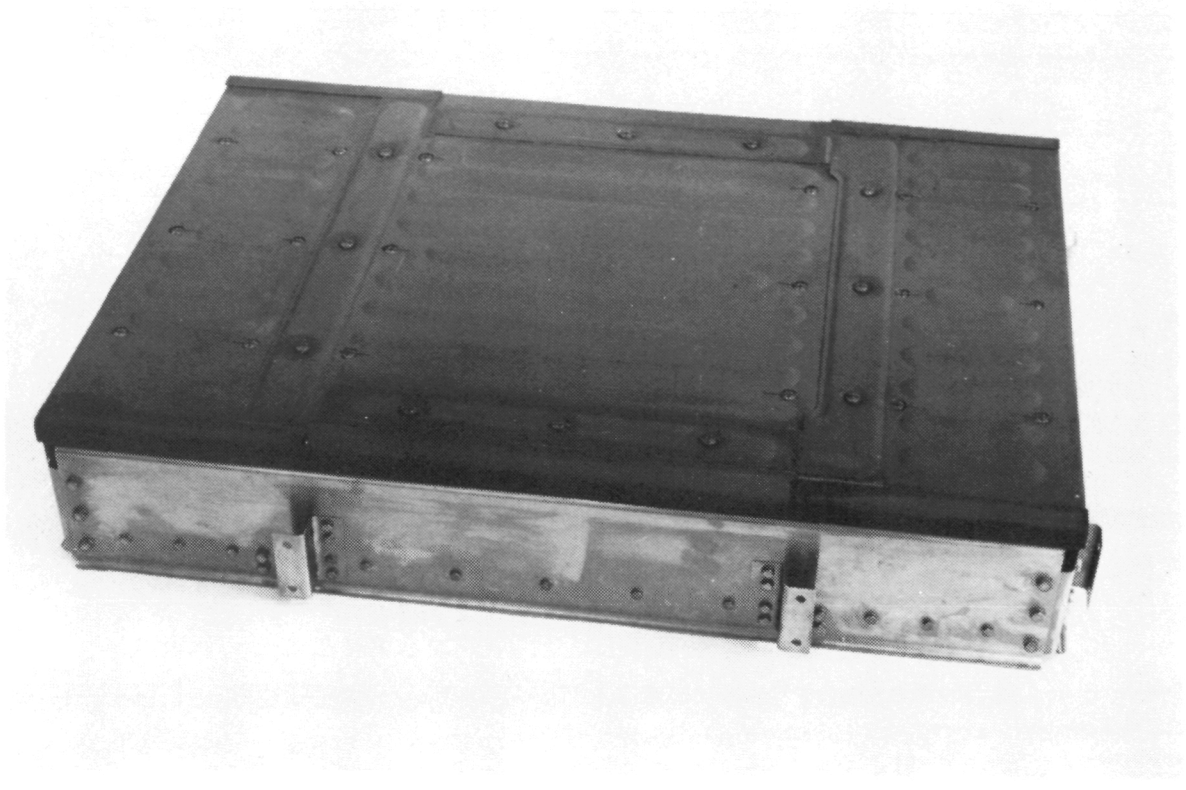

Figure 2-36. Completed TPSTF Test Array

strips. Figure 2-35 shows the heat shields and a cover strip positioned on the heat shield supports before installation of the fasteners and side close-out members. The completely assembled test array is shown in Figure 2-36.

Unit weights of the TPSTF test array components that comprise the full-size, full-scale TPS are presented in Table 2-4. Comparison of the TPSTF weights with those of the contractor test array weights (Table 2-1) shows a reduction in the TPSTF unit weight of approximately 5.90 kg/m^2 (1.21 lb/ft^2). The weight reduction resulted primarily from a redesign of the heat shield support system and a revision of the insulation packaging system. The support system was changed from beam supports to pylon-type supports and also included a reduction in TD Ni-20Cr sheet thickness of the support system from 0.102-cm (0.040-in.) in the beams to 0.025-cm (0.010-in.) for the pylon supports. The insulation packaging was changed from a metallic foil container to the use of high temperature quartz cloth for packaging the fibrous insulation.

Table 2-4

Weights of TPSTF Test Array

Component	Weight kg (lb)		Unit Weight kg/m^2 (lb/ft^2)	
Main Panel	1.69	(3.72)	6.88	(1.41)
Closure Strips	0.30	(0.67)	1.22	(0.25)
Panel Supports	0.29	(0.63)	1.17	(0.24)
Ceramic Pads	0.07	(0.15)	0.29	(0.06)
Insulation Package	1.94	(4.27)	7.91	(1.62)
Bolts	0.28	(0.61)	1.12	(0.23)
			18.59	(3.81)

Section 3
THERMAL PROTECTION SYSTEM INSTRUMENTATION AND TESTING

The full-scale, full-size TPS array was designed to simulate a segment of a complete TD Ni-20Cr metallic radiative thermal protection system including heat shields, heat shield supports, insulations, and the primary structure. In the tests conducted by the contractor, programmed cycles of differential pressure, temperature, and environmental pressure were applied to simulate boost, entry, and cruise flight conditions experienced by a typical TPS area on the lower surface of the Orbiter (Figure 2-5). Simulated boost flight acoustic loads were interspersed with the cyclic pressure and temperature conditions.

The test system used for the Phase II full-size TPS array is shown schematically in Figure 3-1, which also shows the sequence of testing. The test fixture was designed to permit its use in both the Space Simulation Chamber and the Acoustic Facility so that the test array could remain in place except for necessary inspections and instrumentation replacement.

The programmed cycles of differential pressure, main chamber pressure, and temperature are shown in Figure 2-19, while Figure 3-2 presents the sound pressure level spectrum selected for acoustic tests. The main chamber pressure used for the test profile (Figure 2-19) was greater than that predicted for the Orbiter entry flight due to pumping capacity limitations for the main chamber. Also, excessively low pressures in the test fixture would have caused arcing of the quartz lamps. As shown in Figure 2-19, the main chamber pressure was held at 20 torr (0.4 psi) throughout a majority of the test cycle. This test pressure, while higher than the computed ambient pressure during the Orbiter entry flight, was sufficiently low to simulate the low-pressure effects that could cause degradation from chromium depletion under elevated temperatures combined with low-pressure environments (see Appendix C, Reference 2).

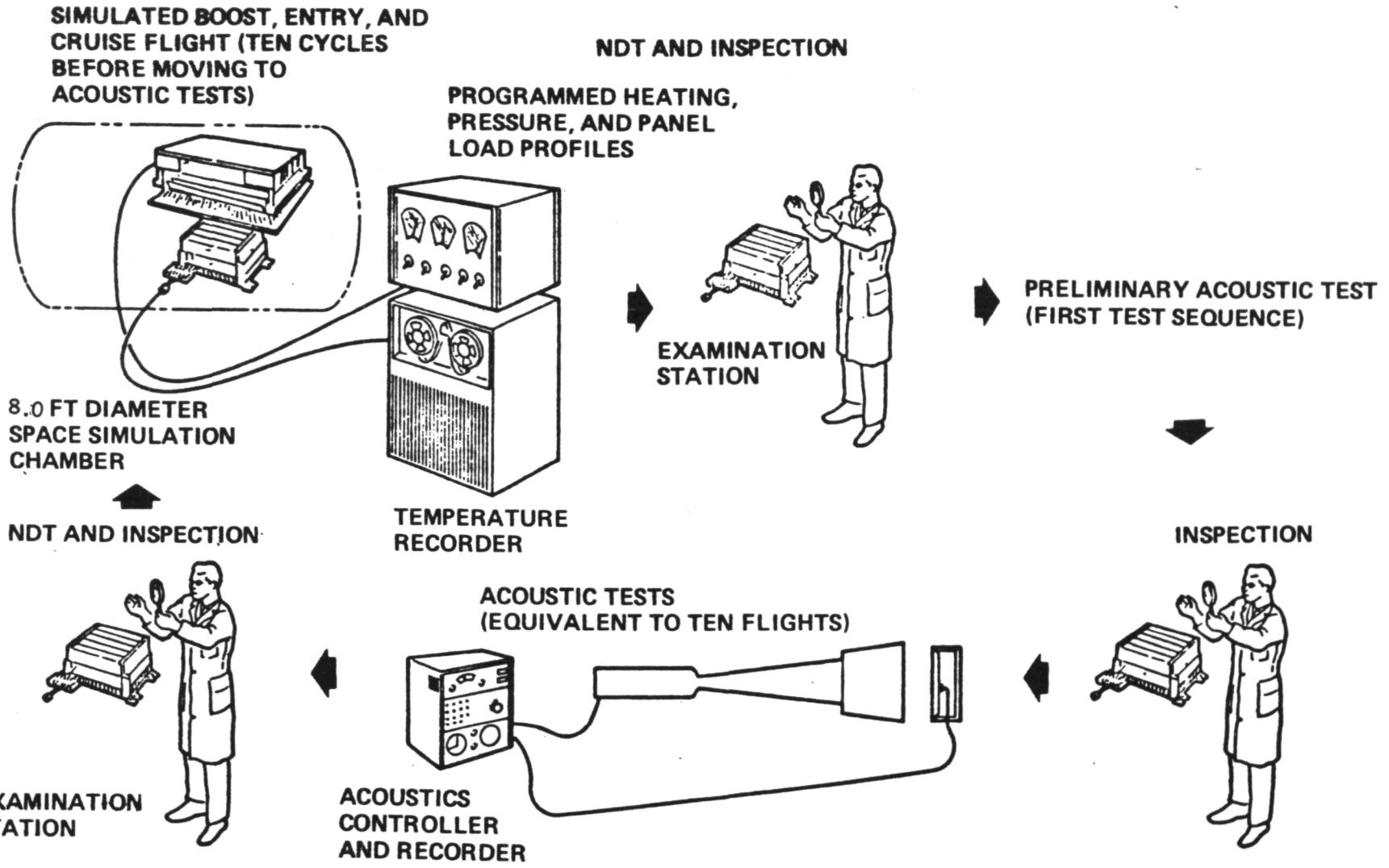

Figure 3-1. Test Sequence for the Full-Scale, Full-Size Test Array

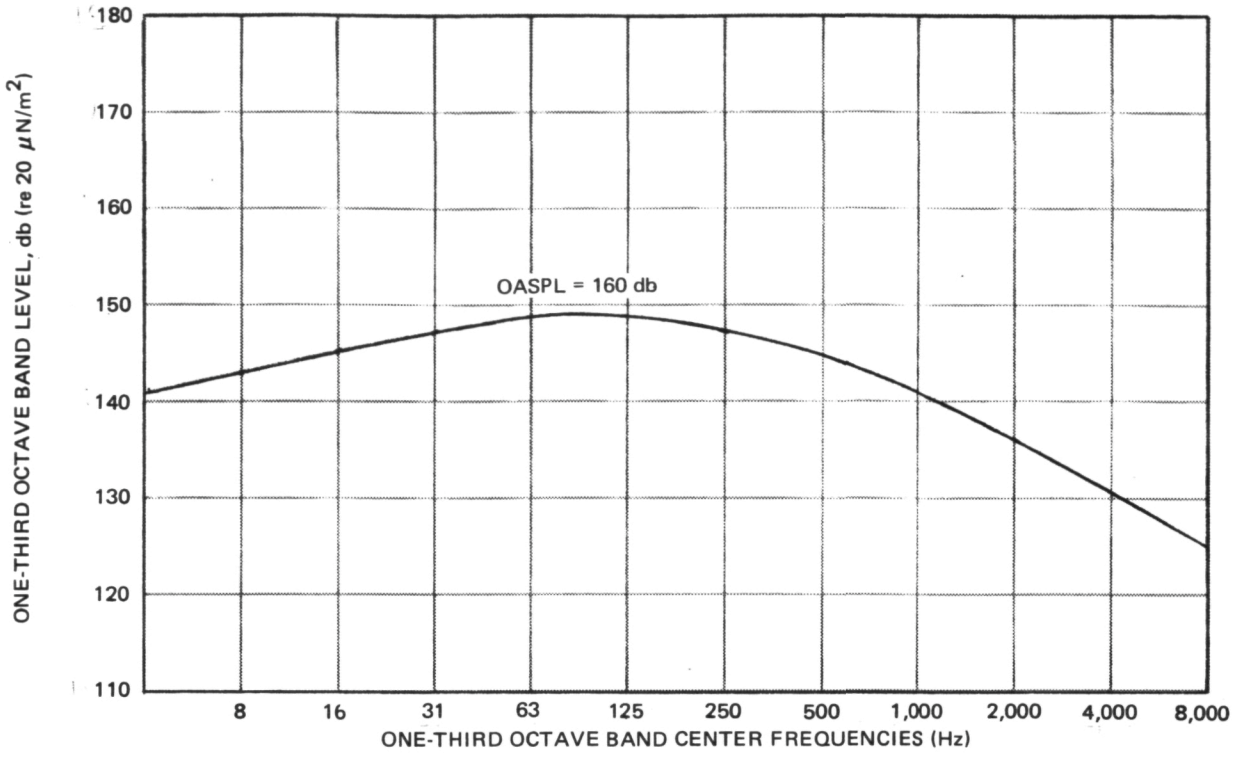

Figure 3-2. Acoustic Test Spectrum

The contractor test array was fabricated at MDAC's Santa Monica location, and checkout of the assembly was also conducted at Santa Monica through use of a wooden mockup which simulated the steel test fixture mounting points (Figure 2-13). After the test array checkout was completed, the TPS was shipped to the MDAC Space Simulation Laboratory at St. Louis for instrumentation and testing.

3.1 TPS ARRAY INSTRUMENTATION

The TPS array was instrumented with strain gages and thermocouples as shown in Figure 3-3. Strain gages were employed to evaluate maximum stresses when differential pressure loads were applied to the panels in the initial tests. All panel stress tests were conducted as preliminary tests at room temperature since the simulated cyclic mission tests with a maximum temperature of 1,478°K (2,200°F) destroyed the strain gages. As shown in Figure 3-3, uniaxial strain gages were mounted on the external surface of the face sheets on both main test panels and on two of the side closeout panels, one of the instrumented

Page intentionally left blank

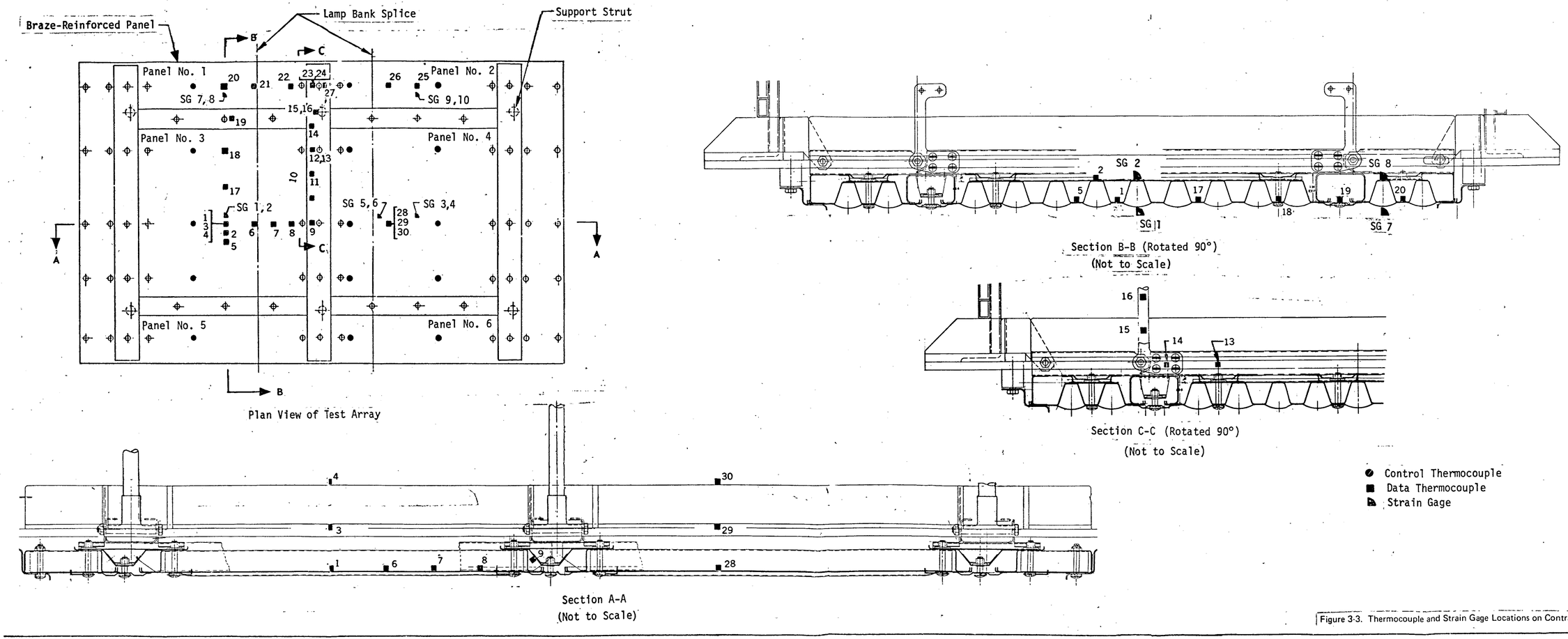

Figure 3-3. Thermocouple and Strain Gage Locations on Contractor Test Array

Page intentionally left blank

side panels being the braze-reinforced panels. Similarly, uniaxial strain gages were placed on the interior side of the panels on the corrugation crowns in positions directly beneath the exterior surface strain gage locations. A total of 10 strain gages were used for the initial panel stress surveys.

Thermocouple locations are also shown in Figure 3-3 for both control thermocouples and data thermocouples. Control thermocouples were located in three transverse rows that corresponded to the approximate centers of the three groups of quartz lamps mounted in the lower half of the test fixture (see Figure 2-8). Data thermocouples were located in the main TD Ni-20Cr heat shields, the insulation packages, the side closeout panels, support beams, and a support strut. Locations for the data thermocouples were selected to provide temperature distribution data in several key areas, including the support beams and struts. Thirty data thermocouples and fifteen control thermocouples were employed on the test array.

3.2 PRELIMINARY TESTS

The heat shield test array is shown installed in the test fixture upper frame in Figures 3-4 and 3-5. The outer surfaces of the instrumented panels are shown in Figure 3-4 and the rear surfaces are shown in Figure 3-5. Insulation packages and the simulated substructure were installed after the photographs of Figures 3-4 and 3-5 were taken.

The TPS array was subjected initially to modal response tests to determine resonant frequencies and modal response shapes of the heat shield array. One of the main panels was excited near its center by an oscillating point force that produced panel accelerations normal to the plane of the array. Accelerometers located at 40 grid points on the array measured the response of the panels as noted in Figures 3-6 through 3-9. A frequency sweep was conducted first to determine the resonant frequencies by observing the phase and magnitude responses of the accelerometers at the various grid points noted in Figures 3-6 through 3-9. The first four resonant frequencies were identified and detailed response shapes were defined by recording the accelerations at each grid position.

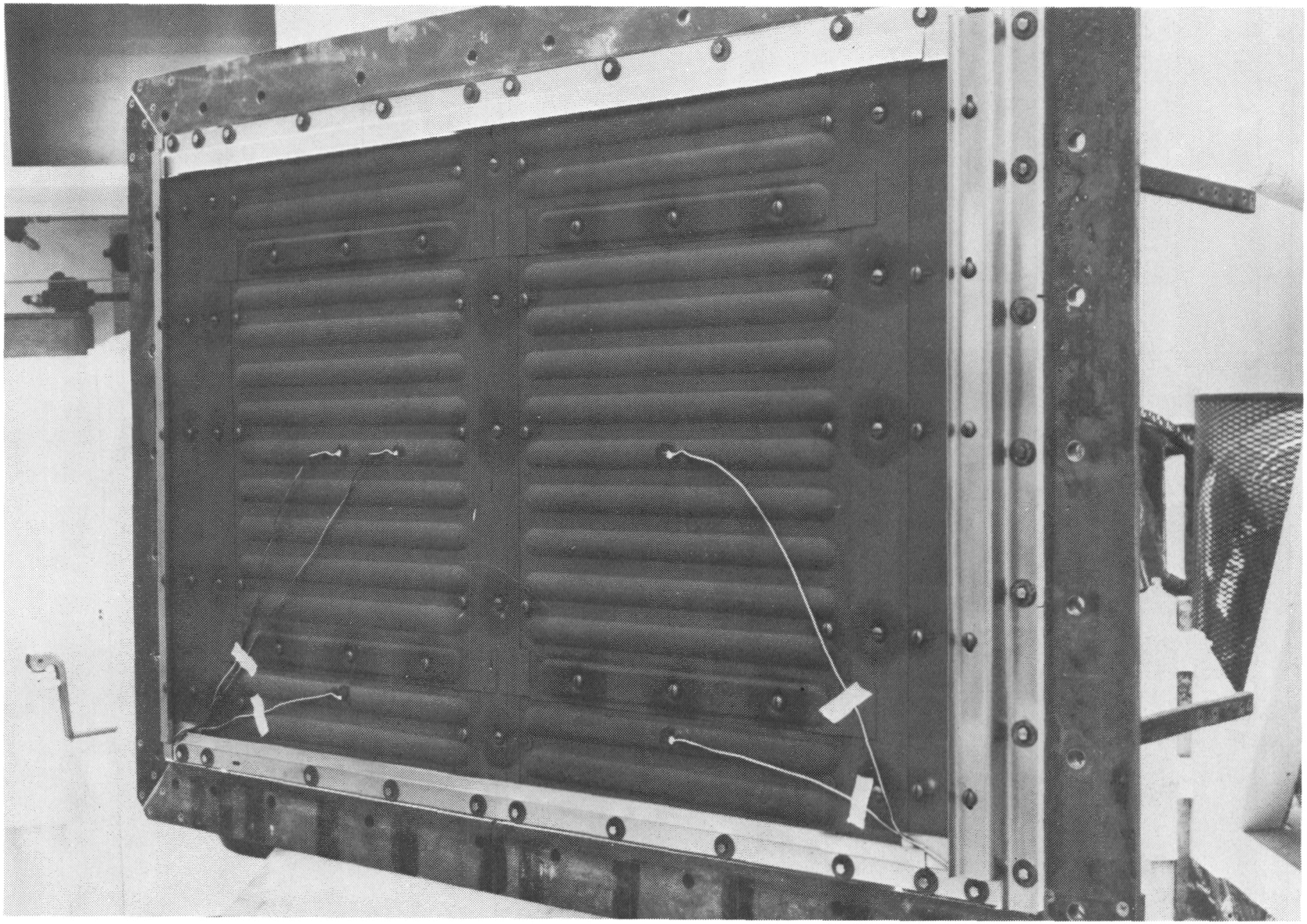

Figure 3-4. External Surface of Test Array Before Test Initiation

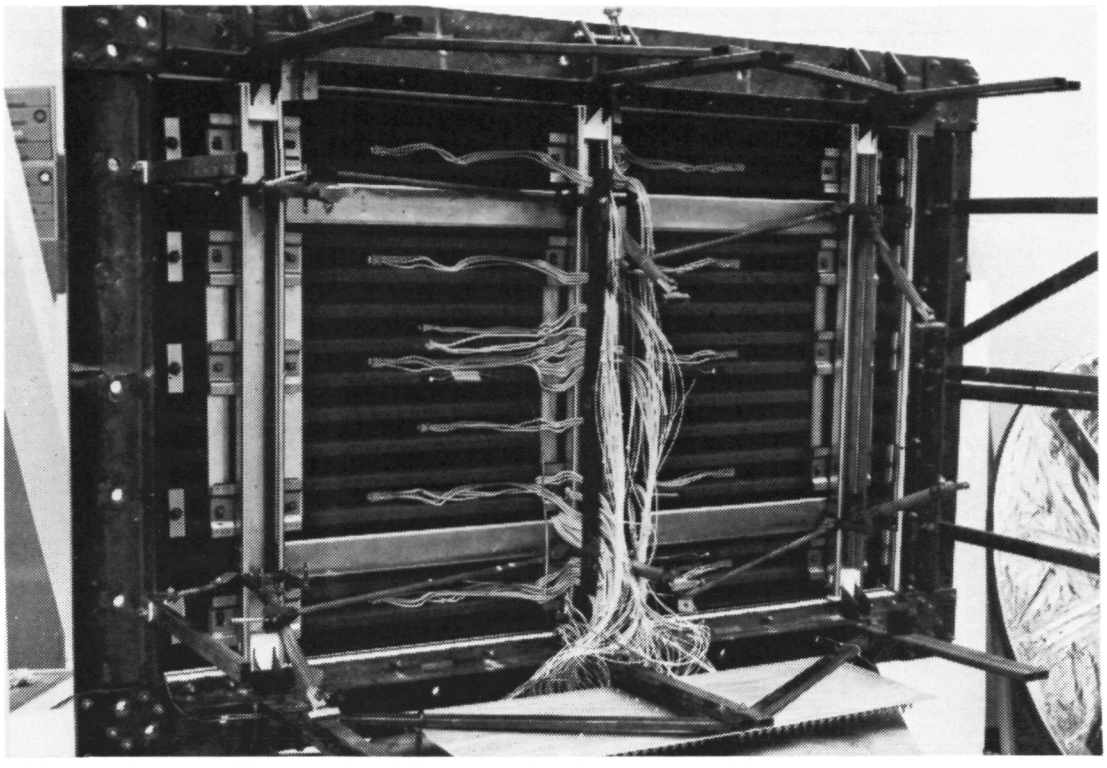

Figure 3-5. Internal Surface of Heat Shield Panels Before Testing

Accelerometer readings were then normalized at each frequency with respect to the maximum acceleration. The first four resonant frequencies occurred at 228 Hz, 233 Hz, 322 Hz, and 330 Hz. The test array normalized mode shapes at each frequency are shown to scale in the perspective sketches of Figures 3-6 through 3-9.

After completion of the initial panel modal response tests in the Vibration and Acoustic facility the test array was moved back to the Space Simulation Laboratory for preliminary stress and thermal tests. The panel stresses caused by differential pressure at room temperature were checked in two separate runs, and both runs resulted in similar stress levels being recorded. The maximum tensile stress at the panel midspan position with a differential pressure of 22.7 kN/m^2 (3.30 psi) was approximately 109.0 MN/m^2 (15,800 psi), which compares favorably with the analytical prediction of 109.8 MN/m^2 (15,900 psi). Similarly, the maximum compression stress at the midspan point was 7.61 MN/m^2 (11,050 psi) compared to a predicted stress of 7.07 MN/m^2 (10,250 psi). Measured strains were converted to stresses using a static modulus of elasticity of 167.8 x 10^3 MN/m^2 (24.3 x 10^6 psi).

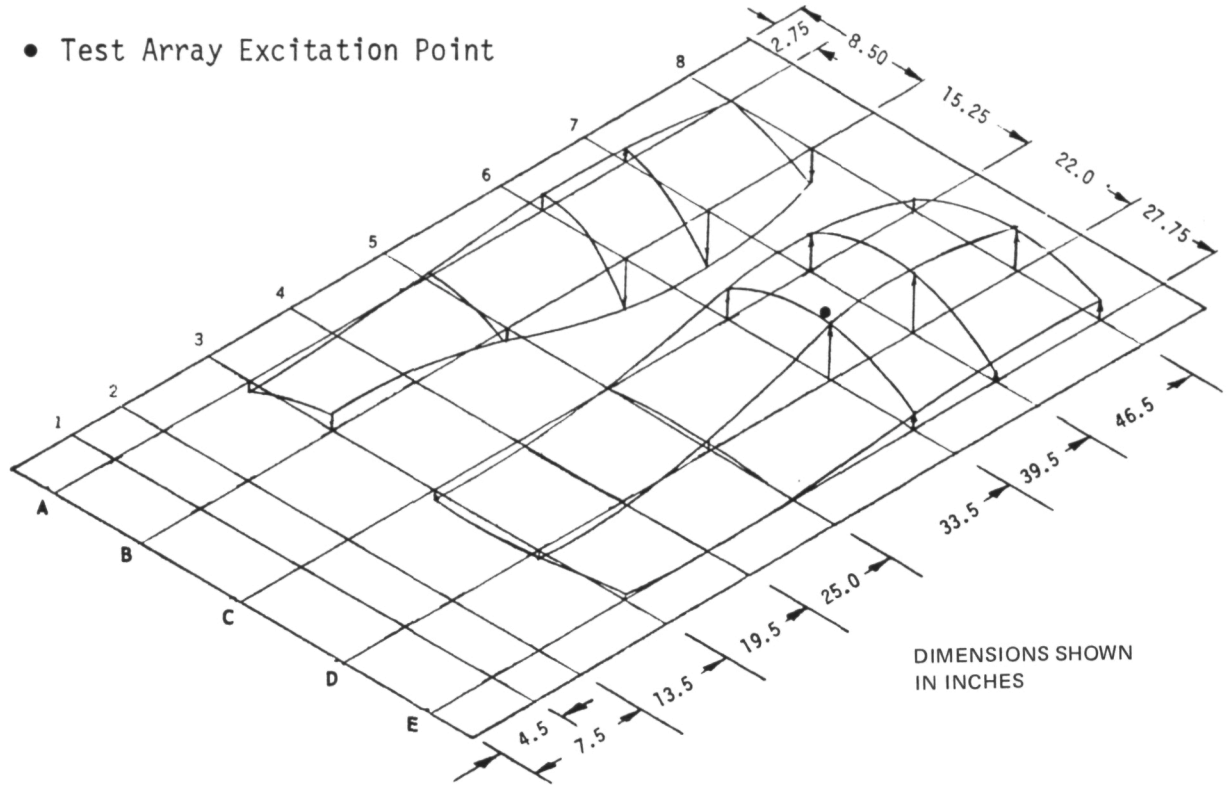

Figure 3-6. Test Array Normalized Modal Response at 228 Hz

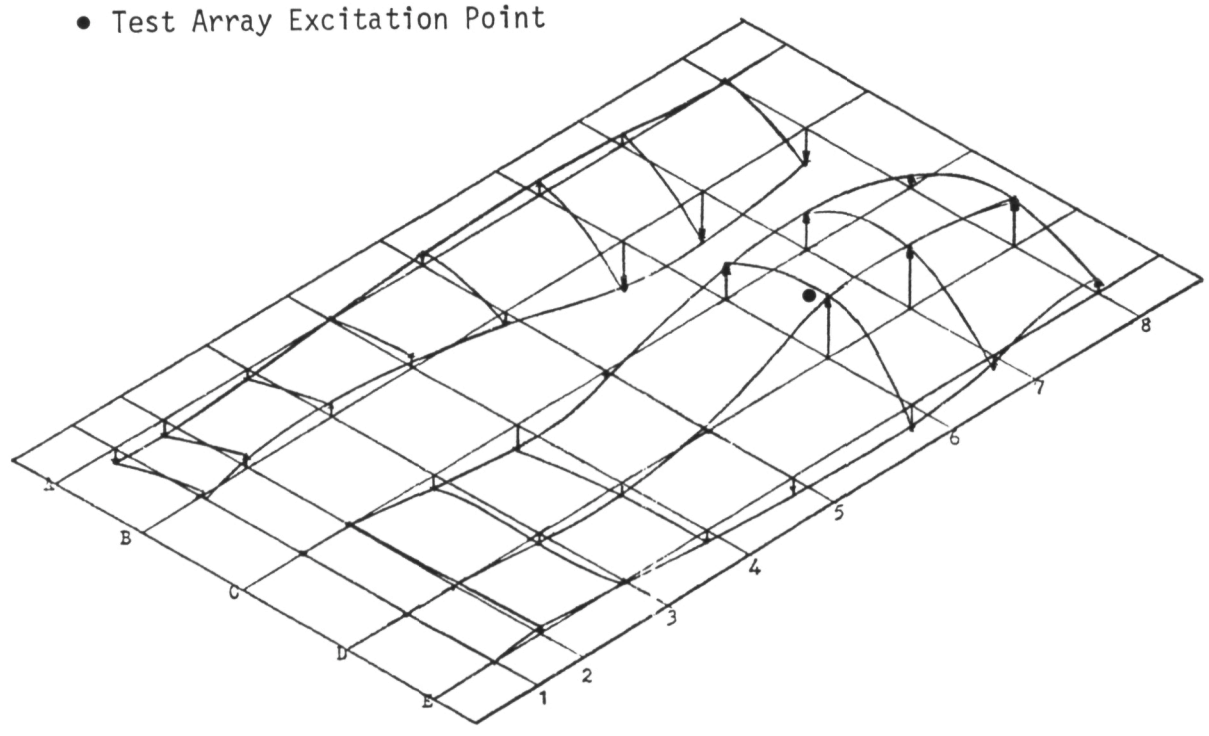

Figure 3-7. Test Array Normalized Modal Response at 233 Hz

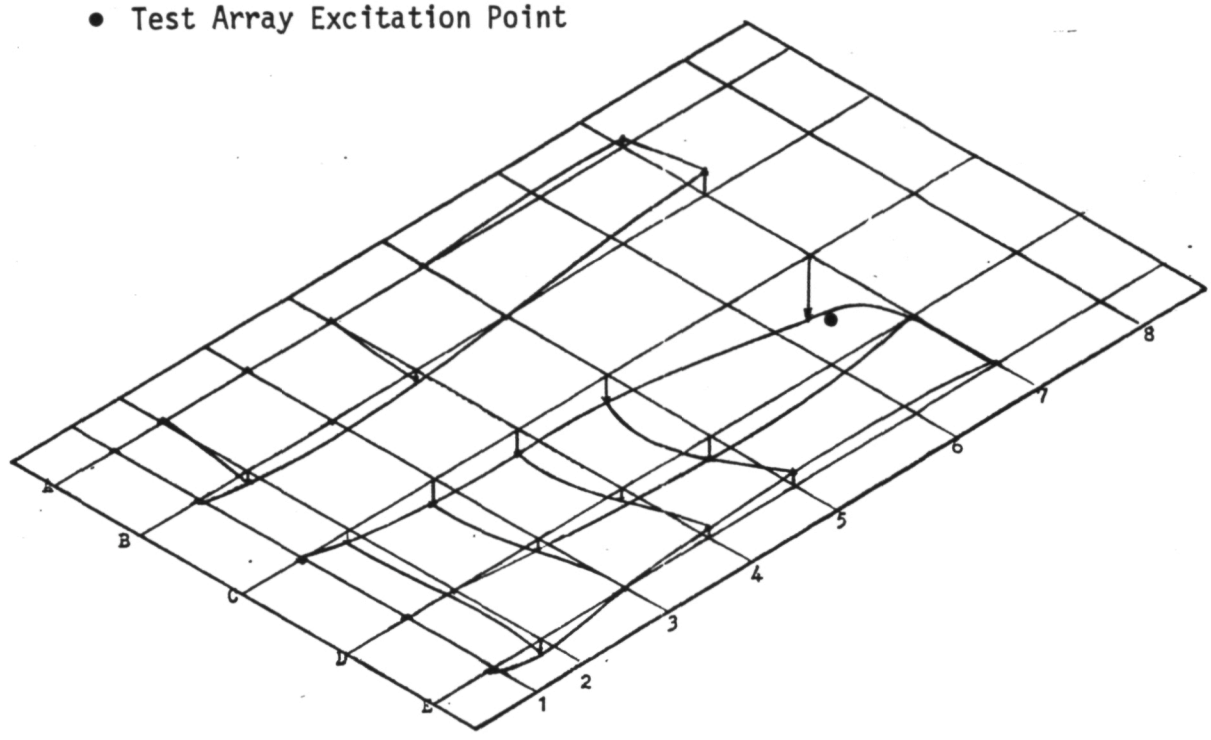

Figure 3-8. Test Array Normalized Modal Response at 322 Hz

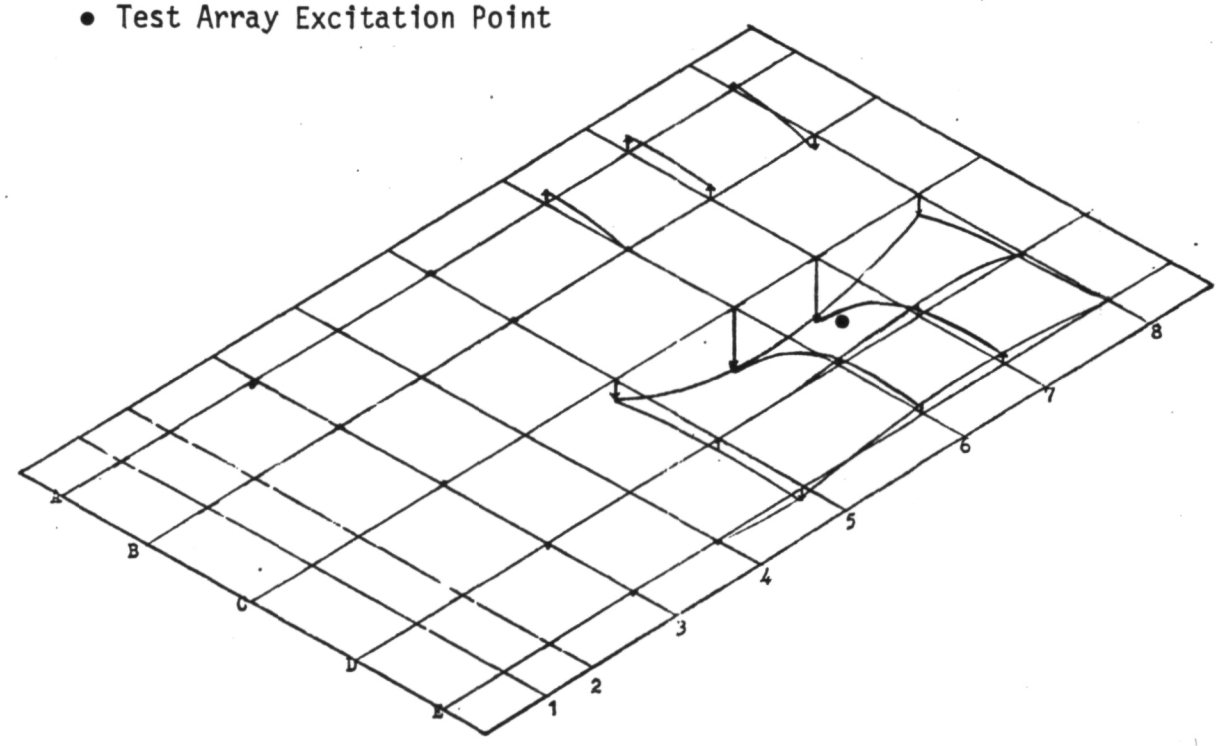

Figure 3-9. Test Array Normalized Modal Response at 330 Hz

The preliminary strain survey on the panels was conducted with the heat shield array mounted in the test fixture and installed in the Space Simulation Chamber. The chamber was vacuum pumped while air at 1 atmosphere pressure was admitted to the pressure box portion of the test fixture so that differential pressure was applied to the heat shield array with the higher (1 atm.) pressure being on the external surface of the array. The pressure in the main test chamber was lowered in steps to permit strain readings to be recorded at approximate intervals of 3.457 kN/m^2 (0.5 psi) differential pressure.

Strain gage locations are shown again in Figure 3-10 to indicate the detailed placement of the gages. Stresses derived from the first strain survey test are presented in Figures 3-11 through 3-13 as a function of differential pressure loads. Stresses at the midspan position on a main panel and at the same position on the braze-reinforced panel are shown in Figure 3-11. The data of Figure 3-11 indicate slightly lower stresses occurred on the braze-reinforced panel when compared to similar stresses on the main panel. Less difference was noted in the compression stresses of the second main panel and its adjoining close-out panel, as can be observed in comparing the stress levels at gage 3 (Figure 3-12) with those of gage 9 (Figure 3-13). However, comparison of the tensile stresses measured at gages 4 (Figure 3-12) and 10 (Figure 3-13) show the main panel to have experienced somewhat higher tensile stresses in the reinforcing corrugation than experienced by the close-out panel.

A preliminary thermal test was next conducted using the full mission temperature profile with a maximum temperature of 1,478°K (2,200°F) without differential pressure loads. The preliminary thermal test caused a sine-wave shaped buckle to occur at one end of the center transverse cover strip due to restricted expansion space at the side edge seals. The cover strip buckle in turn caused some deformation of the edges of the two side close-out panels upon which the cover strip rested. Maximum deformation of the cover strip was estimated to be approximately 0.508 cm (0.20 in.) in a posttest visual examination of the test array. Figure 3-14 shows an overall view of the outer surface of the test array in which noticeable buckling of

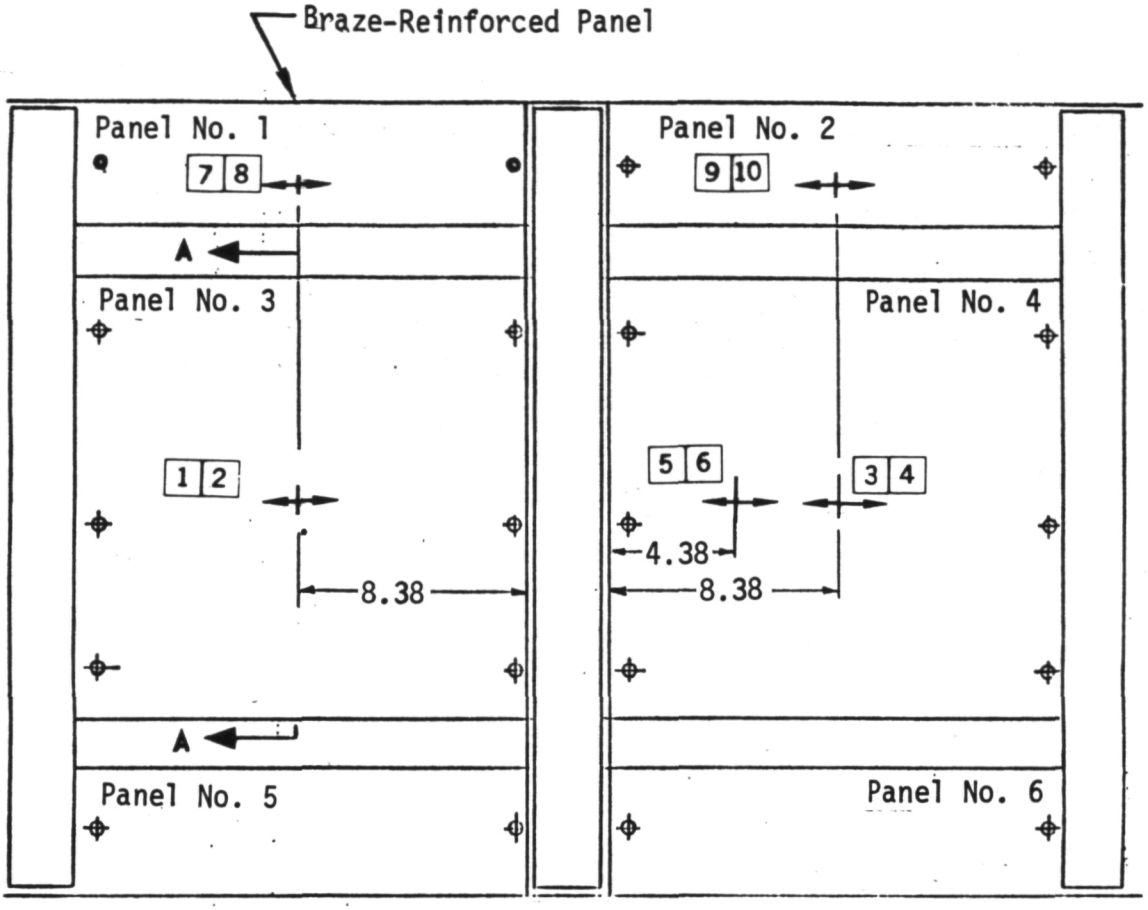

View of External Surface

Dimensions shown in inches.

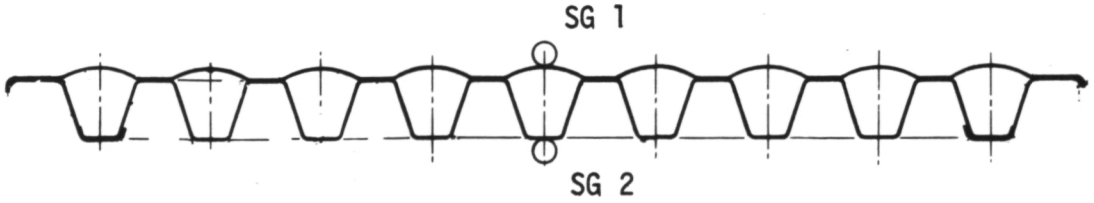

Section A-A (Rotated 90° CW)

Strain Gage Placement Typical for All Locations; Odd Numbered Gages on External Surface, Even Numbered Gages on Internal Surface

Figure 3-10. Strain Gage Locations

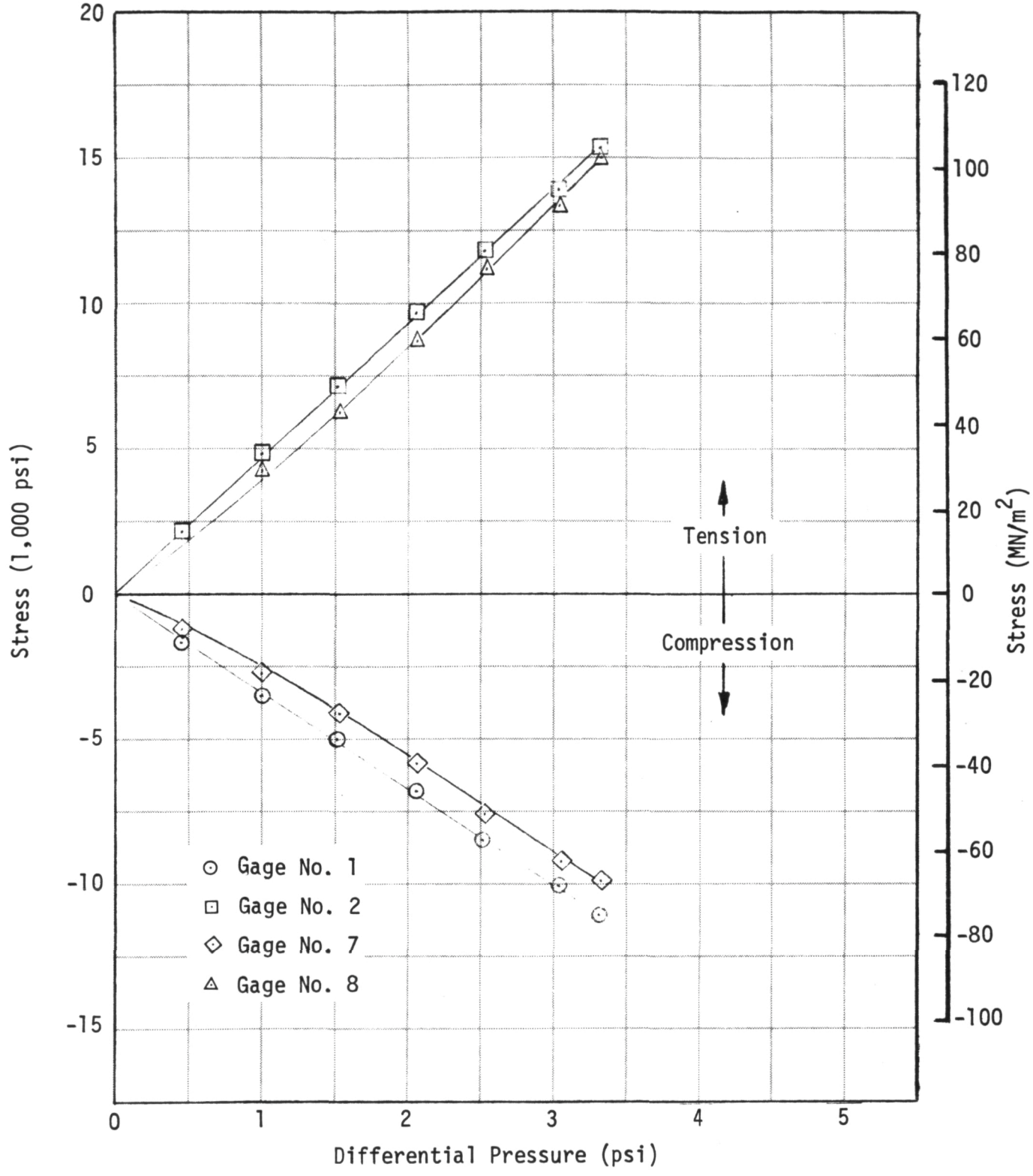

Figure 3-11. Panel Stresses as a Function of Differential Pressure — Gages 1, 2, 7, and 8

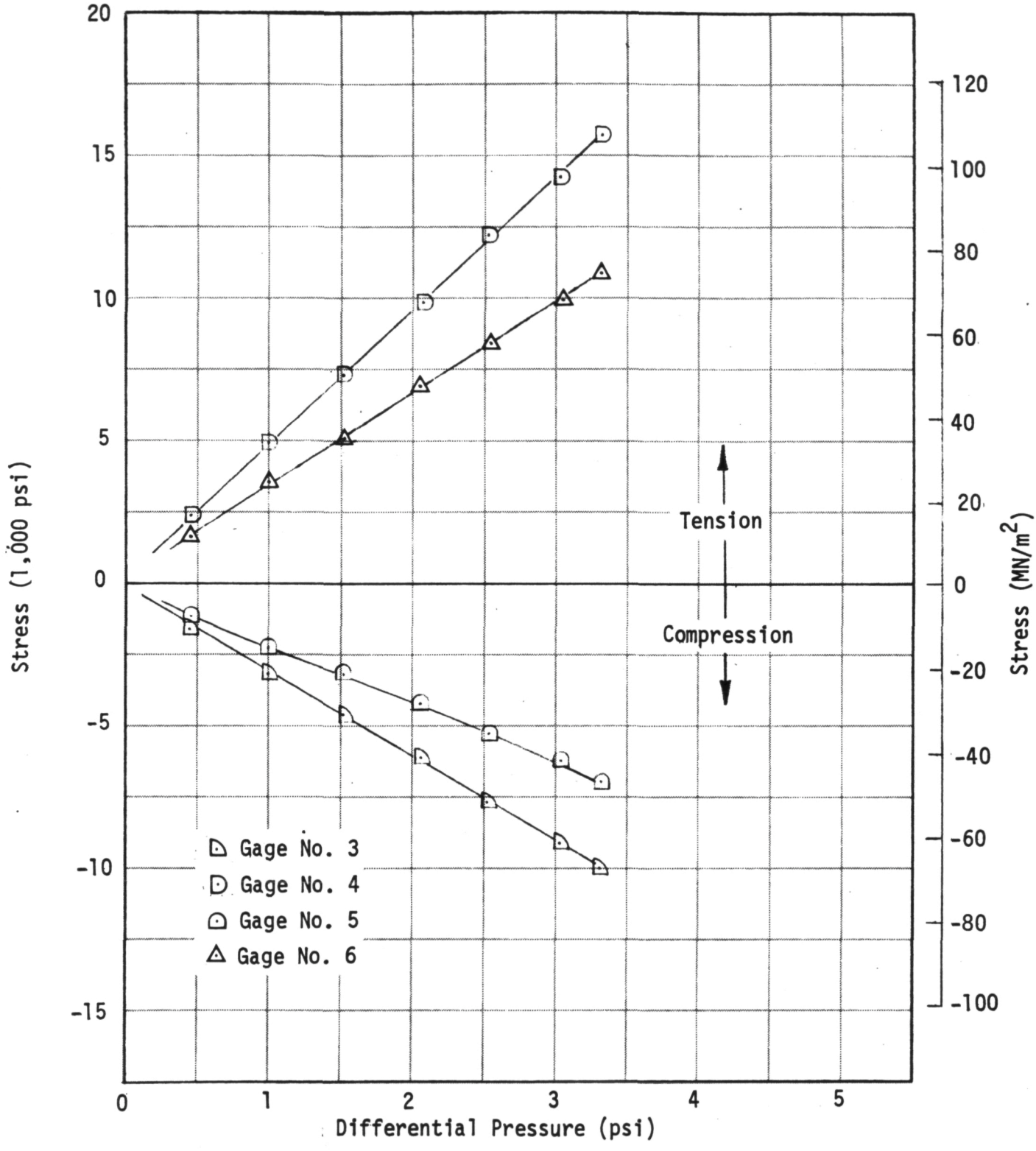

Figure 3-12. Panel Stresses as a Function of Differential Pressure — Gages 3, 4, 5, and 6

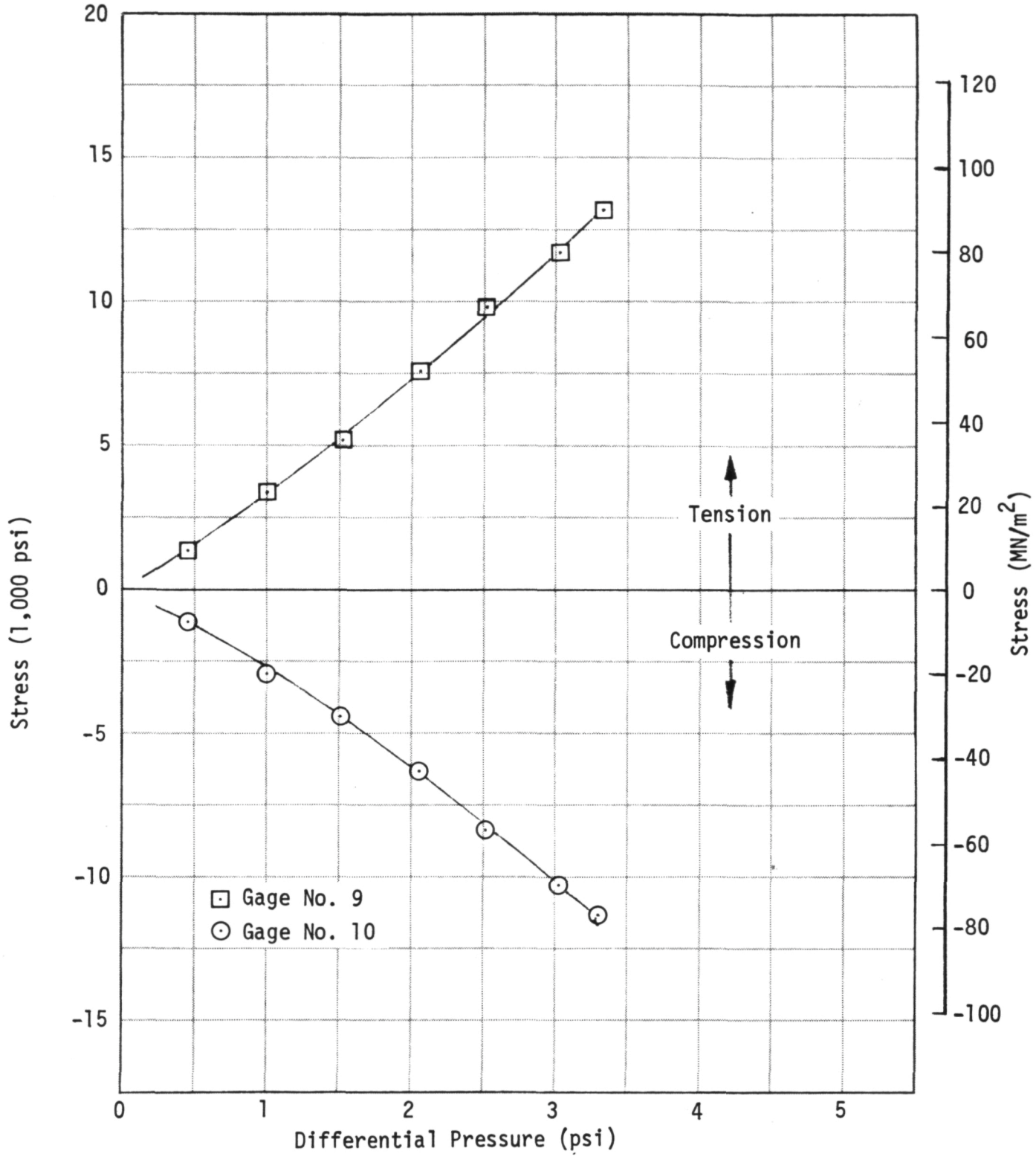

Figure 3-13. Panel Stresses as a Function of Differential Pressure – Gages 9 and 10

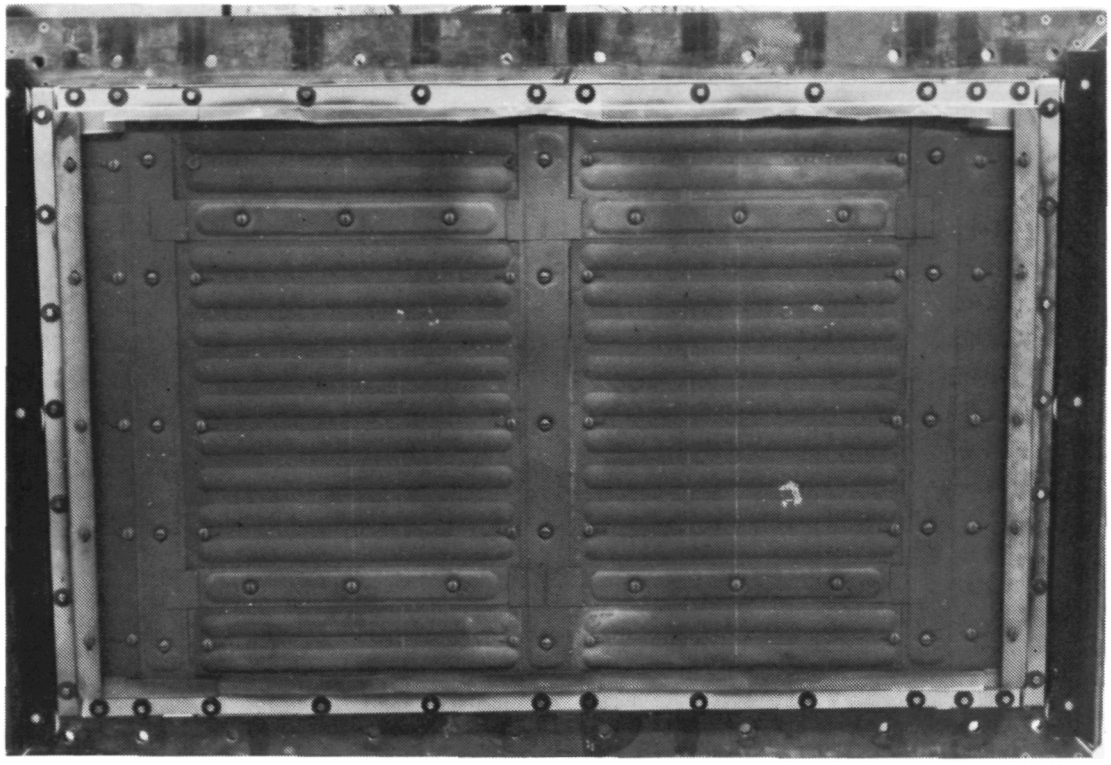

Figure 3-14. Overall View of Test Array After Preliminary Thermal Test

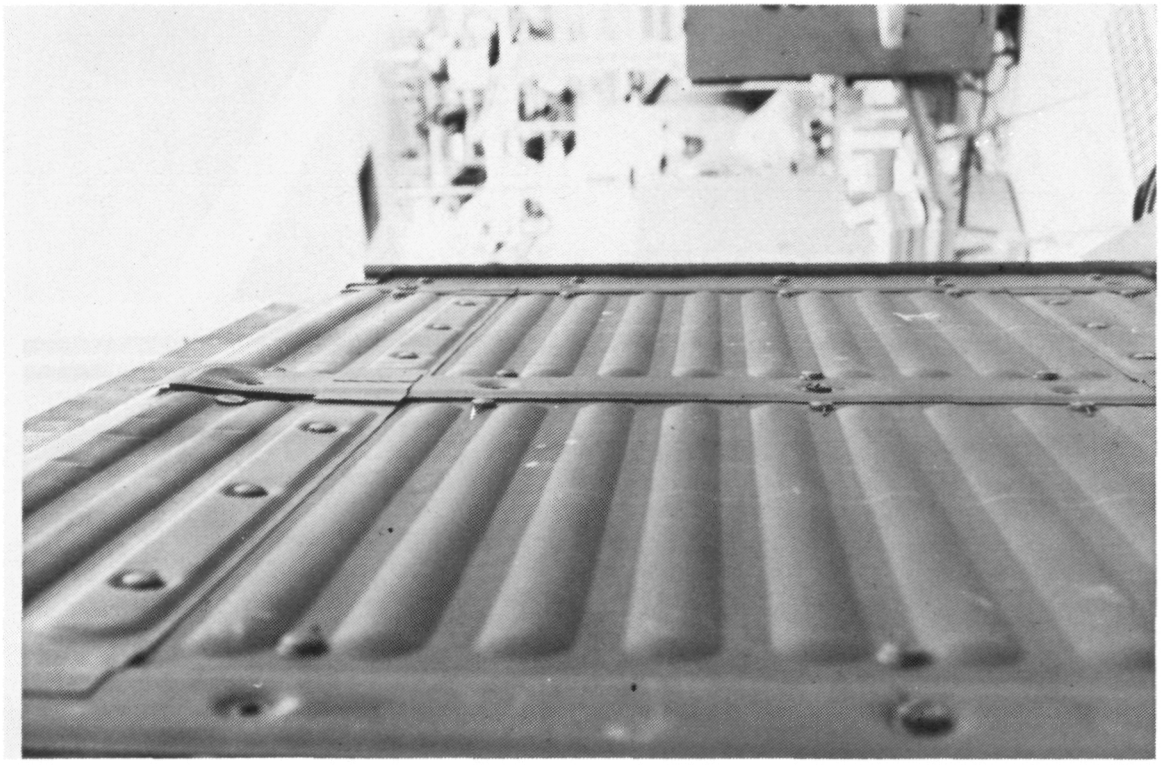

Figure 3-15. Cover Strip Deformation After Preliminary Thermal Test

the lateral edge seals may be seen. The sine-wave shaped buckle in the end of the center transverse cover strip is shown clearly in Figure 3-15 in a photograph taken after the edge seals had been removed along the sides of the test array. Examination of the side close-out panels revealed several fine cracks in the panel face sheets where local bending was induced in the panels when the cover strip buckled. To conduct further examinations of the panel edges and to trim and straighten the cover strip end, the bolts attaching the center cover strip were removed. Figure 3-16 shows the cover strip partially detached. All of the transverse cover strips were then examined for interference with the edge seals, and the ends of the strips were trimmed where necessary. The strips and edge seals were reinstalled, and testing was continued with initiation of combined differential pressure and thermal cycles simulating the Shuttle Orbiter mission profile.

3.3 SIMULATED MISSION CYCLIC TESTS

The first mission cycle was conducted with the objective of checking the control of the programmed pressure and temperature profiles when both were applied

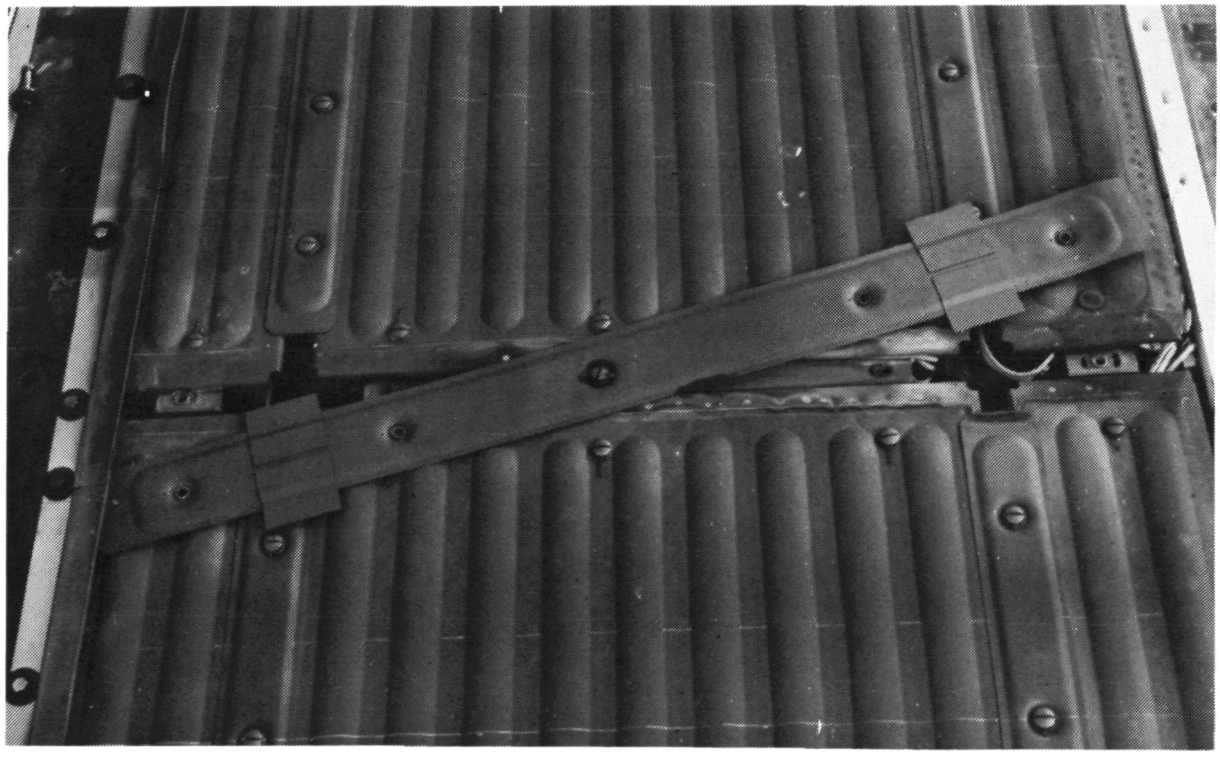

Figure 3-16. Cover Strip Partially Removed

simultaneously. Minor difficulty was encountered in portions of the temperature profile due to failure of some of the control thermocouples. After the first complete mission cycle the test array was removed from the test chamber and the failed thermocouples were replaced. Sufficient space was available to allow the necessary expansion of the transverse cover strips and no further deformations of the cover strip ends were noted. Examination of the panel areas where initial cracking had occurred during the preliminary thermal test showed some additional crack growth. Figure 3-17 presents an overall view of the test array after the first simulated mission cycle, and the areas where face sheet cracks were noted are indicated. Close-up views of two of the areas are shown in Figures 3-18 and 3-19. Several additional face sheet cracks were observed in the main panels at the ends of beads near a panel attach position. The latter cracks, shown in Figure 3-20, were approximately 0.63 cm (0.25 in.) in length. After inspection and thermocouple replacement, the test array was reinstalled in the Space Simulation Chamber and simulated mission test cycles were resumed.

Another inspection of the test array was conducted at the end of the tenth cycle. Some additional growth was noted at existing crack locations as seen in Figure 3-21. The growth that occurred between test cycles 1 and 10 may be noted by comparing Figures 3-18 and 3-21. The maximum damage noted after the tenth test cycle occurred at the end of a side close-out panel. A crack approximately 7.62 cm (3.0 in.) in length, shown in Figure 3-22, was observed across the end of the panel. Smaller cracks, also shown in Figure 3-22, occurred around the ends of the two beads in the panel face sheet. The damage shown in Figure 3-22 was judged to be caused by excessive pressure from the transverse cover strip. Such pressure from the cover strip resulted in local bending in the panel end with high tensile stresses in the face sheet. The inspection conducted at the end of the tenth cycle indicated all damage was local, and therefore additional testing was scheduled.

Testing was continued in the Space Simulation Chamber by applying an additional fifteen test cycles to bring the total number of simulated mission cycles to twenty-five. At this point the test array was removed once again for inspection of the heat shields and instrumentation. Little additional crack

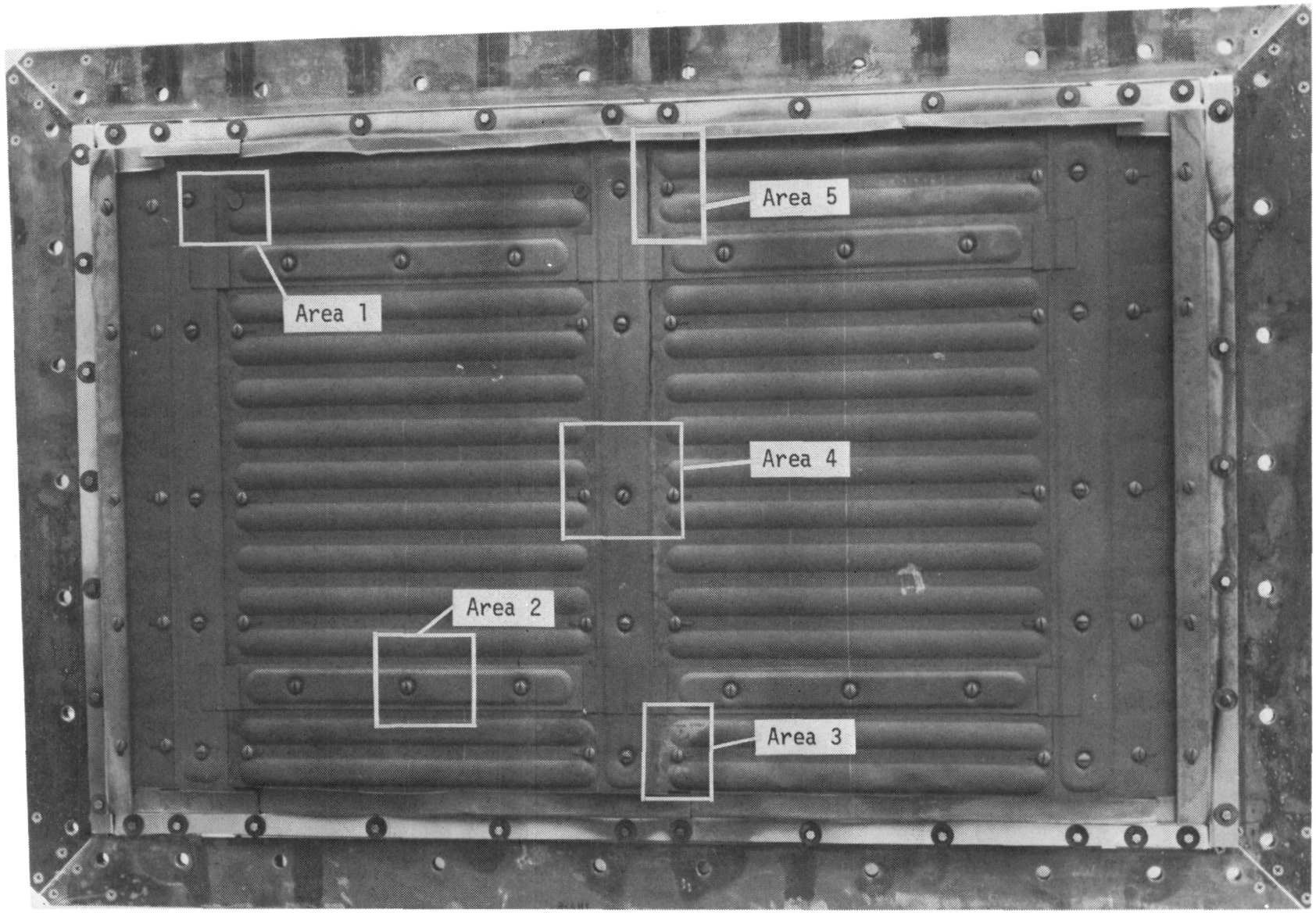

Figure 3-17. Overall View of Test Array After First Mission Test Cycle

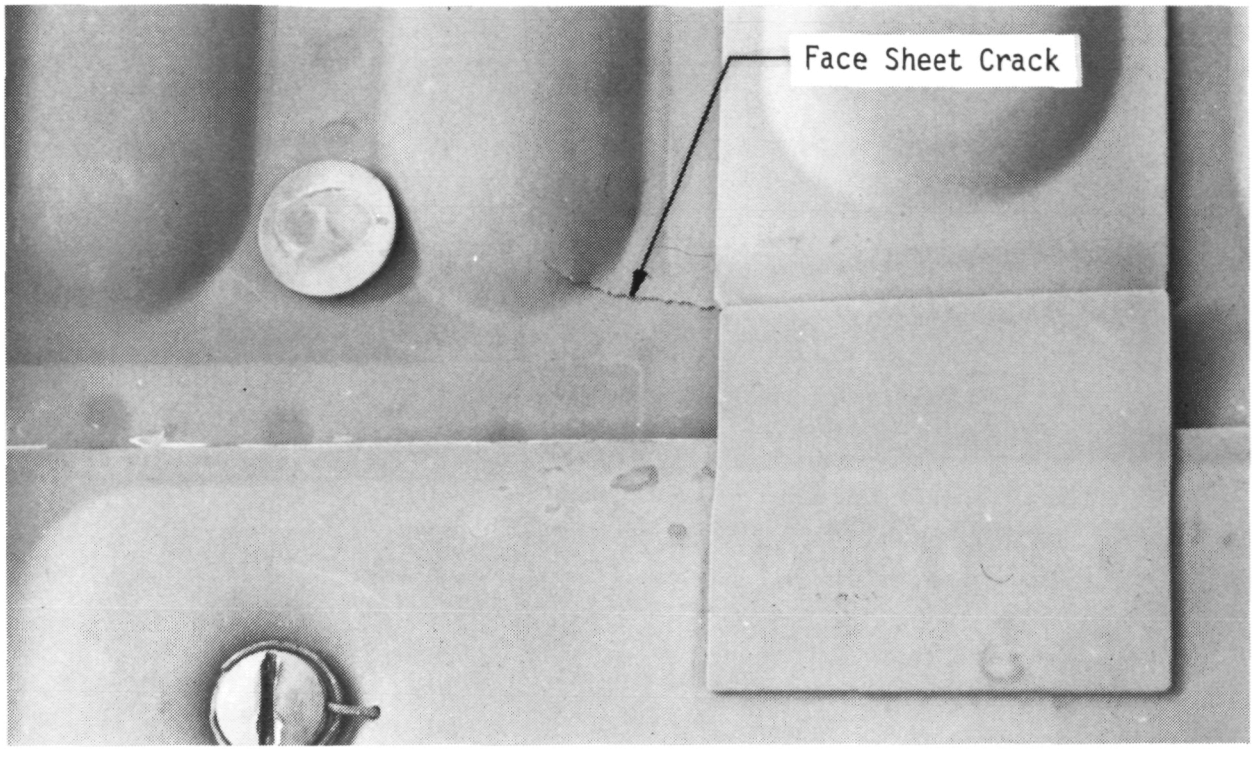

Figure 3-18. Damage In Braze-Reinforced Panel After First Mission Test Cycle

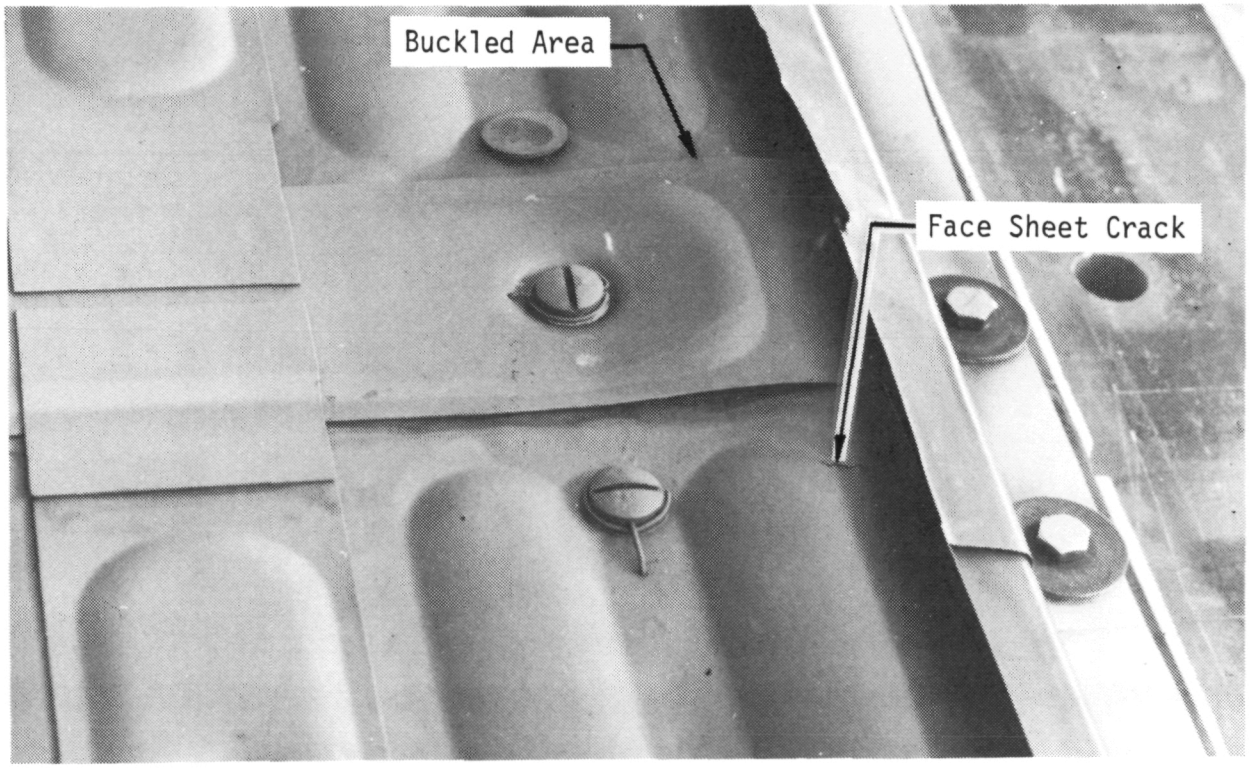

Figure 3-19. Close-up View of Center Transverse Cover Strip (Area 5)

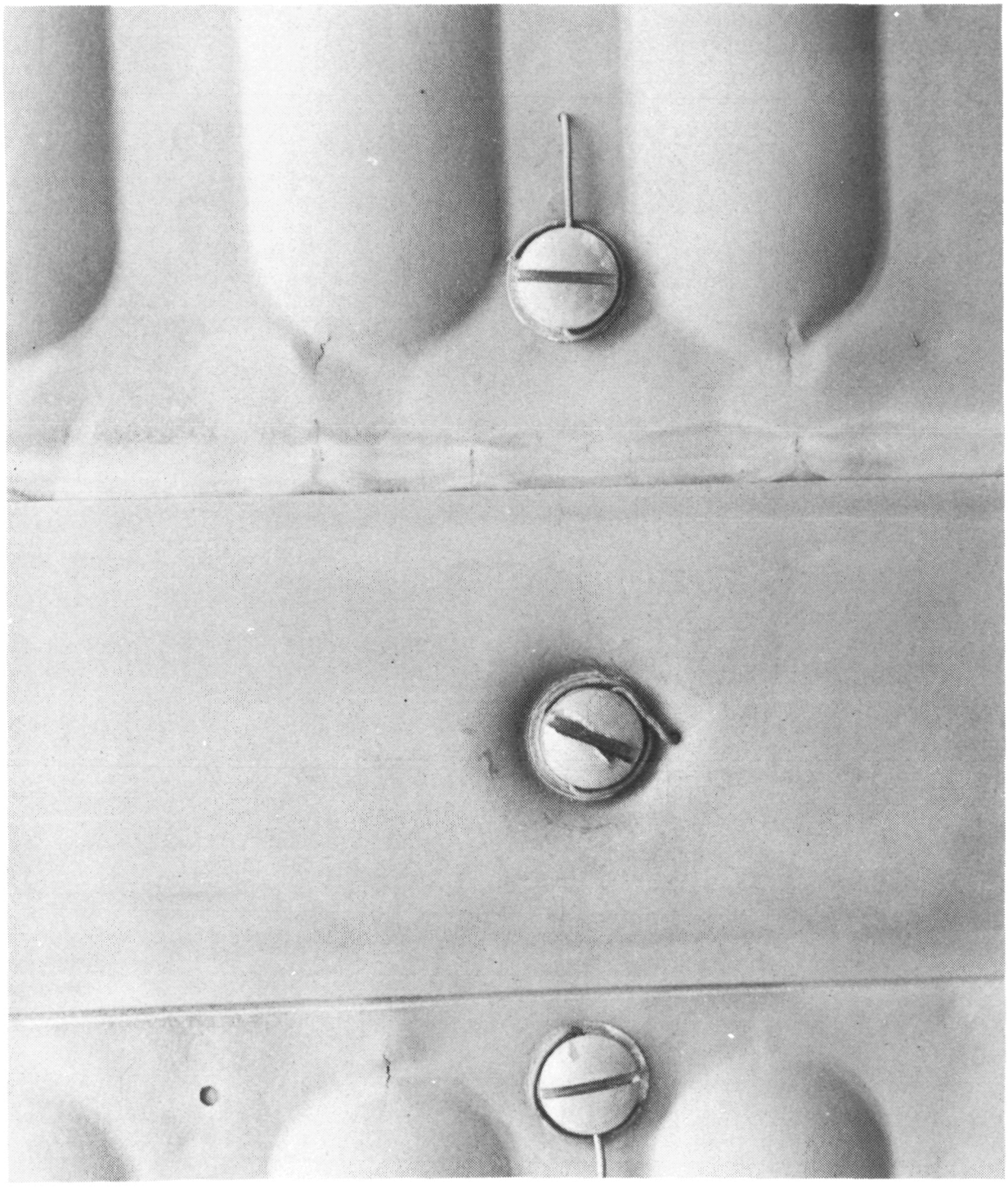

Figure 3-20. Cracks at Bead Ends on Main Panels (Area 4)

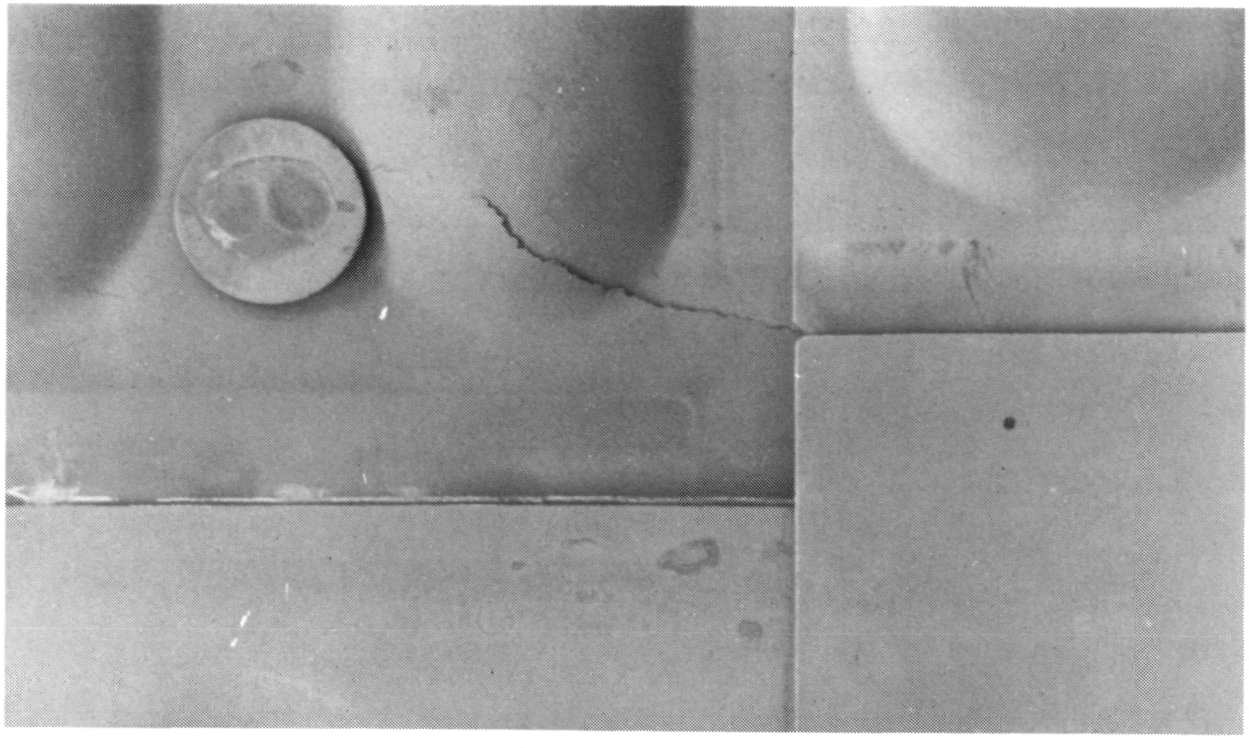

Figure 3-21. Damage in Braze-Reinforced Panel After Tenth Mission Test Cycle (Area 1)

growth was noted on the main panels at the end of the twenty-fifth cycle. Examination of the side close-out panels showed some additional damage in the fracture areas on those panels. Figures 3-23 and 3-24 show areas 2 and 3 (see Figure 3-17) after the twenty-fifth test cycle.

Typical temperature time-histories recorded during tests in the Space Simulation Laboratory are presented in Figures 3-25 through 3-30. Temperatures in the noted figures were recorded during test run number 10, and the values shown are typical of the temperatures recorded in simulated mission pressure and temperature tests conducted with the contractor test array. The programmed external surface temperature is shown in Figure 3-25 for comparison with the panel temperature recorded by thermocouple 1 (Reference Figure 3-3). Comparison of the programmed surface temperature profile with the values of thermocouple 1 shows close adherence of the test array surface temperatures with the test profile. The computed temperature response at the inner surface of the insulation package is also shown in Figure 3-25 for comparison with the data recorded at thermocouple 4. As shown in Figure 3-25, the test temperature on the inner

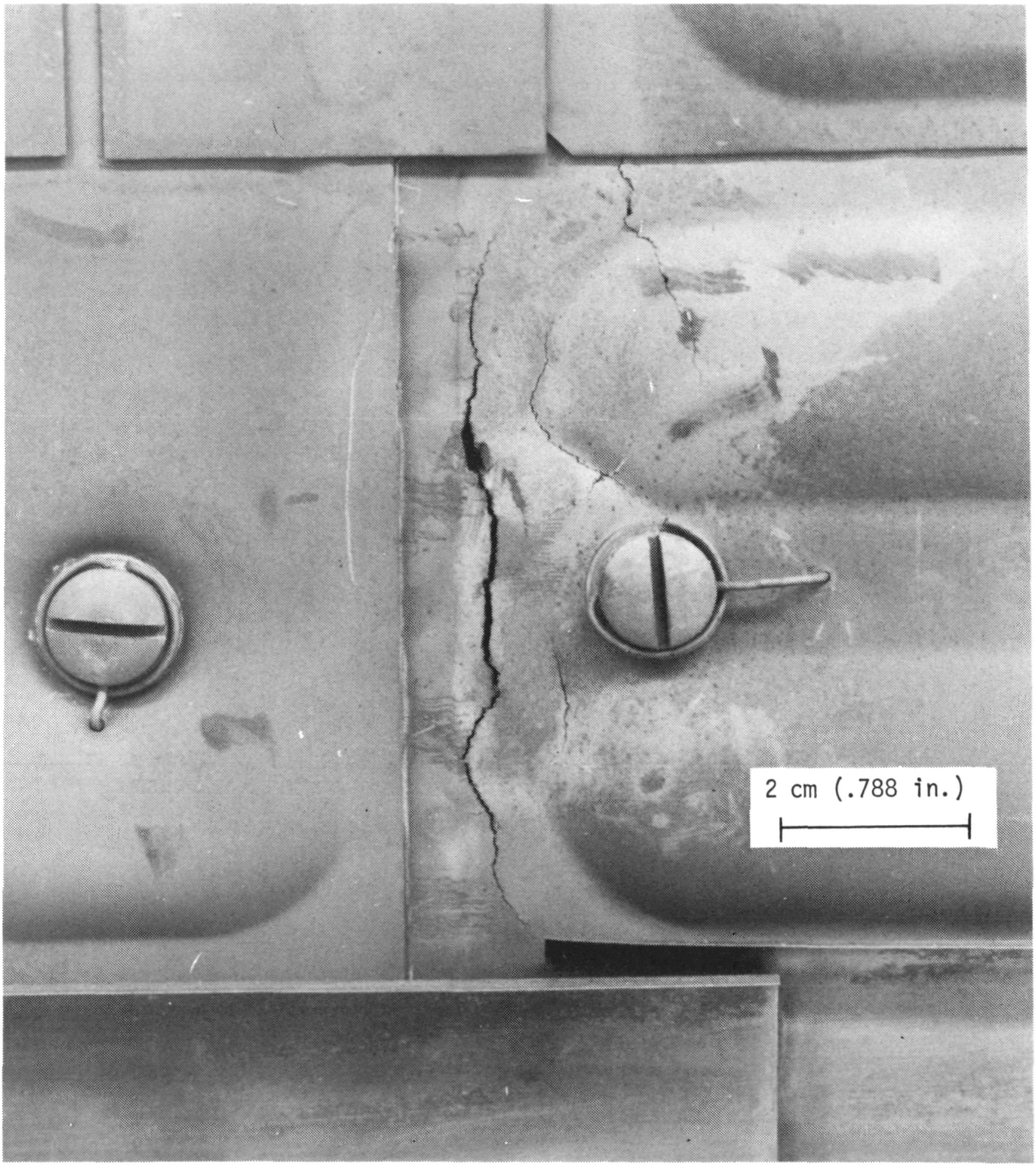

Figure 3-22. Damage in Panel No. 6 After Tenth Mission Test Cycle (Area 3)

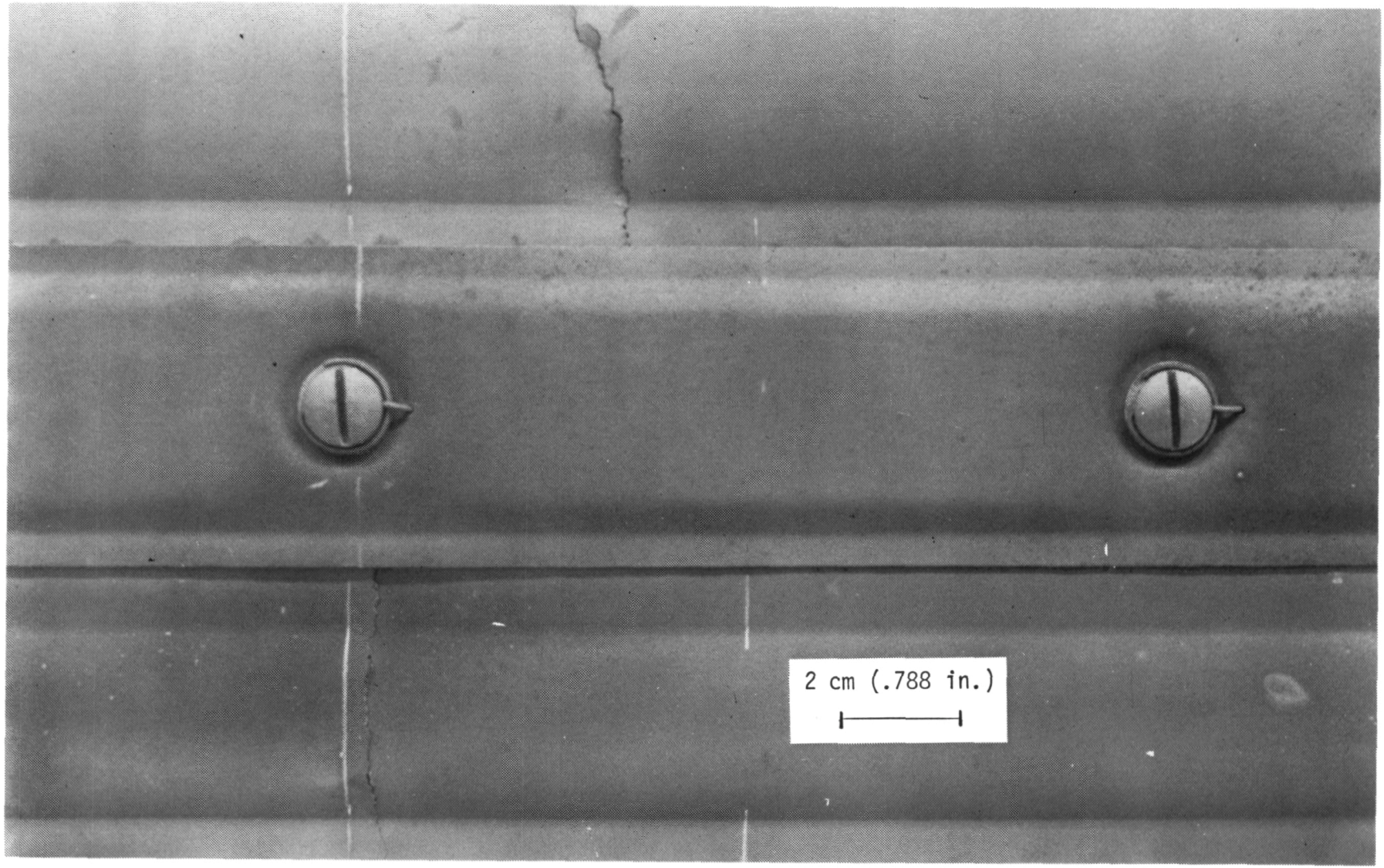

Figure 3-23. Face Sheet Cracks in Area 2 After Twenty-fifth Test Cycle

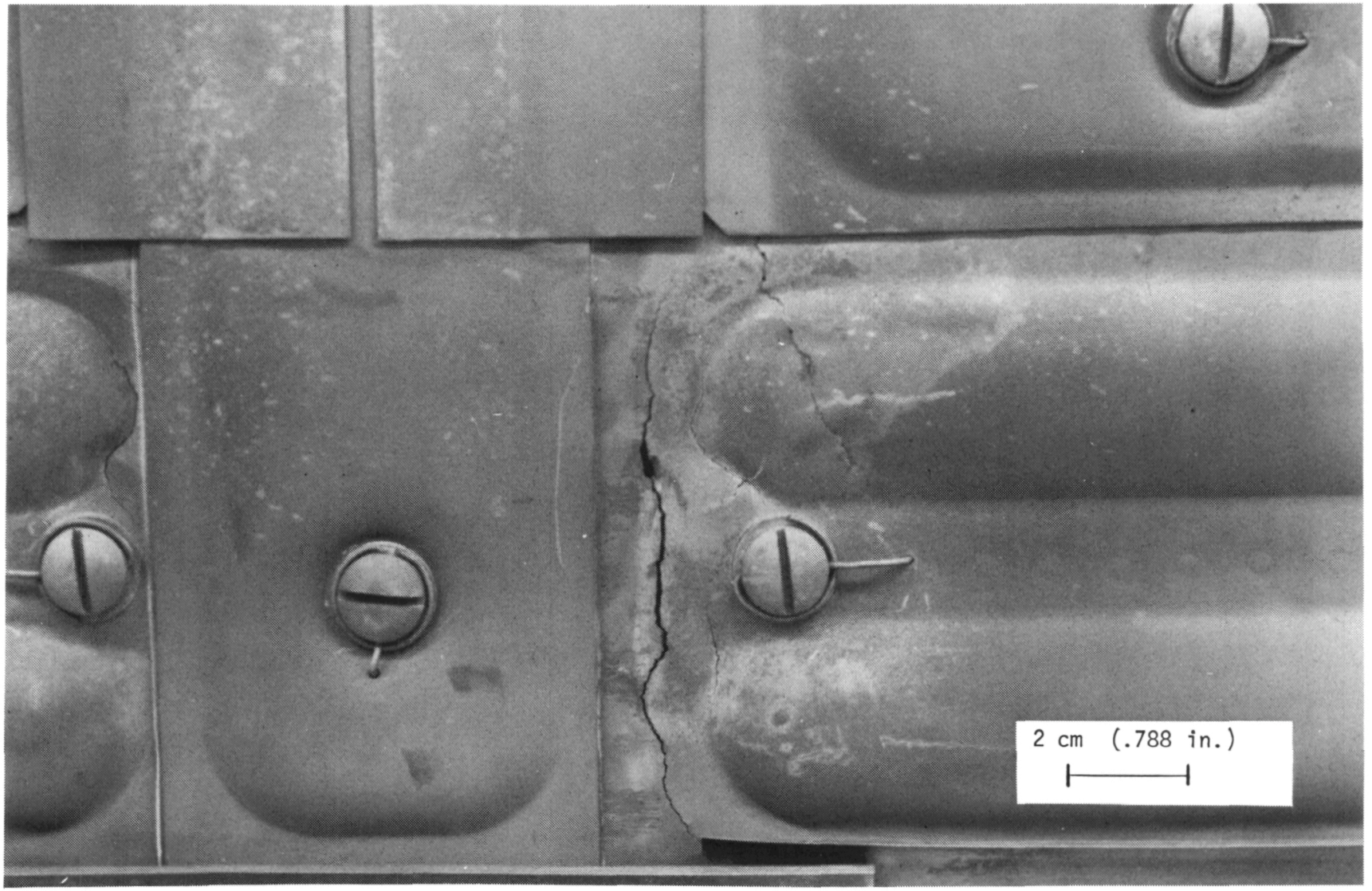

Figure 3-24. Damage in Panel 6 After Twenty-fifth Test Cycle (Area 3)

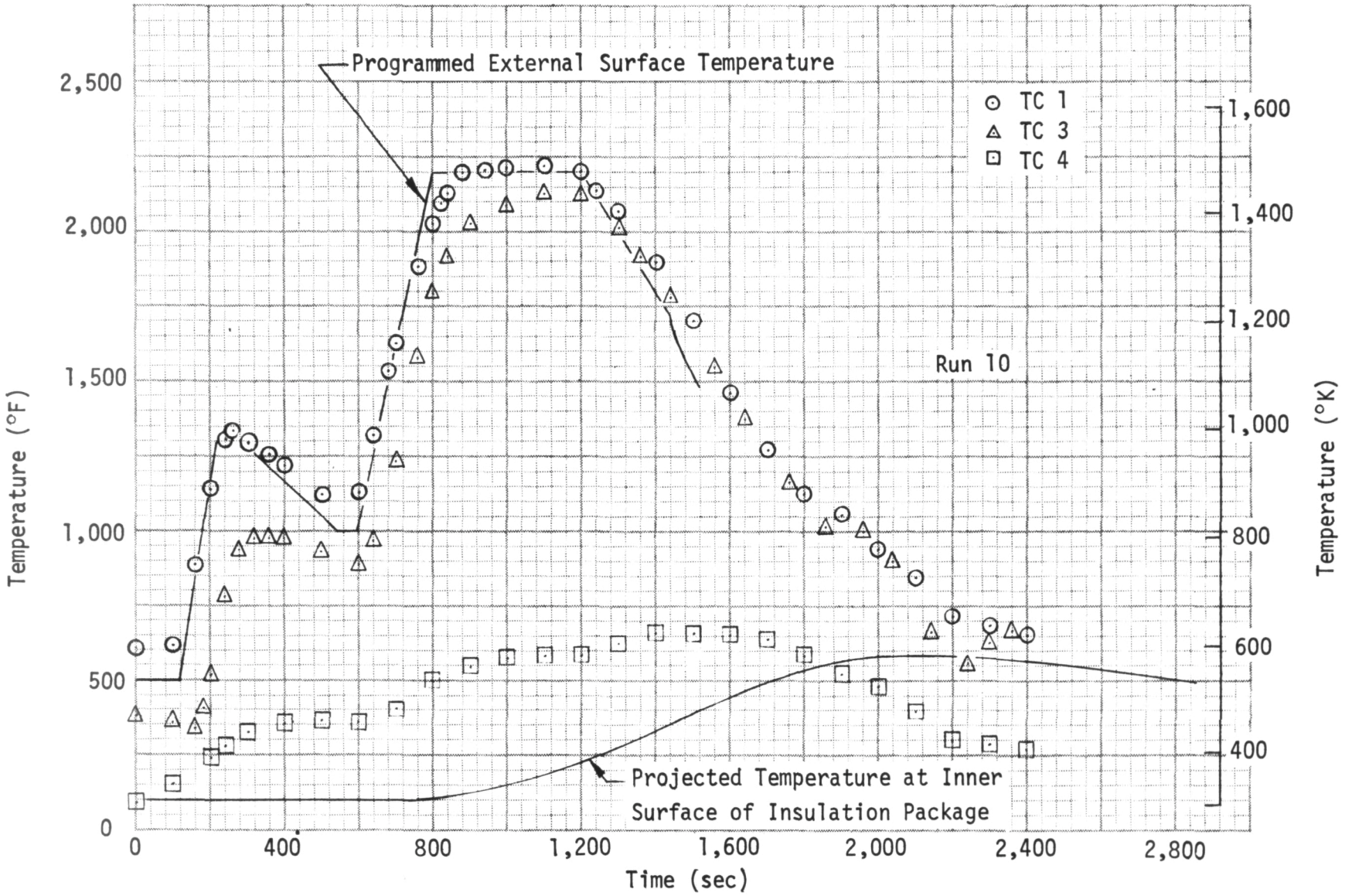

Figure 3-25. Temperature Time-Histories, Thermocouples 1, 3, 4

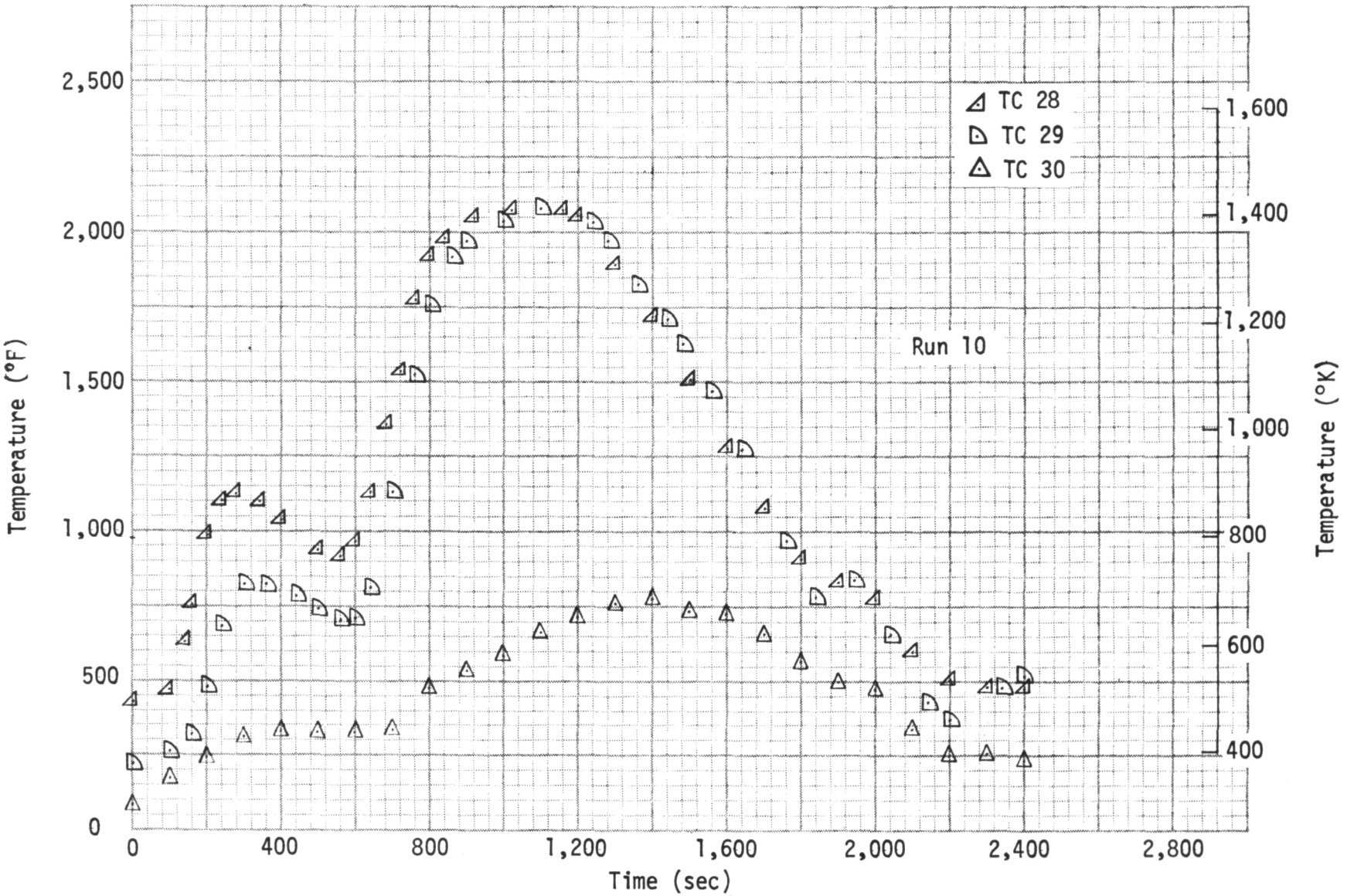

Figure 3-26. Temperature Time-Histories; Thermocouples 28, 29, 30

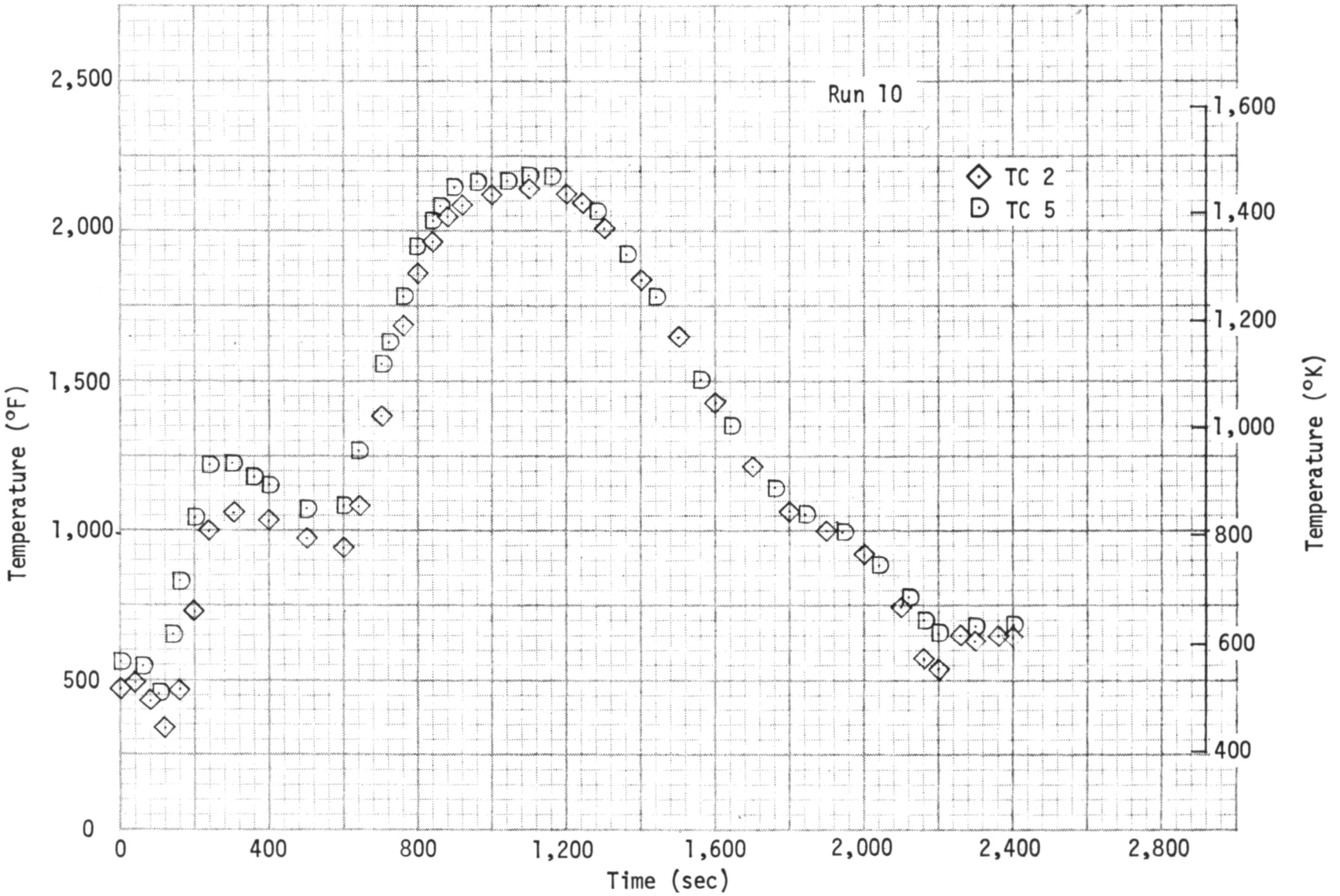

Figure 3-27. Temperature Time-Histories; Thermocouples 2, 5

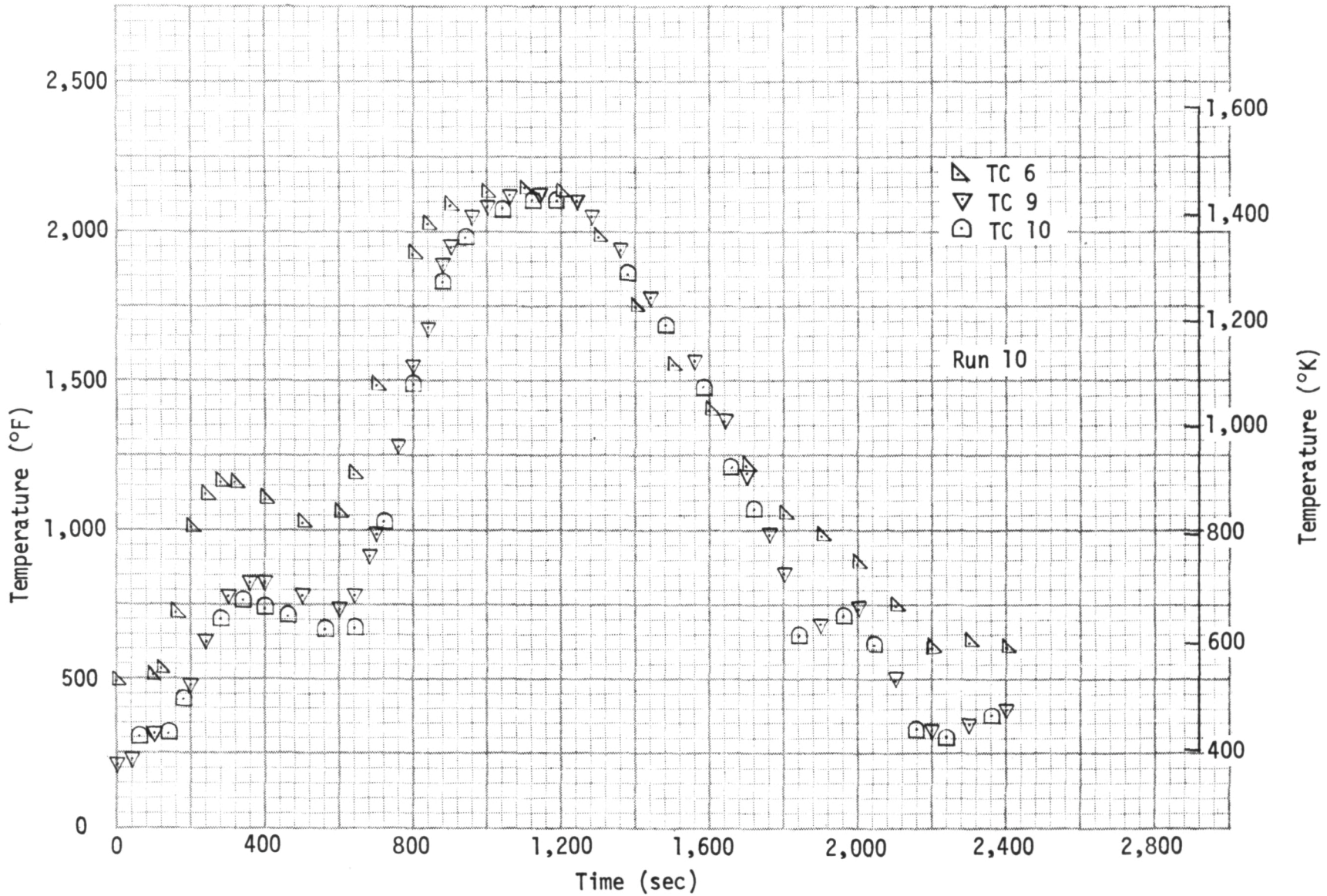

Figure 3-28. Temperature Time-Histories; Thermocouples 6, 9, 10

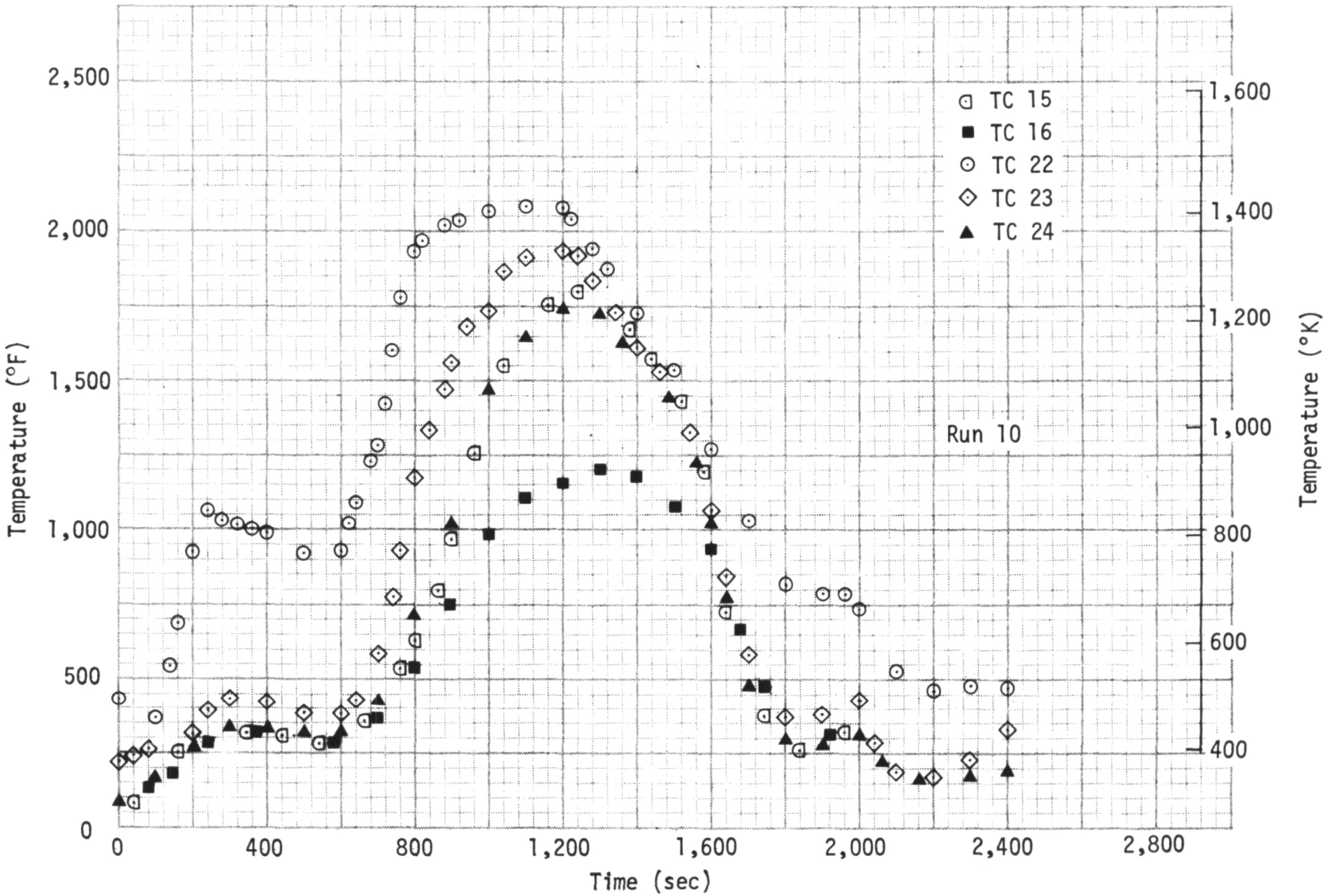

Figure 3-29. Temperature Time-Histories; Thermocouples 15, 16, 22, 23, 24

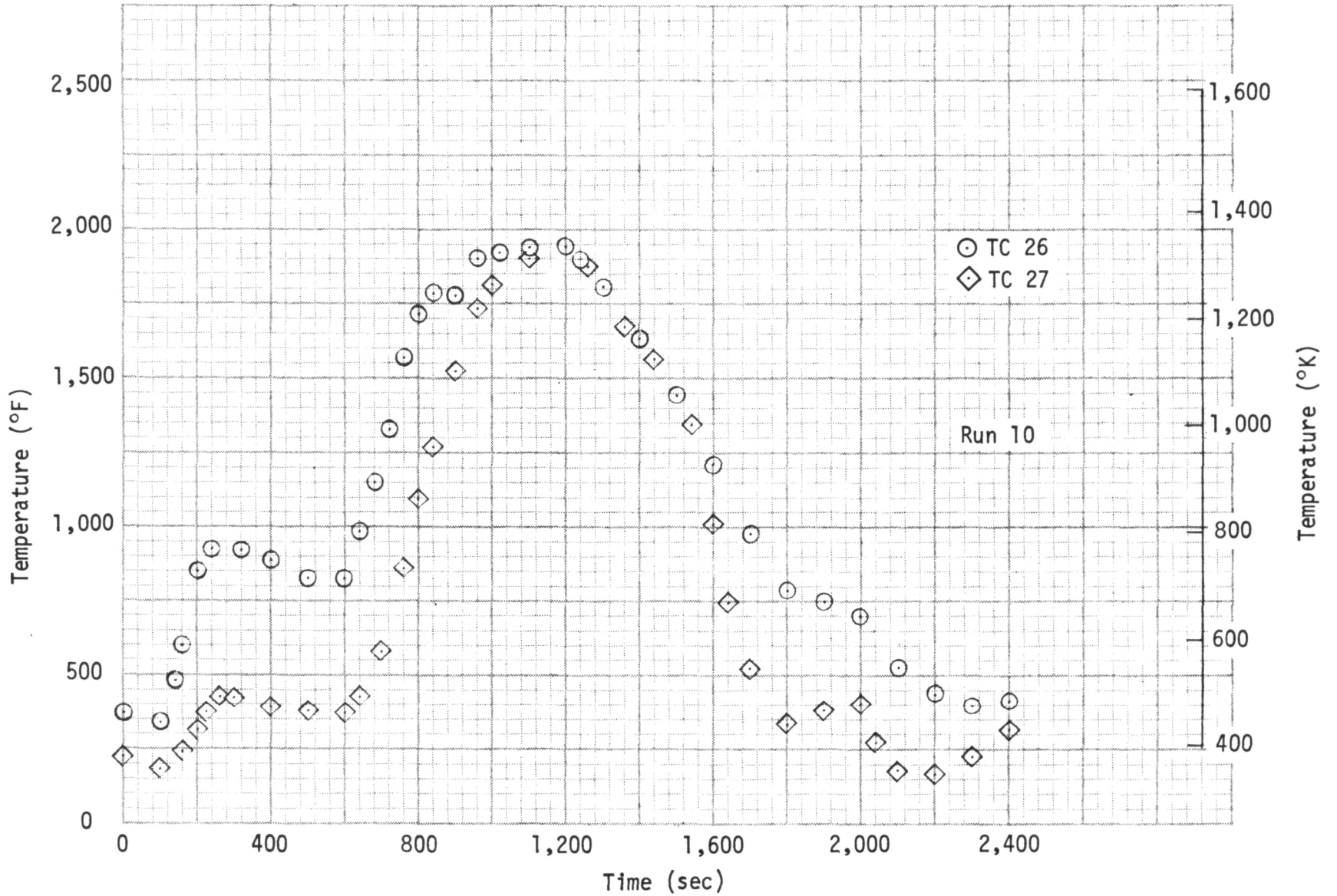

Figure 3-30. Temperature Time-Histories; Thermocouples 26, 27

surface of the insulation peaked earlier and at a slightly higher value than predicted by analysis. Similar temperature responses occurred at the center of the second full-size heat shield, the values there being shown in Figure 3-26 as recorded by thermocouples 28, 29, and 30.

The temperature gradient through the heat shield thickness is shown in Figure 3-27 for a position near the center of panel No. 3 (Reference Figure 3-3). Thermocouple 5 recorded the temperature at the panel surface and thermocouple 2 indicates the temperature at the inner surface of the corrugation stiffener immediately adjacent to the position of thermocouple 5. The maximum gradient through the panel occurs during initial heating, during which time a gradient of approximately 198°K (355°F) was recorded. Gradients near maximum panel temperatures were somewhat less than those shown during initial heating, the maximum gradient when panel surface temperatures were above 1,368°K (2,000°F) being approximately 45°K (80°F). A slight reversal of the gradient occurs during the initial cooldown portion of the test cycle in which the internal temperature at thermocouple 2 is slightly higher than the surface temperature. A maximum reverse gradient of 11°K (20°F) was noted in test run number 10.

The differential pressure recorded in run 10, shown in Figure 3-31, indicates good agreement was maintained with the programmed test profile during a majority of the test run. Pressure drops occurred at two points near the end of the run, both deviations being in non-critical portions of the profile. The data of Figure 3-31 are typical of all test runs conducted in the Space Simulation Chamber during Phase II tests.

After inspection of the heat shields following the twenty-fifth thermal and differential pressure cycle, the test array was moved intact to the Acoustics Laboratory where it was mounted in the test chamber for simulated lift-off acoustic environment tests. The acoustic spectra, shown in Figure 3-2, simulated the projected engine noise at liftoff with an overall sound pressure level of 160 db. The duration of the simulated liftoff acoustic level was selected as 30 seconds for each mission.

The test array, including its holding fixture, was mounted in the acoustic test chamber so that it formed one of the side walls in a rectangular chamber

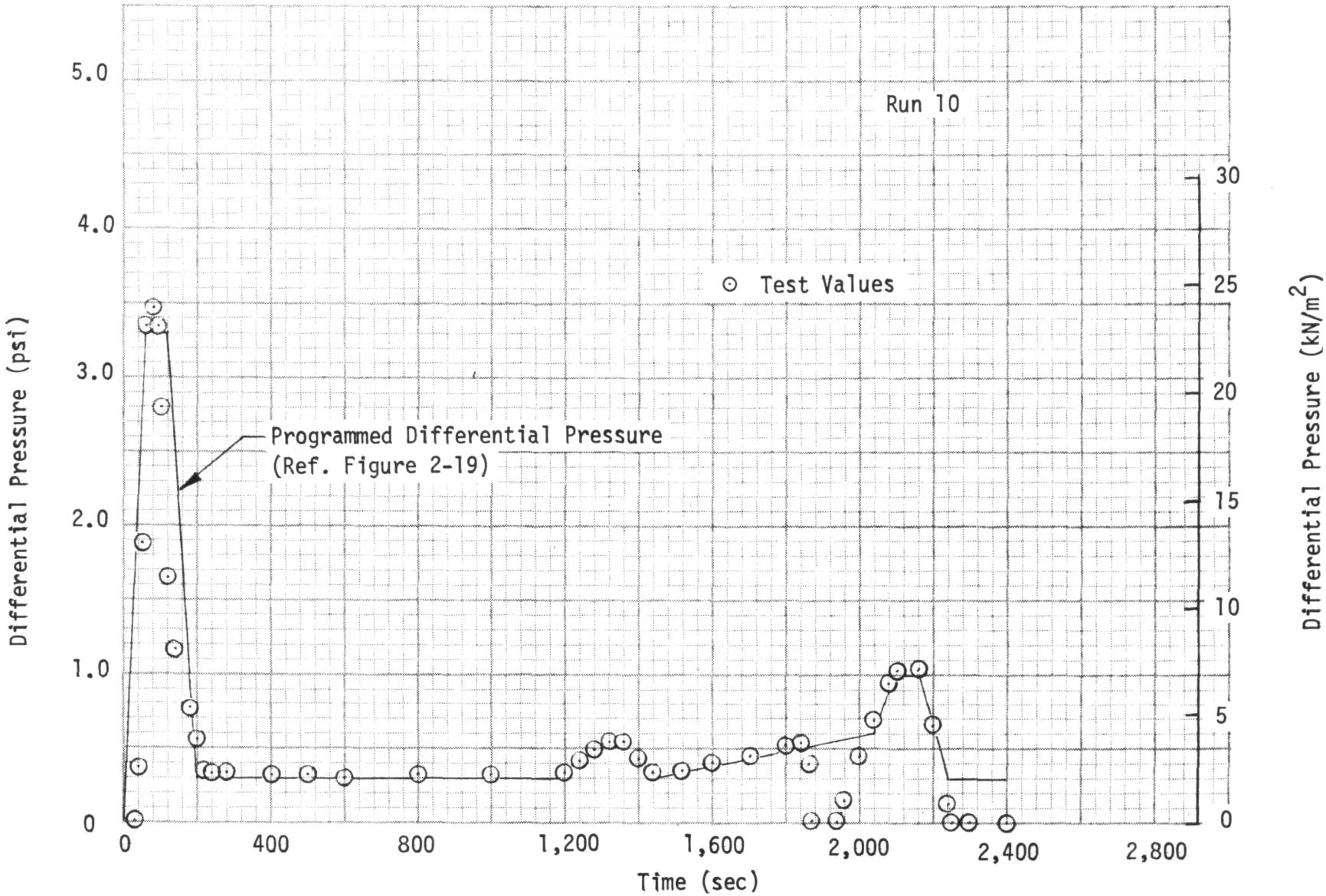

Figure 3-31. Differential Pressure Time-History

which was open at one end and attached to two exponential horns at the other end. The test chamber was approximately 2.14 m (7.0 ft.) in length, 1.22 m (4.0 ft.) in height, and .61 m (2.0 ft.) in width. Existing cracks in the heat shields were marked at their ends so that increases in fracture damage during the acoustic tests could be easily noted.

The initial test at 160 db was conducted for 1.5 minutes, after which the test was stopped and the test array was inspected. No additional damage could be detected in the visual inspection, and testing was resumed. An additional 11.5 minutes of acoustic test time was applied to the test array to simulate a total of 12.5 minutes, the equivalent of 25 missions. Inspection of the array was again made, and no further crack growth could be noted in the heat shields. The tests were continued until a total of 25 minutes of acoustic exposure at 160 db had been reached. Inspections at that point again showed no visible increase in crack lengths on the panels. An additional 25 minutes of testing at 160 db overall sound pressure level was conducted to provide a total of 50 minutes of simulated liftoff acoustic noise levels. Thus, 100 missions were simulated in the acoustic tests. Inspection of the test array was made again, and one of the spring-loaded covers for the recessed fasteners on the braze-reinforced panels was found to have vibrated free and fallen from the assembly. Examination of the cover showed no failure in the part. The areas that had been damaged during testing in the Space Simulation Laboratory were examined visually at the termination of the acoustic tests, and crack lengths were compared with the markings made at the crack tips prior to the start of the acoustic tests. From the examinations made, no crack progression could be detected at any of the previously damaged areas.

3.4 COST STUDIES

Cost studies were conducted to develop projected initial TPS costs, refurbishment rates, and overall TPS unit cost for 100 missions. Refurbishment and cost data were developed for several replacement rates, and results from contractor tests of the full-scale, full-size TPS array were then reviewed to select projected refurbishment requirements and overall costs.

TPS cost studies were based upon fabrication of a TD Ni-20Cr metallic shield system of the same type as produced in Phase II for tests in the Langley 8-ft. HTST and the TPSTF facility. The TPS arrays for Langley test facilities incorporated single-face corrugation-stiffened TD Ni-20Cr heat shields attached to TD Ni-20Cr pylon supports. TD Ni-20Cr fasteners were used to attach the panels and cover strips, and packaged low-density fibrous insulation was installed between the heat shields and the substructure. The panel face sheets, corrugations, and edge members were joined by resistance spot welding to form the assembled heat shields. Similarly, resistance spot welding was employed in joining the panel support members. All cost studies included heat shield panels, panel supports, fasteners, panel cover strips, and insulation packages. The primary structure was not included in the cost studies.

To define costs peculiar to a TD Ni-20Cr radiative thermal protection system, a nominal surface area of 122.5 m^2 (1,320 ft^2) was selected as the vehicle area sustaining temperatures requiring TD Ni-20Cr shields. The same area was previously used in Phase I studies of meteoroid impingement effects on TD Ni-20Cr heat shields (Appendix E, Reference 2). A nominal size of 50.8 by 50.8-cm (20 by 20-inches) was selected for the heat shields, a size that corresponded to the test array panel size in Phase II tests. Thus, 470 TD Ni-20Cr panels were required per vehicle. Six orbiter vehicles were considered as the initial quantity produced, with heat shield requirements for six vehicles being 2,820 panels. A spare panel inventory of 10 percent was assumed, bringing total initial heat shield production to 3,102 panels.

Projected initial TPS costs included the recurring fabrication costs of labor and materials plus non-recurring tooling costs attributable to tooling design, materials and tooling fabrication. No engineering design, development, test, and evaluation costs were included in the cost studies. TD Ni-20Cr material costs were based upon the most recent commercial prices charged for sheet and bar material. Such prices ranged from $100 per pound to $125 per pound, with the higher price being charged for thin gage sheet material such as 0.0254-cm (0.010-inch) thick sheet. A scrappage rate of 25 percent was applied to all TD Ni-20Cr parts. Thus, a factor of 1.25 was applied to weights of finished components to determine the required purchased material.

Refurbishment cost studies were also conducted to define total costs over the span of 100 missions. Refurbishment costs included manhour costs for inspection and replacement of heat shields, replacement of other TPS parts (fasteners, supports, insulation), and additional costs for fabricating the required replacement panels and parts. Based on results from tests with both subsize and full-size TD Ni-20Cr heat shields, the criterion for replacement of a panel was detection of cracks in the heat shield. Manhours required for inspection and refurbishment operations were based on study results presented in Reference 7 for metallic radiative thermal protection systems.

Removal and replacement manhours were based upon observed times in initial assembly and check-out operations of the full-size test arrays combined with component removal operations during tests. As described subsequently, removal and replacement manhours observed in this program agreed closely with those presented in Reference 7. Repair of the TD Ni-20Cr heat shields was not considered feasible since the panel damage observed in both Phase I and Phase II tests occurred predominantly as cracks in the 0.0254-cm (0.010-inch) thick face sheets or edge members. Consequently, replacement of panels or other TPS components was considered as the only refurbishment operation for the TD Ni-20Cr TPS with the criterion for replacement being detection of cracking in the heat shield, support structure, or attachment parts.

Refurbishment costs were defined for heat shield replacement rates per mission of 1 percent, 2 percent, 4 percent, and 6 percent. For an assumed replacement rate of 1 percent per mission, each vehicle would have its entire array of TD Ni-20Cr heat shields replaced by the end of 100 missions. For a 2 percent replacement rate, an entire set of 470 panels would be used as replacements by the end of 50 missions. Panel requirements per vehicle are presented in Figure 3-32 as a function of replacement rate and number of missions. The initial complement of panels in Figure 3-32 reflects the assumed 10 percent spares inventory. Phase I and Phase II test results from contractor tests of TD Ni-20Cr TPS arrays showed a minimum replacement requirement for components other than the external heat shields. Consequently, a replacement rate for support structures, insulation, and fasteners was selected as one-tenth the rate for heat shield panel replacement.

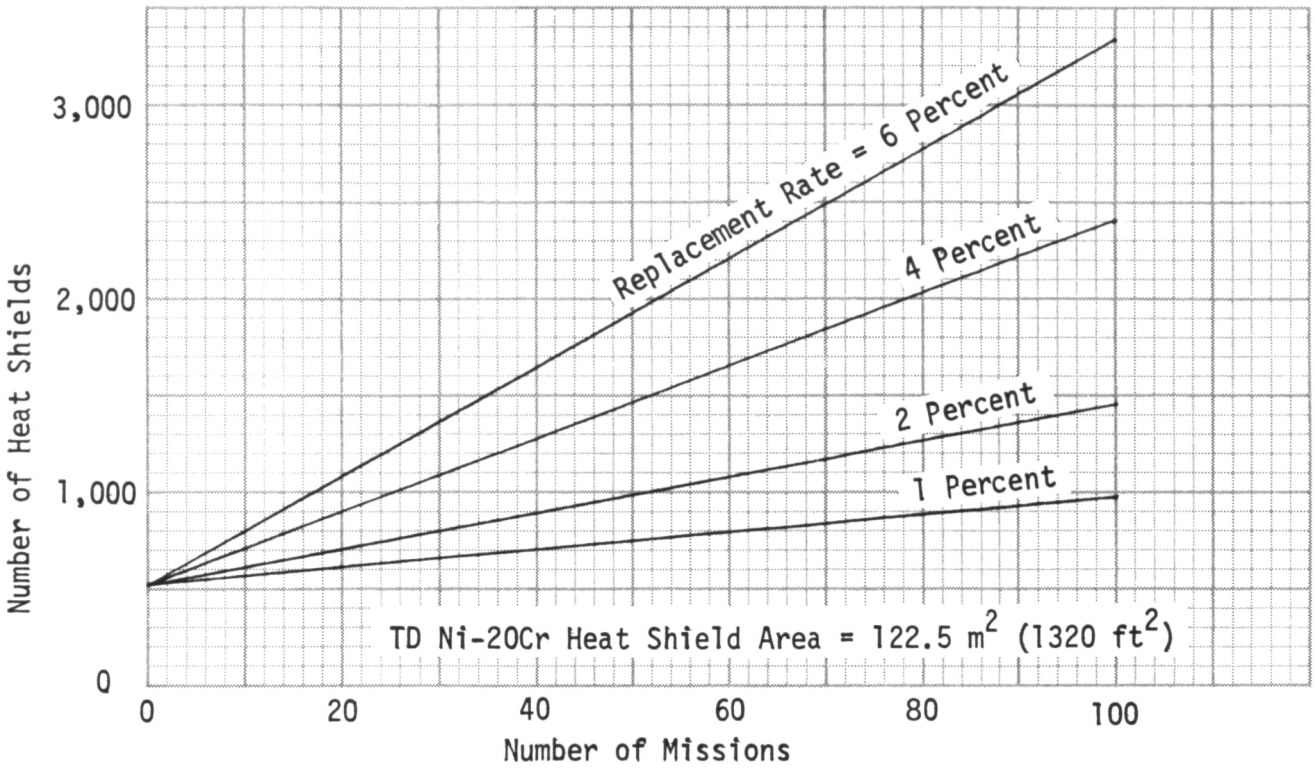

Figure 3-32. TD Ni-20Cr Heat Shield Requirements Per Vehicle

The assumptions made in projecting the initial TPS costs and the ensuing refurbishment costs are summarized as follows:

A. TD Ni-20Cr heat shields cover an area of 122.5 m^2 (1,320 ft^2) on each of six orbiter vehicles. An individual heat shield planform size of 50.8 by 50.8-cm (20 by 20-inches) was assumed.

B. The TPS configuration and fabrication approaches used for cost studies were the same as those applied in Phase II test arrays designed for the Langley 8-ft HTST and the TPSTF facilities.

C. Projected initial cost was based on recurring fabrication costs and non-recurring tooling costs. Design, development, test and evaluation costs were not included in cost projections.

D. A 10 percent heat shield spares inventory is maintained.

E. Refurbishment manhour requirements are based on study results presented in Reference 7.

F. Replacement of support structures, fasteners, and insulation occurs at one-tenth the rate of panel replacement.

The TD Ni-20Cr TPS costs per vehicle are shown in Figure 3-33 as a function of number of missions and replacement rate of heat shields. Figure 3-34 presents the TD Ni-20Cr TPS costs per vehicle in terms of unit costs, or dollars per unit surface area.

Test results from both phases of the program were reviewed to define a projected replacement rate for heat shields in a TD Ni-20Cr thermal protection system applicable to the Shuttle Orbiter. Design deficiencies in the attachment design of the Phase I test panels were considered significant in a majority of the damage incurred during the early portion of Phase I testing. Similarly, test fixture restrictions were considered to have contributed largely to the early damage incurred by the contractor test array in Phase II tests. As a result of test evaluations, a replacement rate of four percent was selected as a projected rate for the TD Ni-20Cr TPS. A replacement rate of four percent per flight would require 2,397 panels to be manufactured per vehicle, or a total of 14,382 heat shields for six vehicles.

Initial costs were independent of replacement rate, and from Figure 3-34 the initial unit cost is projected as $721 per square foot of TPS surface area. The projected initial cost, as well as refurbishment cost projections, are based on 1974 dollars. As also shown in Figure 3-34, the unit cost per vehicle for 100 missions would be $1,943 per square foot for the projected refurbishment rate of four percent per flight.

3.5 DESIGN ADEQUACY AND LIFE EXPECTANCY

Results from Phase II tests conducted by MDAC were used to assess the adequacy of the TPS design and to evaluate life expectancy for TD Ni-20Cr heat shields in Shuttle applications. The evaluations for design adequacy and life expectancy were both closely related to assessment of reburbishment costs discussed in Section 3.4.

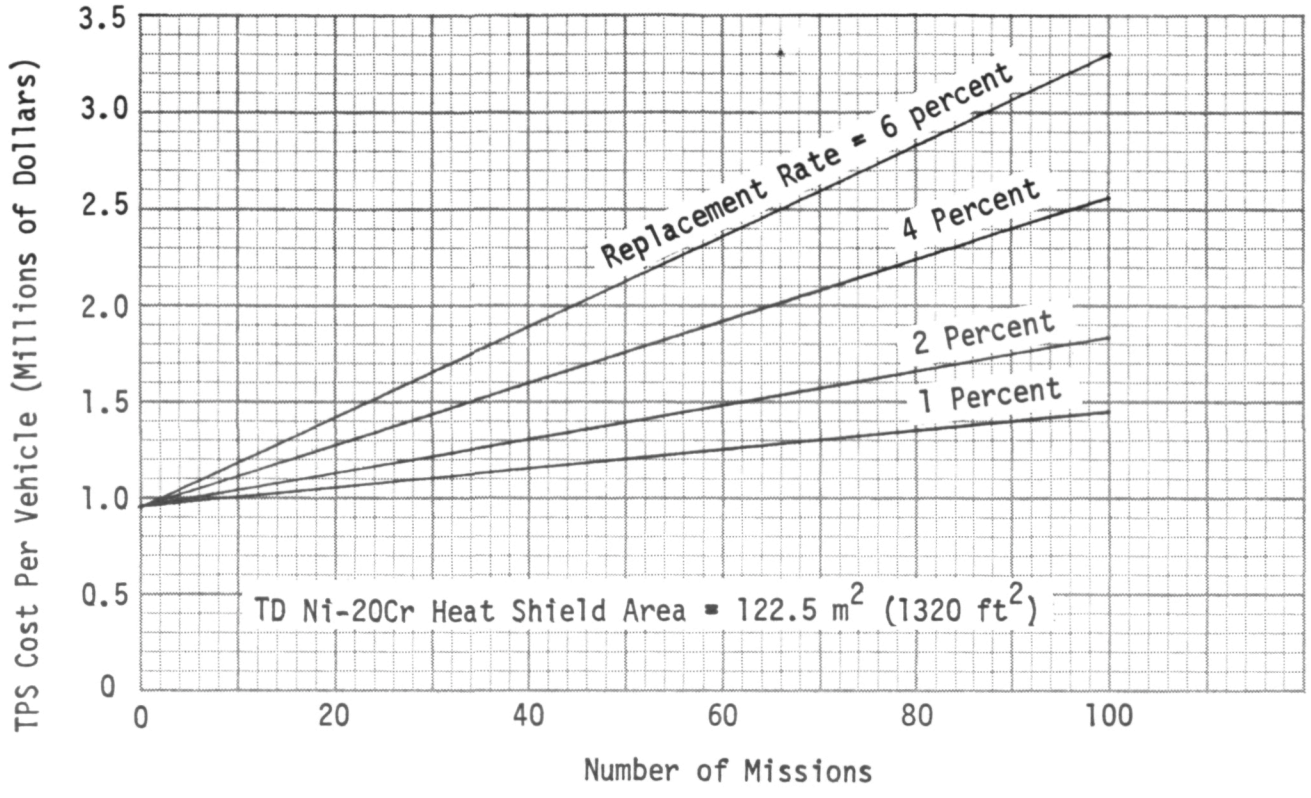

Figure 3-33. TD Ni-20Cr TPS Costs Per Vehicle

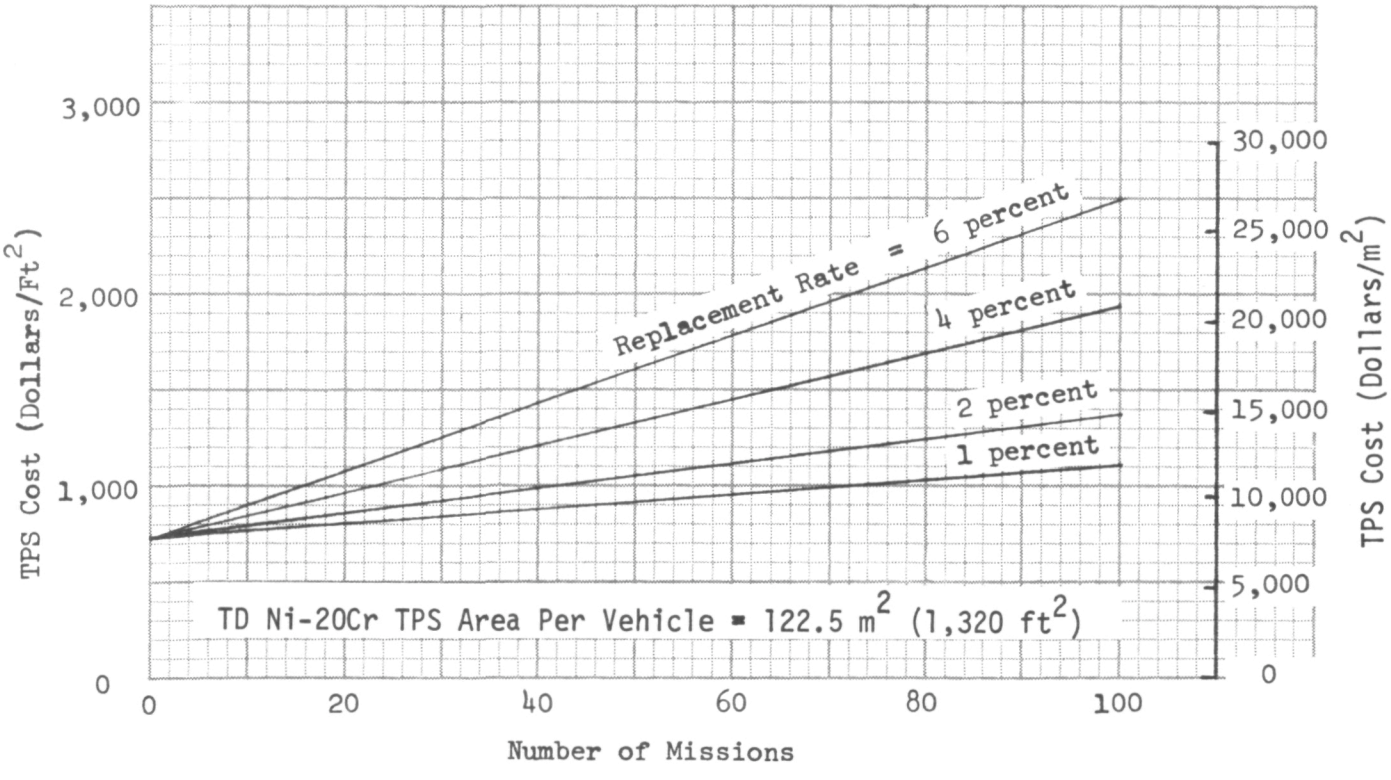

Figure 3-34. TPS Unit Cost Per Vehicle

The TD Ni-20Cr heat shield design developed in this program was considered to be a viable basic approach that has the following desirable features:

A. Removal and replacement of any individual panel may be made without loosening or removing adjacent panels.

B. The surface heat shields are relatively low in weight with high stiffness in bending and torsion. Unit weight for the panels in the contractor test array was 7.09 kg/m^2 (1.45 lb/ft^2) including closure strips and fasteners.

C. The fasteners were secured externally. This approach eliminated the need for locknuts or internal lockwiring, both of which were considered to cause higher maintenance and refurbishment costs.

Improvements to the heat shield design were considered desirable in two specific areas. Firstly, an improved method of positioning the cover strips should be incorporated in the design to prevent inducing bending moments near the panel edges where the cover strips are seated on the heat shield's external surface. Secondly, an improved fastener design is required that would incorporate a self-locking feature and would be shorter in length to reduce fastener weight. Additional studies and tests should also be conducted with the objective of decreasing the number of fasteners per unit area. Such a reduction could reduce weight, initial cost, and refurbishment costs.

Average life expectancy for the TD Ni-20Cr heat shields was based on the performance of the main panels in tests conducted at McDonnell Douglas. In such tests the main panels showed significantly less deterioration than shown by the side close-out panels. The poorer performance of the close-out panels was due primarily to deformation of the cover strips near their ends that resulted from interference by the test fixture seals. In contrast, the cover strips in the area of the main test panels appeared to suffer no deformation, and consequently the main heat shields showed only minor degradation during tests. Coinciding with a replacement rate of four percent, the average heat shield life expectancy was projected as 12 to 15 missions.

3.6 INSTALLATION AND INSPECTION EVALUATIONS

Installation requirements and ease of replacement were assessed for the Phase II heat shield design and attachment system. Evaluations of panel installation were based on experience in the initial assembly of the three test arrays and in disassembly and reassembly operations conducted with the contractor test array during testing at the Space Simulation Laboratory.

Installation of the heat shields was considered to be relatively simple, the basic steps being placement of the panel on the heat shield supports, alignment of the retaining nuts with the panel holes, installation of six retaining bolts, and lockwiring the bolts externally. Installation time ranged from 25 to 30 minutes per panel. Cover strips were then added to close the expansion space between panels, each cover strip requiring three bolts that were also lockwired externally. For flight vehicle installation, an average of two cover strips per heat shield would be required. Installation time per cover strip ranged from 4 to 5 minutes in the observed assembly operations with the test array. Total installation time per panel, including cover strip installation, ranged from 33 to 40 minutes. Panel removal time was more difficult to assess because removal operations involved other components such as edge seals or close-out panels. Also, only partial removal of some components was required in most instances. Estimates for panel removal times, while not as firmly defined as those for installation, were judged to be in the same range as installation times. The total time for removal and replacement of the TD Ni-20Cr heat shields ranged from 66 to 80 minutes (1.10 to 1.33 hr.). In terms of manhours per square foot, the removal and replacement time ranged from 0.42 to 0.51 hr/ft^2. The panel removal and replacement times observed in this program compare favorably with those reported in the studies of Reference 2, in which the projected removal and replacement time for 20-in. by 20-in. metallic radiative panels was 0.47 $manhours/ft^2$.

Inspections of panels and other components were performed at various stages during fabrication and assembly of the test arrays. Basic inspection procedures included visual inspection of the detail parts to find obvious defects and dimensional checks to assure accuracy within specified tolerances. In addition to the basic inspection procedures, NDT techniques were evaluated for effectiveness in finding defects and in assessing the suitability of parts and assemblies containing minor defects. Three types of defective parts were noted during early fabrication efforts in building the three full-size, full-scale test arrays. The first type consisted of out-of-tolerance parts that were easily detected by basic inspection procedures. The second type of defect consisted of fine cracks that occurred in the early development stages of some formed parts. During development of the formed parts, a number of fine cracks were detected by visual inspection with the use of a 10X magnifying glass. More extensive examinations were also conducted with dye-penetrant checks of areas that are particularly susceptible to cracking in TD Ni-20Cr formed parts, such areas being the heel lines of contours on hydropress-formed parts and the external surfaces of brake-formed straight bends. A sample development part checked by dye-penetrant inspection is shown in Figure 3-35. Dye-penetrant inspection proved to be an exceptionally good technique for detecting very fine cracks in formed parts. Forming tools were changed where necessary during development work by increasing the radii at bead edges and other critical areas to eliminate cracks in the parts.

The third type of defect consisted of material expulsion at spot welds on the main heat shield panels and on the closeout panels. This condition can be caused by slight changes in spotweld machine settings or by changes in material thicknesses within a sheet of material. Tests were previously conducted to evaluate radiography as an NDT method for detecting expulsion at spot weld positions in panel assemblies. Defective spot welds were produced by intermittantly using above normal current settings on the spot welder so that expulsion occurred on some of the spot weld positions. The defective panel was x-rayed and the resulting x-ray was examined for indications of defective positions on the panel. Sections which appeared to show expulsion were subsequently cut from the panel and micrographs of the

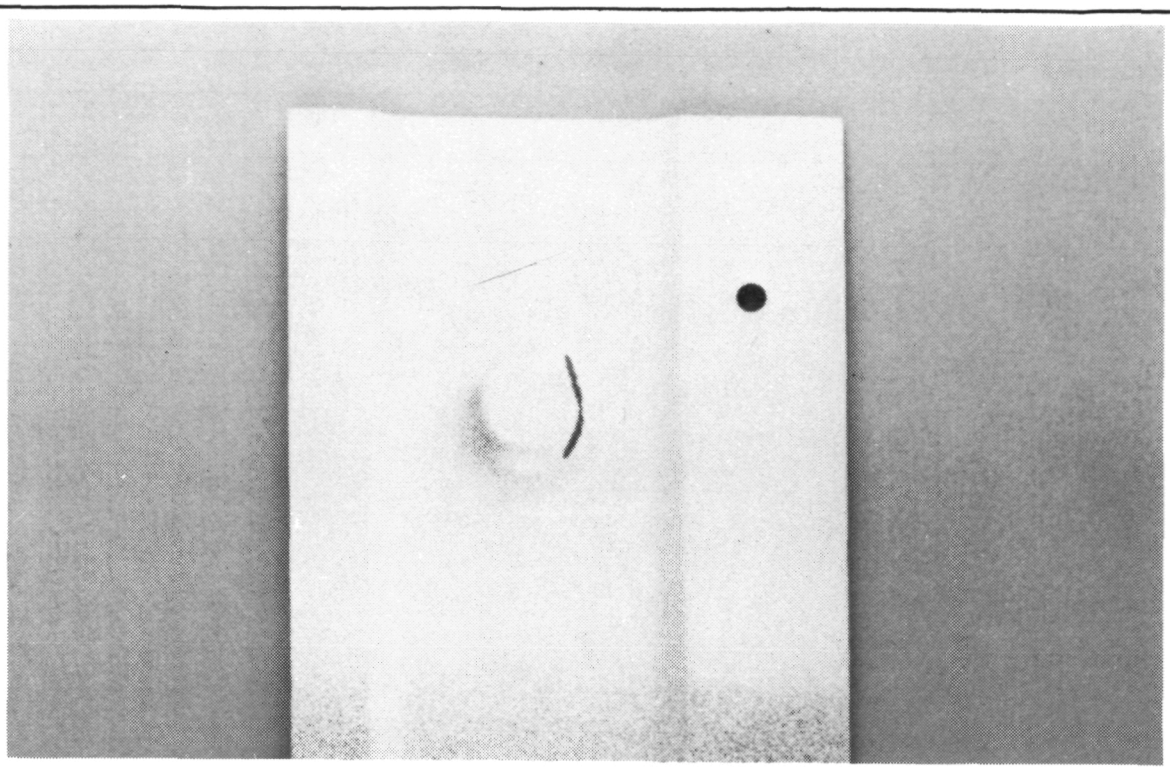

a. Overall View of Area With Crack

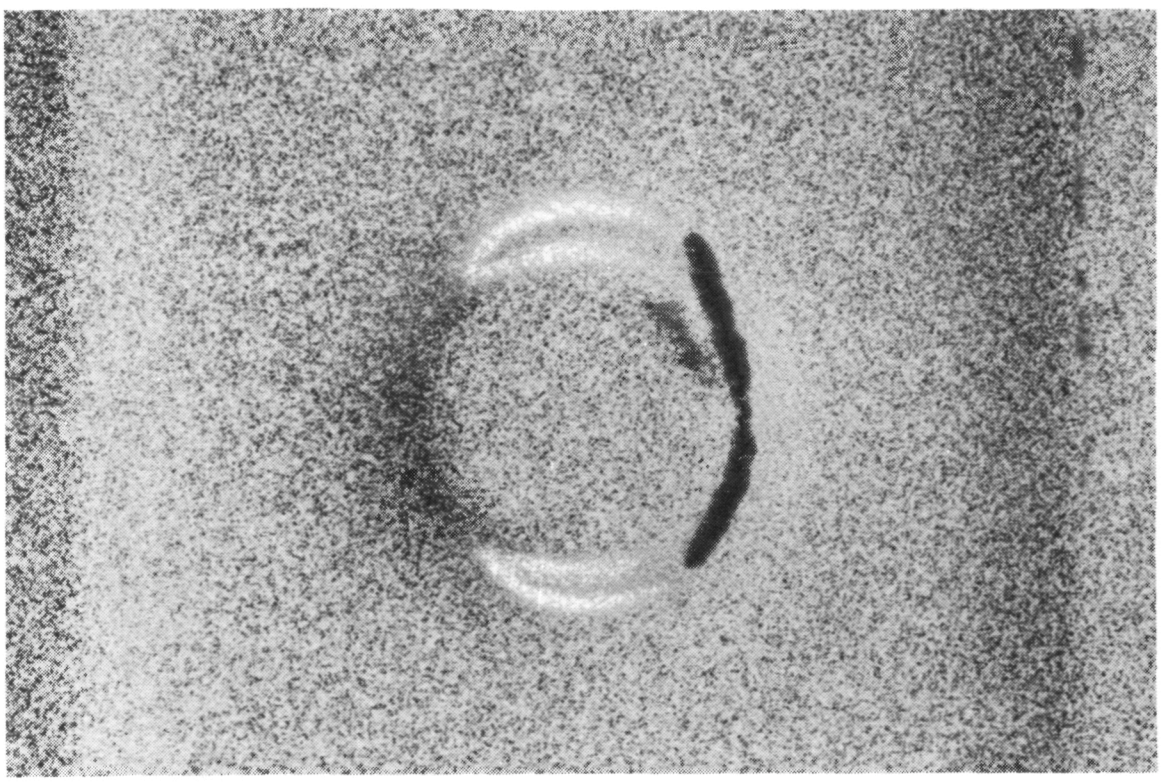

b. Closeup of Crack Exposure By Dye-Penetrant

Figure 3-35. Dye-Penetrant Inspection of Formed Cover Strip

mounted spot welds were made to confirm the defect. A sample of the panel x-ray is shown in Figure 3-36. The lighter areas at spot weld positions in the panel x-ray indicate a thinning of the spot welds caused by greater transverse compression in the material where above-normal current was used. Such areas were visually confirmed by noting excessive indentation on the surface of the panel at spot weld positions that appear as lighter areas in the x-ray of Figure 3-36.

The x-ray NDT method has proven to be a satisfactory method for checking spot-welded components for material expulsion at the welds. In addition to evaluation of radiography as an NDT method, spot weld machine settings were checked regularly during panel fabrication by testing sample spot-welded single lap-shear test specimens using the same settings as those employed for assembly of the panels. Minimum strength values were established for each combination of sheet thicknesses, and test samples were strength checked intermittantly during spot welding operations to assure satisfactory machine settings.

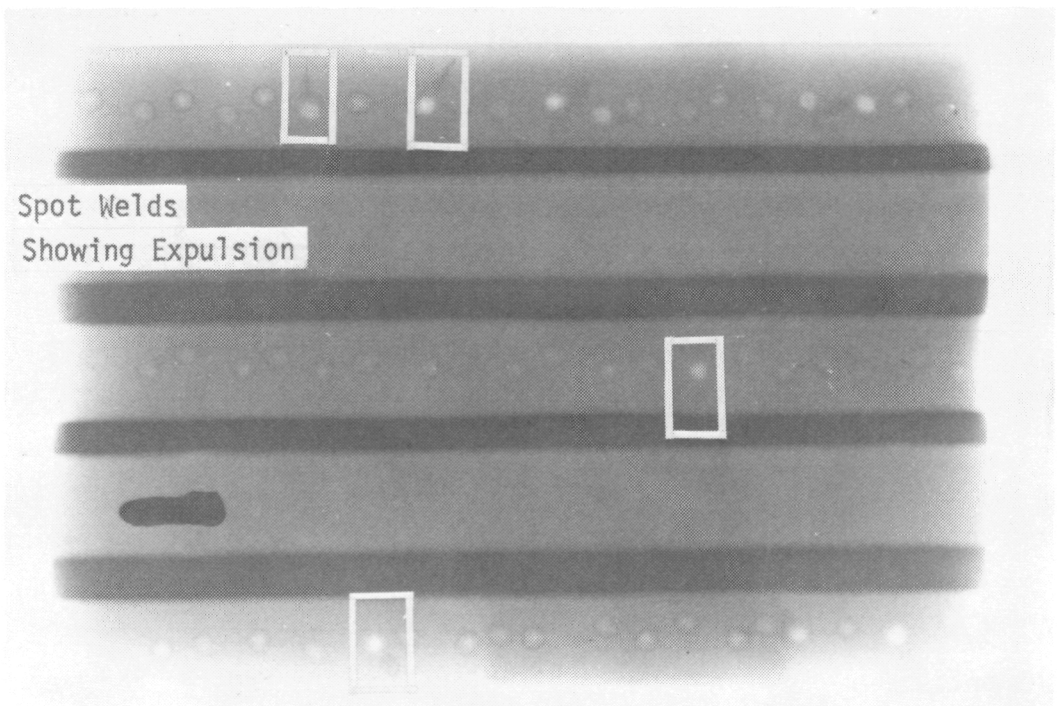

Figure 3-36. X-ray of Spot-Welded Panel

As described in Section 2, braze-reinforcement of a spot-welded panel was used on only one close-out panel in the contractor test array. Consequently, evaluations of NDT methods for the braze-reinforced panel were not made during Phase II. However, the differences in coloration shown in Figure 2-18 indicate the possibility of using normal photography or visual inspection to evaluate the extent of braze alloy flow in braze-reinforced spot-welded panels.

Section 4
CONCLUSIONS

The work performed in Phase II included design, fabrication, and testing of a full-scale full-size TD Ni-20Cr heatshield array simulating a Shuttle Orbiter TPS. Test results were evaluated to determine reuse capabilities, refurbishment requirements, TPS weight, and cost aspects that are associated with the use of a TD Ni-20Cr radiative TPS on the Space Shuttle Orbiter. Results of Phase II efforts led to the following conclusions:

A. Behavior of the full-scale, full-size panels in Phase II tests confirmed the results of Phase I subsize panel tests in that no significant permanent deformations were observed on the full-size TD Ni-20Cr heat shields.

B. Based on Phase II test results, the required replacement of TD Ni-20Cr heat shields during operational service of the shuttle is expected to be approximately four percent per orbital mission. Support structure, insulation packages, panel close-outs, and fastener replacement rate was indicated to be approximately one-tenth that of the TD Ni-20Cr heat shields.

C. Based on program results, a projected initial cost for a TD Ni-20Cr metallic radiative thermal protection system is $721 per square foot of TPS surface area. Costs were based on 1974 dollars and included the external heat shields, heat shield supports, insulation packages, panel close-outs, and fasteners.

D. Damage sustained by the TD Ni-20Cr heat shields as a result of simulated mission tests was confined to cracks in the 0.0254 cm (0.010 in.) thick panel face sheets. Face sheet cracking resulted primarily from local bending near the panel ends caused by pressure from the external cover strips. Excessive cover strip pressure appeared to result from buckling of the cover strip ends when thermal expansion was restricted by the test fixture edges.

E. Refurbishment costs, based on a heatshield replacement rate of four percent per mission, were added to the projected initial cost to yield a projected total TD Ni-20Cr TPS, cost of $1,943 per square foot for 100 missions.

F. The design approach used in the Phase II full-size full-scale TPS heat shields provided for replacement of individual panels without removal or loosening of any adjacent panels. This design feature allowed minimum refurbishment time and led to projected minimum labor costs in refurbishment operations.

G. Heat shield panel removal and replacement time observed in this program agreed closely with previous studies reported in Reference 7.

REFERENCES

1. Klingler, L. J., W. R. Weinberger, P. G. Bailey, and S. Baranow. Development of Dispersion-Strengthened Nickel-Chromium Alloy (Ni-Cr-ThO_2) Sheet for Space Shuttle Vehicles. NASA CR-120796, December 1971.

2. Johnson, R., Jr., and D. H. Killpatrick. Evaluation of Dispersion Strengthened Nickel-Base Alloy Heat Shields for Shuttle Application. Phase I Summary Report, NASA CR-132360, May 1973.

3. Fritz, L. J. Characterization of Mechanical and Physical Properties of TD Ni-Cr (Ni-20Cr-2ThO_2) Alloy. Contract NAS3-15558, Monthly Reports Nos. 1 (7 July 1971) through 15 (1 October 1972).

4. Johnson, R., Jr., and D. H. Killpatrick. Dispersion-Strengthened Metal Structural Development. AFFDL-TR-68-130, Part I (1968).

5. Gulbransen, E. A., and W. R. McMillan. Oxide Film on Nickel-Chromium Alloys. Industrial and Engineering Chemistry, Vol. 45, No. 8, August 1953, pp. 1734-1744.

6. Deveikis, W. D., and L. R. Hunt. Loading and Heating of a Large Flat Plate at Mach 7 in the Langley 8-Foot High Temperature Structures Tunnel. NASA TN-D-7275, September 1973.

7. Haas, D. W. Refurbishment Cost Study of the Thermal Protection System of a Space Shuttle Vehicle. NASA Report CR-111832, 1 March 1971.